UNIVERSITY OF MARYLAND

National Transportation Center

Project ID: NTC2016-SU-R-03

ECONOMIC IMPACTS FROM CHALLENGES IN PAVEMENT ENGINEERING IN AN UNCERTAIN CLIMATE FUTURE

Final Report

by

Dr. Shane Underwood
Assistant Professor
Civil, Environmental and Sustainable Engineering
Arizona State University

Dr. Mikhail Chester
Associate Professor
Civil, Environmental and Sustainable Engineering
Arizona State University

Padmini Gudipudi
Postdoctoral Research Scholar
Arizona State University

for

National Transportation Center at Maryland (NTC@Maryland)
1124 Glenn Martin Hall
University of Maryland
College Park, MD 20742

December, 2017

ACKNOWLEDGEMENTS

This project was funded by the National Transportation Center @ Maryland (NTC@Maryland), one of the five National Centers that were selected in this nationwide competition, by the Office of the Assistant Secretary for Research and Technology (OST-R), U.S. Department of Transportation (US DOT).

DISCLAIMER

TABLE OF CONTENTS

LIST OF TABLES

LIST OF FIGURES

EXECUTIVE SUMMARY

Climate change and extreme weather events have become issues of greater relevance to transportation engineering professionals. However, there remains relatively weak science for how climate change hazards can impact transportation infrastructure, the personal and commercial use of the infrastructure, the economic disparities that may occur from inconsistent geospatial and temporal influences, and how these impacts should be best managed. Recently the National Cooperative Highway Research Program evaluated how climate change *might* introduce hazards to transportation infrastructure. The outcomes provided, in very general terms, scenarios for the potential impact of these changes. While useful for planning, operations, and disaster management uses, these findings do not provide tangible information for designers on the engineering controls that may emerge in response to greater climatological uncertainty nor the economic impacts associated with the uncertainty.

In this report a series of analysis are shown to better understand the role of projected increases in temperatures on the structural capacity and longevity of pavements. This work uses current pavements and the projection of their performance under different climate scenarios to quantify the effects of a failure of engineering process to adapt. In the first study flexible interstate pavements are examined using an average of relatively high warming and relatively low warming scenarios. Geospatial differences in impacts are identified. In the second study a smaller number of pavements (five) are examined closely using a larger number of models in addition to the ensemble median. Climatological indices are identified from these simulations and applied to the entire US. Again, geospatial impacts are identified. Finally, in the third analysis asphalt binders are used a surrogate measure for pavement performance under different temperature regimes. An ensemble of 38 climate models across high and low warming scenarios are applied. In this analysis the changes in performance are linked to economic impacts using a life cycle cost analysis.

The specific locations impacted most greatly depended somewhat on the method used in the study. However, this study does show that modest average global temperature increases may result in predictable changes in infrastructure performance since pavements are affected more by extreme temperatures than mean temperatures. It is also evident that some regions of the country, particularly the mid-west and southeast may be more prone to impacts than other regions. The results of this study provide a unique, and large-scale perspective on the issue of climate change and its impacts on the pavement infrastructure.

1.0 INTRODUCTION

1.1 BACKGROUND

Climate change and extreme weather events have become issues of greater relevance to transportation engineering professionals (Meyer et al. 2014). However, there remains relatively weak science for how climate change hazards can impact transportation infrastructure, the personal and commercial use of the infrastructure, the economic disparities that may occur from inconsistent geospatial and temporal influences, and how these impacts should be best managed. The impacts themselves will result from intense precipitation, heat/cold stress, and other non-physical challenges that degrade infrastructure quality and longevity that climate change science suggests will occur in the future (NRC 2008, Anderson et al. 2015, Cambridge Syst. 2015, Koetse and Rietveld 2009, Rosenzweig et al. 2011, Huang 1993, Yoder and Witczak 1975). Because these transportation systems constitute large civil investments (US$7.7 trillion in assets and US$45 billion annual expenditures (USDOT 2015a)) and underpin an economic vibrancy (USDOT 2015b) and private citizen expenditures equal to 8.9% of GDP (USDOT 2015a)), the impacts may be substantial. Transportation infrastructure is built to last decades, but engineering protocols in the United States assume climate stationarity, which may result in accelerated degradation, and, consequently, increased costs. Additional costs are a concern since the American Society of Civil Engineers estimates that infrastructure needs US$3.6 trillion in the next decade, with a large fraction of that currently unfunded (ASCE 2013). At present, engineers assume a stationary climate when selecting pavement materials, meaning that they may be embedding an inherent negative performance bias in pavements for decades to come. With warming trends observed and accelerating across the U.S. (Melillo et al. 2014), and with scientific consensus for future warming, continued use of such data will likely expose some areas to more rapid degradation (Knutti and Sedlacek 2013, Mearns et al. 2012, Woldemeskel et al. 2016, Wuebbles et al. 2014).

In 2008, the National Cooperative Highway Research Program (NCHRP) evaluated how climate change might introduce hazards to transportation infrastructure. These hazards were described in broad terms across all transportation modes, but encompassed a range of potential impacts from increased shipping seasons in cold-weather ports to operational challenges due increased coastal and inland flooding events (Humphrey 2008). While useful for planning, operations, and disaster management uses, these findings do not provide tangible information for designers on the engineering controls that may emerge in response to greater climatological uncertainty nor the economic impacts associated with the uncertainty. With respect to pavements this report suggested that future increases in very hot days and heat waves may lead to concerns with pavement integrity. They also recognized that changes in subgrade moisture levels (either by changes to the water table depth or through precipitation) could alter the bearing capacity and thus performance of this infrastructure, and conclude that the typical design scope for pavements (10-20 years), may help to mitigate these impacts. With this guidance, for example, one resulting scenario may be that designs are adjust to a higher overall level of reliability, which will increase infrastructure costs and maintain current levels of performance. In an alternative vision the engineering could remain the same and performance could reduce by either overall system deterioration and/or increased

frequency of catastrophic failures. Currently the knowledge to accurately assess the economic impact of these (or other) scenarios inclusive of user/freight delay does not exist.

Reviews of other studies on climate change impacts reveals some gaps in accurately quantifying the impacts using distresses directly. For example, Anderson et al. (2015) quantify the potential impact to Arizona transportation infrastructure using the number of projected days above 38°C. This approach is not addressing the fact that pavements are designed with materials specific to the location in which they are placed and thus the number of days above a single fixed temperature does not indicate the impacts fairly across areas that are already climatologically diverse. In addition, Anderson et al. (2015) do not account for the interactive impacts of soil conditions, traffic, and structure. In another study involving the state of Texas, researchers recognized the difference in materials across regions, but did not project how an increase in temperature might affect performance with respect to the continuation of historical trends (Cambridge Syst. 2015).

Chinowsky and Arndt (2012) developed an economic dynamic-stressor model based on empirical performance impacts from precipitation and temperature). These models reflect, but do not predict the precise impact of climate change on materials. This approach has been codified into a planning system and used extensively to assess the economic impacts of climate change on pavement infrastructure (Schweikert et al. 2014). A limitation in these network level analyses is that they ignore the actual engineering details of the infrastructure. They essentially overlay climate variables in terms of changes in temperature and/or precipitation on top of the existing infrastructure and identify where the two (infrastructure and climate change) intersect. Such an approach does not account for the fact that the pavement performance is a cumulation of many interactive factors (materials, structures traffic, and climate).

An engineering analysis was completed by Daniel et al. (2014) to evaluate the impact of climate change on the performance of New England pavements. Climate prediction data was incorporated into the pavement design process and results were compared with design/analysis completed using the historical data. The study concluded that climate change predictions may have a substantial effect on pavement distresses, specifically that pavement life may decrease from between 16 years to 4 years and maintenance cost may also increase by 100%. Meagher et al. (2012) used climate change projections from the North American Regional Climate Change Assessment Program to evaluate designs of flexible pavements in New England. In this study the authors used only temperature data and found that changes in alligator cracking for secondary and interstate pavements was negligible but for the increase ranged from 4% to 16% depending on the precise location. Other studies have concluded that rutting and pavement failure occurs much earlier than anticipated leading to the frequent new construction and maintenance of roadway infrastructure (Harvey et al. 2004, Mills et al. 2009, Mndawe et al. 2013).

Most of these studies mentioned above focus on temperature data alone from the climate prediction models to study the impact of climate change on the pavement performance. However, two recent studies used changes in precipitation levels along with temperature data from climate prediction models and reported that climate change shows significant impact on the pavement life (Heitzman 2011, Mndawe et al. 2015). These studies integrate both temperature and precipitation data, but do not indicate whether one or the other factors has a greater impact. Very little data is found isolating the impact of precipitation. Many of the studies that exist echo that of Gaspard et al. (2007), which

studied pavements performance after Hurricane Katrina and found that pavements submerged during the hurricane were weaker than the ones that were not. In case of flexible pavements, the damage observed is more than the damage observed for rigid pavements.

Overall, existing evidence suggests that climate change will impact the performance and maintenance of the pavement infrastructure. However, there are some limitations in the existing literature: 1. Most of the existing studies are limited to one pavement structure, location, and/or one climate region. Even taken collectively the literature uses dissimilar models and other underlying assumptions making it impossible to gain a comprehensive view of impacts, 2. Most current studies focus on one or maybe two climate models and do not include different potential emission scenarios in the analysis, thus it becomes very difficult to infer or ascertain the certainty/uncertainty in the predicted outcome, and 3. Current studies do not identify the relative significance of projected temperature versus precipitation on predicted pavement performance.

1.2 STUDY OBJECTIVE

The objective of this research is to investigate the impacts of unaccounted for climate change on pavement infrastructure.

1.3 SCOPE OF WORK

Evaluating the effects of future climate factors on pavement infrastructure is not a simple problem since these impacts depend on current traffic conditions, the conditions and engineering of existing infrastructure, and an analytical model to predict how climate interacts with these factors. This study therefore carried out a multi-tiered analysis process involving both system and project specific analyses. Final conclusions are drawn based on the combined interpretation of these analyses.

1.4 RELEVANCE TO CENTER THEMES

This research directly addresses economic competitiveness. The construction and maintenance of highway infrastructure represents a substantial burden for state and local transportation agencies. Proper planning and design of this infrastructure can reduce these costs and permit more effective distribution of funds. States and regions experiencing greater climatological changes may be particularly vulnerable and face substantial hurdles to remain economically competitive. Nationally, ensuring that current transportation infrastructure investments are strategically directed so as to mitigate these uncertainties (by investing in major commercial routes that are along corridors less prone to future climate uncertainties for example) may lead to a more resilient transportation infrastructure that maintains and improves the global economic competitiveness of the country. The findings from this study will add another dimension to the discussion of climate projections as it directly addresses the expected impacts on pavement infrastructure. It will provide an assessment of the do-nothing scenario wherein procedures do not change as well as establish a framework for future studies that may establish goals for infrastructure design and construction and/or development of new materials technologies to ensure effective long-term development of the transportation infrastructure.

2.0 STUDY 1: EVALUATION OF FLEXIBLE PAVEMENTS ON THE PRIMARY FREIGHT NETWORK

2.1 INTRODUCTION

The overall goal of this project is to assess the sensitivity of the pavement infrastructure along key interstate routes to freight movement projections. The interstates selected for this study are shown in Figure 1 and include I-5, I-10, I-15, I-35, I-40, I-70, I-75, I-80, I-90, I-94, and I-95. These interstates are selected based on the vehicular traffic they carry, the strategic importance to freight movement (port connectivity), their inclusion in the MAP-21 Primary Freight Network (MAP 21 2012), and their geographic diversity. The total mileage length of all these routes is 22,900 miles, which is approximately 48% of the total interstate system. The selected interstates represent approximately 70% of the total freight traffic occurring on all interstates (FHWA 2013). The method used to organize this analysis into manageable pieces and still obtain an accurate assessment involved segmenting the routes into smaller and more uniform sections. This segmentation was based principally upon traffic, climate, and subsurface since these factors are known to contribute substantially to pavement performance. In addition, state boundaries were also used to segment the interstates as each state has its own set of pavement specifications, which will affect the materials utilized along each segment. In total there are 211 segments that have been analyzed for this study, and these are described in more detail below.

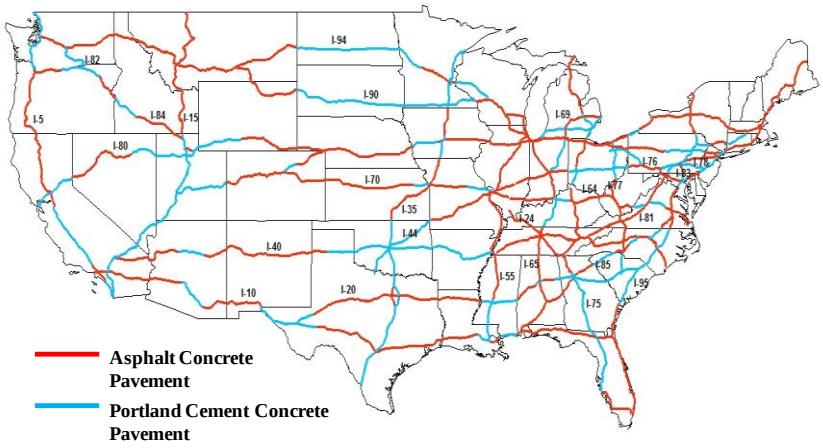

Figure 1: Map of selected interstates.

2.2 SEGMENTATION RULES

The four main factors determining the stability of a pavement section are the traffic carried by the section, the climate in the area of the pavement, the soil over which the pavement is built, and the materials used in the paving layers. All other factors being equal if a pavement carries more traffic the process of deterioration will be faster and the probability of failure of the section will increase.

Likewise, more extreme temperatures, greater amounts of precipitation, and inferior soils can hasten pavement deterioration. Materials are generally project specific, but are selected and designed following the guidelines and specifications laid out by State Departments of Transportation. The paragraphs below detail the rules applied in three of these categories (traffic, climate, and soil). The fourth criteria, state boundaries, were identified through geospatial mapping of the interstate routes.

2.2.1 Traffic

To segment the interstate routes by traffic, each available traffic segment (mile marker in some cases or larger sections in other cases) was ranked on a scale of 1 to 5. The assignment was based on the Average Annual Daily Truck Traffic (AADTT) values in the base year (2012);

- 5 = > 20,000,
- 4 = 15,000 – 20,000,
- 3 = 10,000 – 15,000,
- 2 = 5,000 – 10,000, and
- 1 = < 5,000.

To populate this traffic database, data was collected through the various state Departments of Transportation, where it was found that each department generally follows its own format. Some provide the exact AADTT data on a mileage basis, but most do not. Some of the states provide the traffic values by sections on their county maps while some states provide it in other formats such as *.kml (Google earth) and *.shp (GIS applications). In cases where states provided only the average annual traffic, the department's design documentation was reviewed to identify either site specific or generally applied truck factors.

2.2.2 Soil

The second factor considered for the segmentation of interstates was the soil type for the region. The extensive mapping effort completed under NCHRP 9-23B was used for this purpose. In this project, researchers compiled soil maps, like that shown in Figure 2, by reviewing available databases and applying certain empirical predictive equations to estimate engineering properties. In this figure, each colored region represents an area of approximately uniform soil conditions. The database is available as an online application (http://nchrp923b.lab.asu.edu/index.html). An example of the output from this application is given in Figure 3, where it is seen that soil characteristics for a particular site are compiled as a function of depth according to AASHTO classification and engineering properties. In the AASHTO classification system soils are denoted as either A1, A2, A3, A4, A5, A6, or A7 with A1 denoting highly course and A7 denoting very fine soil. The strength of a pavement and the drainage conditions depend on its subgrade soil.

For the process of segmentation, the soil properties need to be known on a mile-by-mile basis, and this required some processing of the database. In this database information can be obtained from by two methods, both of which are discussed here. In the first method, the user chooses to search for route information and is taken to a second screen where he/she selects state, route type (Interstate in this case), and milepost are first selected. The web application then identifies the

latitude and longitude coordinates, which the user must then paste into the appropriate boxes on the main screen of the application. Next, the user selects the 'Get Map' button and the soil layer corresponding to that particular point is displayed in color. By then moving the cursor on top of the colored map region and selecting the region a soil unit, referred to as a 'MapChar', is then displayed and the user enters this into the report box to generate a soil unit report. In the second method the soil report selection procedure is the same, but to identify the search 'MapChar', the user first gets a state-wide map and then manually identifies the requisite milepost locations.

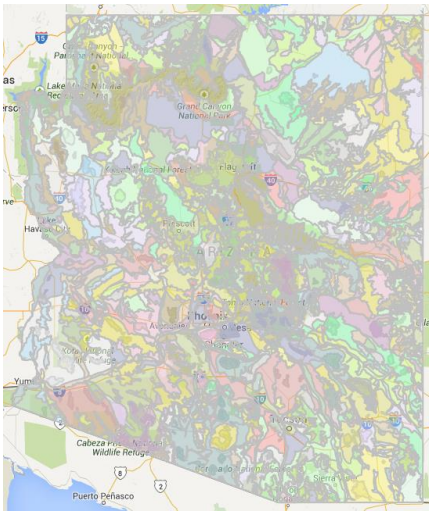

Figure 2: Example map in NCHRP 9-23B soil map application (State of Arizona).

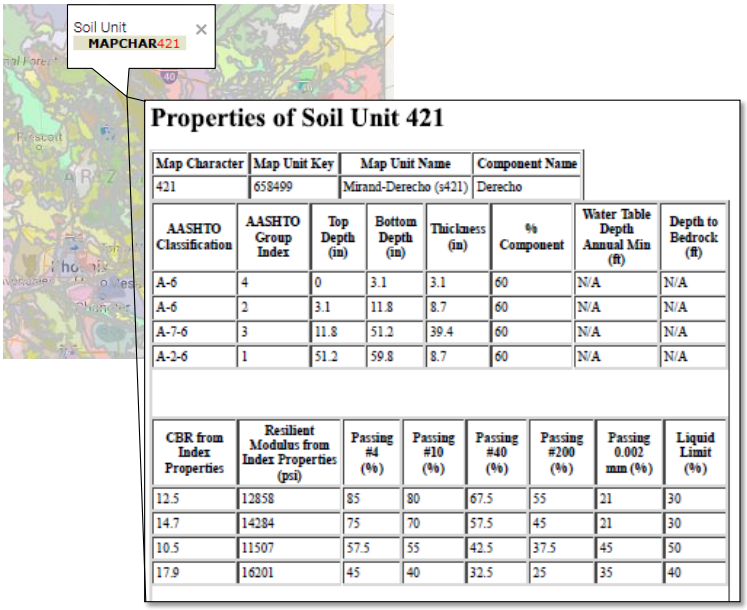

Properties of Soil Unit 421

Map Character	Map Unit Key	Map Unit Name	Component Name
421	658499	Mirand-Derecho (s421)	Derecho

AASHTO Classification	AASHTO Group Index	Top Depth (in)	Bottom Depth (in)	Thickness (in)	% Component	Water Table Depth Annual Min (ft)	Depth to Bedrock (ft)
A-6	4	0	3.1	3.1	60	N/A	N/A
A-6	2	3.1	11.8	8.7	60	N/A	N/A
A-7-6	3	11.8	51.2	39.4	60	N/A	N/A
A-2-6	1	51.2	59.8	8.7	60	N/A	N/A

CBR from Index Properties	Resilient Modulus from Index Properties (psi)	Passing #4 (%)	Passing #10 (%)	Passing #40 (%)	Passing #200 (%)	Passing 0.002 mm (%)	Liquid Limit (%)
12.5	12858	85	80	67.5	55	21	30
14.7	14284	75	70	57.5	45	21	30
10.5	11507	57.5	55	42.5	37.5	45	50
17.9	16201	45	40	32.5	25	35	40

Figure 3: Engineering parameters from NCHRP 9-23B application.

The soil unit report describes the AASHTO type of soil present in that region, the thickness of each layer, water table depth (if known), depth to bedrock, and the other engineering properties of the soil. The search databases identified and functions developed by the NCHRP 9-23b research team are capable of estimating the soil properties at multiple depths (more than 60 inches in some

cases). Some soil units are completely homogenous with depth, e.g., they show the same soil type for the entire profile. However, in some cases there are two or more types of soils present. In such cases, the weakest type of soil present at that location is considered. For example, if a given location contains an A2 soil for the top 3 inches and A4 soil for the next 12 inches, the soil type of the location is set as A4 for the segmentation process.

Based on its engineering properties, the high quality soils are given a low rating and the lower quality soils were given a higher rating. The rating scale is as follows.

- A1 & A2 – 1
- A3 – 2
- A4 – 3
- A5 – 4
- A6 & A7 – 5

2.2.3 Climate

The third factor considered in segmentation was current climate with special reference to the total precipitation over the region. One of the main reasons for pavement failure is the seepage of water into the pavement and its effect on the subgrade. Hence the effect of precipitation on the pavement deterioration was also used. In order to accommodate the severity of damage caused due to rainfall on the pavement segments, the following methodology was used.

Those places experiencing no or very little rainfall are least susceptible to pavement deterioration due to water seepage, and following the general convention followed in this report, those places were given a rating 1. Analysis of rainfall data for the 51 major cities in the US, Table 1 shows that the annual rainfall distribution in these cities fell into the range of approximately 15 to 60 inches per year as shown in Figure 4.

Table 1: Rainfall data for 51 major US cities.

City	Rain (in.)	City	Rain (in.)	City	Rain(in.)
Atlanta, GA	49.7	Jacksonville, FL	52.4	Portland, OR	43.5
Austin, TX	34.2	Kansas City, MO	39.1	Providence, RI	47.2
Baltimore, MD	41.9	Las Vegas, NV	4.2	Raleigh, NC	46.0
Birmingham, AL	53.7	Los Angeles, CA	12.8	Richmond, VA	43.6
Boston, MA	43.8	Louisville, KY	44.9	Riverside, CA	10.3
Buffalo, NY	40.5	Memphis, TN	53.7	Rochester, NY	34.3
Charlotte, NC	41.6	Miami, FL	61.9	Sacramento, CA	18.5
Chicago, IL	36.9	Milwaukee, WI	34.8	Salt Lake City, UT	16.1
Cincinnati, OH	41.9	Minneapolis, MN	30.6	San Antonio, TX	32.3
Cleveland, OH	39.1	Nashville, TN	47.3	San Diego, CA	10.3
Columbus, OH	39.3	New Orleans, LA	62.7	San Francisco, CA	20.7
Dallas, TX	37.6	New York, NY	49.9	San Jose, CA	15.8
Denver, CO	15.6	Oklahoma City, OK	36.5	Seattle, WA	37.7
Detroit, MI	33.5	Orlando, FL	50.7	St. Louis, MO	41.0
Hartford, CT	45.9	Philadelphia, PA	41.5	Tampa, FL	46.3
Houston, TX	49.8	Phoenix, AZ	8.2	Virginia Beach, VA	46.5
Indianapolis, IN	42.4	Pittsburg, PA	38.2	Washington, DC	39.7

Additional investigations also showed that there were also areas, like Laurel mountain in Oregon and Forks in Washington, that receive exceptionally high rainfall of more than 80 inches per year (NCDC 2010). Owing to the fact that the overall resolution of this study was larger than the scale of many of these microclimates, the index ranges were established based on the city-wise analysis. As shown in Figure 4 the distribution of precipitation in these cities was close to normal with a mean of 37 inches and a standard deviation of 14 inches. Using this distribution as a guide and with the desire to choose ranges with convenient rainfall totals and spaced in approximately one standard deviation intervals, the rating system of 1-5 was devised with the following ranges;

- 5 = > 60 inches per year
- 4 = 45 – 60 inches per year,
- 3 = 30 – 45 inches per year,
- 2 = 15 – 30 inches per year, and
- 1 = < 15 inches per year.

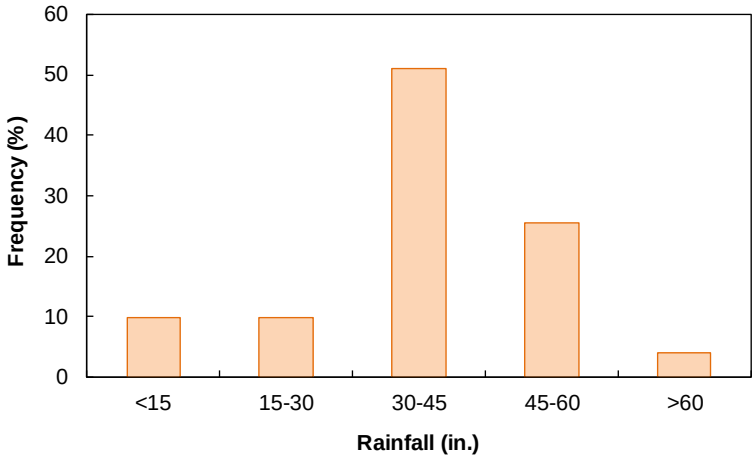

Figure 4: Rainfall distribution in 51 major cities.

2.2.4 Combining Factors and Selecting Analysis Segments

The final segmentation of the interstate routes was based on the combined effect of all these factors, which was calculated by averaging the ratings of each of the three individual factors. Mileage sections with average ratings within the same whole point score were then taken to be a single section. Whenever there was an increase or decrease to the next whole point, a section was assigned to another segment. So for example, if generic section A had an average score of 3.4 and the following section (Section B) had a score of 3.9 they were taken to exist in the same segment. If Section B had a score of 4.1 the two sections would be assigned to different segments. The routes were also divided at the state boundaries because the design and construction details varied between states. Exceptions to the state boundary rule were made in cases where the interstate traversed one of the states for fewer than 40 miles. Additional limits on maximum and minimum length were assigned (200 and 50 miles respectively).

Finally, segments to be included for analysis were selected based on their primary material type. In this chapter primary attention was given to flexible pavements. Since many of these freight networked sections were high volume roadways and since transportation departments prefer

portland cement concrete pavements in these applications, many of the available test segments were eliminated.

2.3 INTERSTATE SEGMENTS

In total 110 segments were extracted for analysis. These segments cover a total of 13,306 miles and 33 states. The sections are summarized in Table 2 through Table 4. In the following paragraphs a brief summary of the segmentation of each interstate is given.

Table 2: Summary of Analysis Segments for North-South Interstates.

Interstate	State	Length (Miles)	Sections			
			Name	Length (Miles)	MP	Description
I-15	ID	122	I15-ID-2	122	76 to 197	Bingham County to Montana border
	MT	396	I15-MT-1	199	0 to 199	Idaho border to Jefferson County
			I15-MT-2	197	200 to 396	Jefferson County to Canadian border
I-55	IL	156	I55-IL-1	156	0 to 156	East St. Louis to McLean County
	MO	216	I55-MO-1	96	0 to 96	Arkansas state line to Cape Girardeau
			I55-MO-2	120	97 to 216	Cape Girardeau to Illinois state line
	MS	186	I55-MS-2	186	104 to 186	Hinds County to DeSoto County
	TN	82	I55-TN-1	82	0 to 82	Mississippi state line to Blytheville
I-65	AL	366	I65-AL-1	181	0 to 181	Mobile County to Elmore County
			I65-AL-2	185	182 to 366	Elmore County to Limestone County
	TN	120	I65-TN-1	120	0 to 120	Giles County to Robertson County
I-69	MI	215	I69-MI-1	108	0 to 108	Branch County to Shiawassee County
			I69-MI-2	107	109 to 215	Shiawassee County to St. Clair
I-75	FL	180	I75-FL-2	180	195 to 374	Sarasota County to Alachua County
	GA	86	I75-GA-4	86	271 to 356	Fulton County to Tennessee border
	KY	173	I75-KY-1	88	0 to 88	Tennessee border to Madison County
			I75-KY-2	85	89 to 173	Madison County to Ohio border
	MI	180	I75-MI-3	180	220 to 399	Ogemaw County to Chippewa County
	TN	142	I75-TN-1	142	0 to 85	Georgia border to Kentucky border
I-77	VA	67	I77-VA-1	67	0 to 67	Carroll County to Bland County
I-81	NY	189	I81-NY-1	130	0 to 130	Broome County to Ellisburg
			I81-NY-2	59	131 to 189	Ellisburg to Orleans
	TN	76	I81-TN-1	76	0 to 76	Dandridge to Virginia border
	VA	288	I81-VA-2	144	162 to 305	Botetourt County to Frederick County
			I81-VA-2	144	162 to 305	Botetourt County to Frederick County
I-85	AL	80	I85-AL-1	80	0 to 80	Montgomery to Georgia border
	NC	93	I85-NC-1	93	0 to 93	Cleveland County to Davidson County
	VA	68	I85-VA-1	68	0 to 68	Mecklenburg County to City of Petersburg
I-95	CT	111	I95-CT-1	111	0 to 111	New York border to Rhode I. border
	FL	383	I95-FL-1	76	0 to 76	Miami-Dade County to Palm Beach County
			I95-FL-2	130	77 to 206	St. Lucie County to Brevard County
			I95-FL-3	177	207 to 383	Brevard County to Georgia border
	GA	112	I95-GA-1	112	0 to 112	Florida border to South Car. border
	MA	107	I95-MA-1	107	0 to 91,	Rhode I. border to Maine border
	MD	47	I95-MD-1	47	0 to 47	Virginia border to Baltimore
	ME	304	I95-ME-1	156	0 to 156	New Hampshire border to Somerset County
			I95-ME-2	148	157 to 304	Somerset County to Canadian border
	VA	174	I95-VA-1	101	0 to 101	North Carolina border to Hanover County
			I95-VA-2	73	102 to 174	Hanover County to Maryland border

Table 3: Summary of Analysis Segments for East-West Interstates (1 of 2).

Interstate	State	Length (Miles)	Sections			
			Name	Length (Miles)	MP	Description
I-10	AZ	248	I10-AZ-1	137	0 to 137	California border to Maricopa County
			I10-AZ-3	111	283 to 393	Pima County to New Mexican border
	CA	251	I10-CA-1	102	0 to 102	Los Angeles County to Riverside County
			I10-CA-2	149	103 to 251	Riverside County to Arizona border
	FL	363	I10-FL-1	175	0 to 175	Alabama border to Gadsden County
			I10-FL-2	188	176 to 363	Gadsden County to Duval County
	LA	207	I10-LA-1	154	0 to 154	Texas border to Lafayette County
			I10-LA-3	53	222 to 274	Jefferson County to Mississippi border
	NM	164	I10-NM-1	164	0 to 164	Arizona border to Texas border
	TX	334	I10-TX-3	161	278 to 438	Pecos County to Sutton County
			I10-TX-4	127	439 to 565	Sutton County to Kerr County
			I10-TX-5	46	566 to 611	Kerr County to Bexar County
I-20	LA	190	I20-LA-1	190	0 to 190	Caddo County to Madison County
	TX	387	I20-TX-2	177	85 to 261	Ward County to Taylor County
			I20-TX-4	101	427 to 527	Tarrant County to Van Zandt County
			I20-TX-5	109	528 to 636	Van Zandt County to Harrison County
I-24	GA	89	I24-GA-1	89	0 to 89	Georgia state line to Rutherford
	KY	131	I24-KY-1	131	0 to 131	Clarksville to Williamson County
	TN	91	I24-TN-1	91	0 to 91	Rutherford County to Hamilton County
I-40	AZ	214	I40-AZ-2	112	147 to 258	Yavapai County to Navajo County
			I40-AZ-3	102	259 to 360	Navajo County to New Mexico border
	CA	155	I40-CA-1	155	0 to 155	Barstow County to Arizona border
	NC	422	I40-NC-1	162	0 to 162	Tennessee border to Iredell County
			I40-NC-2	98	163 to 260	Iredell County to Orange County
			I40-NC-3	162	261 to 422	Orange County to New Hanover County
	NM	374	I40-NM-1	155	0 to 155	Arizona border to Cibola County
			I40-NM-2	102	156 to 257	Cibola County to Guadalupe County
			I40-NM-3	117	258 to 374	Guadalupe County to Texas border
	TN	225	I40-TN-3	160	218 to 377	Davidson County to Knox County
			I40-TN-4	65	378 to 442	Knox County to North Carolina border
	TX	67	I40-TX-1	67	0 to 67	New Mexico border to Potter County
I-44	MO	137	I44-MO-2	137	154 to 290	Pulaski County to St. Louis
I-64	IN	124	I64-IN-1	124	0 to 124	Posey County to Floyd County
	KY	119	I64-KY-2	119	65 to 183	Woodford County to Boyd County
	VA	167	I64-VA-2	167	133 to 299	Albemarle County to City of Chesapeake
I-70	CO	451	I70-CO-1	91	0 to 91	Utah border to Garfield County
			I70-CO-2	184	92 to 275	Garfield County to Denver County
			I70-CO-3	176	276 to 451	Denver County to Kit Carson County
	IL	138	I70-IL-1	138	0 to 138	Missouri border to Indiana border
	MD	93	I70-MD-1	93	0 to 93	Pennsylvania border to Baltimore County
	PA	169	I70-PA-1	54	0 to 54	W. VA border to Westmoreland County
			I70-PA-2	115	55 to 169	Westmoreland County to Maryland border
I-76	CO	121	I76-CO-2	121	67 to 187	Morgan County to Nebraska state line
I-78	NJ	72	I78-NJ-2	72	0 to 72	Town of Alpha to New York

Table 4: Summary of Analysis Segments for East-West Interstates (2 of 2).

Interstate	State	Length (Miles)	Sections			
			Name	Length (Miles)	MP	Description
I-80	NJ	68	I80-NJ-1	68	0 to 68	Pennsylvania border to Bergen County
	NV	306	I80-NV-1	183	0 to 183	California border to Humboldt County
			I80-NV-2	123	184 to 306	Humboldt County to Osino
	WY	231	I80-WY-2	141	174 to 314	Sweetwater County to Albany County
			I80-WY-3	90	315 to 404	Albany County to Nebraska border
I-84	ID	162	I84-ID-2	162	0 to 116	Elmore County to Oneida County
	NY	71	I84-NY-1	71	0 to 71	Port Jervis to Connecticut state line
	OR	103	I84-OR-1	103	0 to 76	Multnomah County to Wasco County
	UT	110	I84-UT-1	110	0 to 110	Box Elder County to Summit County
I-90	ID	68	I90-ID-1	68	0 to 68	Washington border to Montana
	MA	136	I90-MA-1	136	0 to 136	New York border to Suffolk County
	MT	545	I90-MT-1	155	0 to 155	Idaho border to Missoula County
			I90-MT-2	85	156 to 240	Missoula County to Deer Lodge County
			I90-MT-3	160	241 to 400	Deer Lodge County to Gallatin County
			I90-MT-4	75	401 to 475	Gallatin County to Yellowstone County
			I90-MT-5	70	476 to 545	Yellowstone County to Wyoming border
	NY	386	I90-NY-1	106	0 to 108	Pennsylvania border to Victa
			I90-NY-2	136	108 to 242	Victa to Utica
			I90-NY-3	144	242 to 385	Utica to Massachusetts border
	WA	297	I90-WA-1	149	0 to 149	King County to Grant County
			I90-WA-2	93	150 to 242	Grant County to Lincoln County
			I90-WA-3	55	243 to 297	Lincoln County to Idaho border
	WY	209	I90-WY-1	135	0 to 135	Montana border to Campbell County
			I90-WY-2	74	136 to 209	Campbell County to South Dakota border
I-94	MN	143	I94-MN-2	143	115 to 259	Todd County to Wisconsin border
	MT	249	I94-MT-1	119	0 to 119	Yellowstone County to Custer County
			I94-MT-2	130	119 to 249	Custer County to North Dakota border

2.4 PAVEMENT PERFORMANCE PREDICTIONS

For each of the analysis sections, detailed information on the climate, traffic, materials, and structural conditions were obtained from the respective Departments of Transportation. These inputs were then used with the NCHRP 1-37A Mechanistic-Empirical analysis method to predict the performance of the pavement infrastructure under the state of the practice traffic projections. These predicted performance metrics formed the baseline, or control conditions for the current study. Subsequent to these control predictions a second set of predictions were made using climate change model predictions for climate. The relative change in performance metrics were then used to identify interstate sections expected to be more sensitive to climate change.

2.4.1 Pavement Performance Definitions

When engineers consider pavement performance they generally focus on the overall pavement smoothness as well as the distresses of fatigue cracking, rutting, and thermal cracking. Of these three distresses the first two can be readily associated with load related phenomenon, while the third stems from the pavement response to temperature changes. The process of fatigue cracking occurs through the repeated application of load cycles, which while individually not large enough to cause a structural pavement failure do contribute some incrementally small amount of damage

in the pavement system. The distress generally appears first as cracks longitudinal or transverse to the travel direction and isolated to the wheel paths, **Error! Reference source not found.**(a). With c ontinued loading these cracks generally coalesce and grow until they reach a regular cracked pattern that resembles the scale pattern of an alligator, **Error! Reference source not found.**(b). T his pattern leads to the colloquial name for this type of distress: alligator cracking. In most low severity cases fatigue cracking can be mitigated through proper maintenance operations, but if this process does not occur in time then water can infiltrate the pavement system and lead to relatively rapid structural failure.

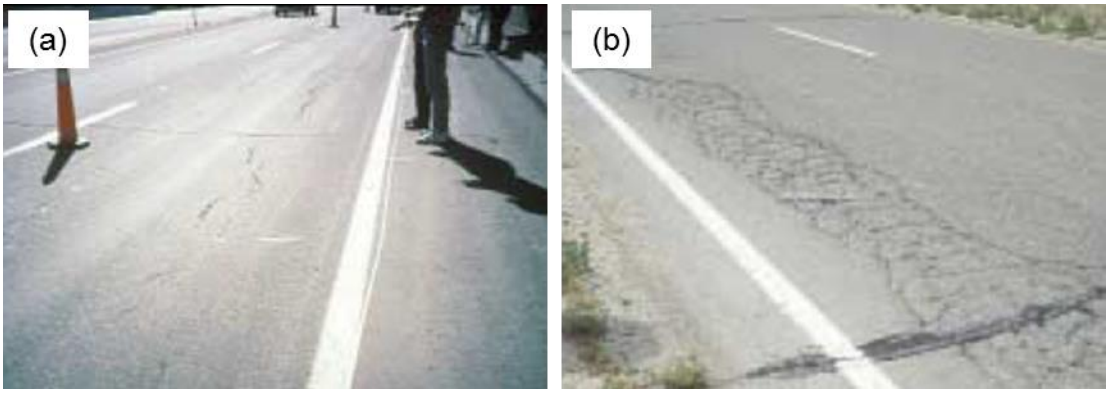

Figure 5: Examples of fatigue cracking in asphalt pavements; (a) low severity and (b) high severity (Miller and Bellinger 2003).

The second load associated distress of principle interest is rutting, which manifest as longitudinal depressions in the pavement surface, **Error! Reference source not found.**. Rutting can occur b ecause of extreme deformation in any single pavement layer or due to relatively small accumulation across any of the individual layers. In the case of rutting the major concern is with respect to safety as water can accumulate in these depressions and lead to hydroplaning. In some extreme cases the depressions can be accompanied by large upheavals on either side, which can pose additional safety concerns from lane changes.

Figure 6: Examples of rutting distress in asphalt pavement.

2.4.2 Mechanistic-Empirical Analysis

As outlined in the introduction chapter and summarized in **Error! Reference source not found.** b elow, the NCHRP 1-37A Mechanistic-Empirical analysis method uses a three-step approach to

predict pavement performance. Step 1 consists of the development of input values for the analysis. During this stage, potential structural options are identified for consideration in Step 2 (analysis). Also in this stage, pavement materials characterization and traffic input data are developed. The enhanced Integrated Climatic Model (EICM), a climatic effects modeling tool, is used to model temperature and moisture within each pavement layer and the sub grade. The climatic model considers hourly climatic data described later on. The pavement layer temperature and moisture predictions from the EICM are calculated hourly over the design period and coupled with secondary effects models to estimate material properties for the foundation and pavement layers as functions of temperature and/or moisture condition. To produce an accurate analysis that considers both daily and monthly variations in temperature, the hourly changes are used to compile five different representative temperature profiles for each month. Subsequent analysis then treats these profiles, referred to as quintiles, as the potential temperature variations for a given month. Step 2 of the design process is the structural/performance analysis. The structural section is analyzed incrementally over time using the pavement response and distress models, and the outputs of the analysis are the accumulated damage and the expected amount of distress and smoothness over time. Step 3 involves the assessment of the structural viability of the pavement based on the damage accumulation and the distress summary of the analysis. In the following paragraphs a brief introduction to the damage and damage modeling process are presented.

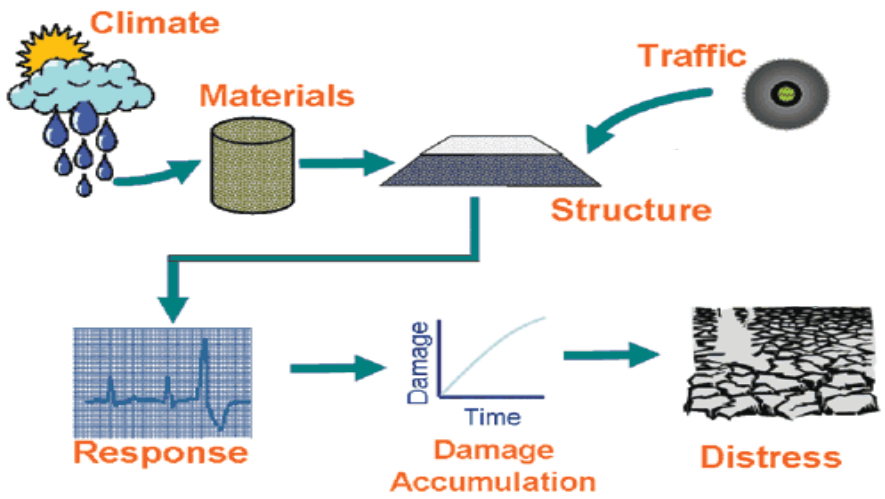

Figure 7: Schematic overview of mechanistic-empirical analysis process.

2.4.2.1 Pavement Response Modeling

There are many methods that exist for predicting the stress and strains response of flexible pavements to vehicular loading, e.g., layered elastic analysis, layered viscoelastic analysis, elastic and viscoelastic based finite element modeling, etc. Of these, the layered elastic analysis (LEA) technique has been chosen for use in the mechanistic-empirical process because of its overall simplicity, widespread familiarity, general accuracy (if used properly), and (most importantly) computational efficiency. The mathematical details of the LEA process are presented in great detail elsewhere, here the implementation of this method as it relates to the current work are presented.

As the name implies, LEA treats all pavement layers as linear elastic, meaning that the stress and strain are assumed to be perfectly proportional to one another at all levels. This constant of proportionality, the Elastic modulus, forms the primary mechanical property of interest and must be estimated for each and every pavement layer and sub-layer. Other important assumptions in the linear elastic analysis process include:

- The materials are homogeneous and isotropic;
- The applied load has a circular footprint;
- The layers are all perfectly horizontal and extend in infinite directions in the plane perpendicular to the applied load (the x-y plane);
- The mechanical properties are independent of x-y location (but can vary by depth, z);
- The bottom layer is infinitely thick; and
- All layers/sub-layers are fully bonded.

An important part of any structural analysis process is identifying the important locations where the response should be identified. This facet of structural analysis is also true in the case of pavements, but the process is complicated somewhat because, while the nature of loading is always the same (vertical load to the horizontal pavement surface), the positioning of these loads can change (for example with a single, tandem, tridem, or quad loading axle). The specific implementation of LEA in the mechanistic-empirical analysis used here overcomes this shortcoming by analyzing a pre-determined matrix of x-y locations that allow the results to be generalized to any likely condition. Figure 8 demonstrates the method used, which exploits the linear superposition principle that stems from the use of linear elasticity as the basic mechanical theory in the response modeling.

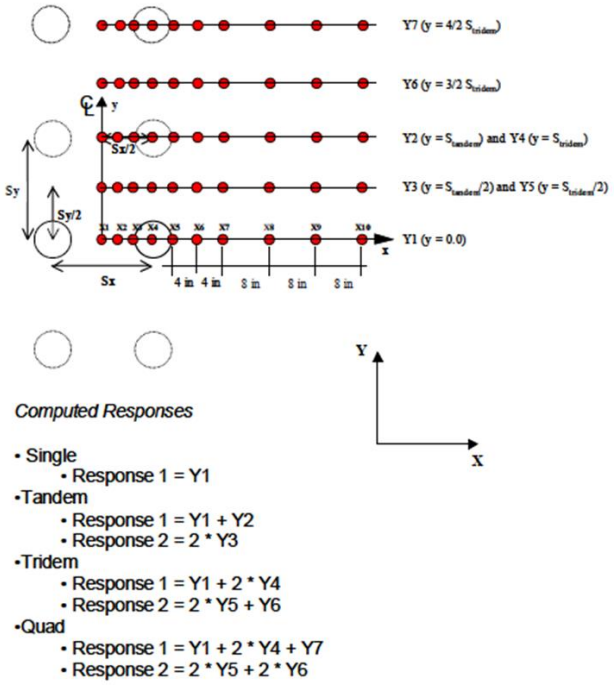

Figure 8: Summary of method used to consider multiple axle configurations in the LEA (ARA 2004).

In addition to coordinates in the x-y plane there are also relevant analysis points at different depths. The depth-wise locations for the response variables are framed with respect to either the fatigue or rutting distresses. In the case of the fatigue cracking phenomenon these depths include the surface of the AC layer, the strain at a depth of 0.5 inches, and at the bottom of the asphalt layer. The first two responses are used to evaluate top-down cracking while the third response is used for the bottom-up cracking prediction. For rutting predictions, the relevant strain response depths include the mid-depth of each structural layer/sub-layer, the top of the subgrade, and six inches below the top of the subgrade.

2.4.2.2 Fatigue Cracking Prediction

Fatigue cracking is predicted based on the cumulative damage concept, e.g., Miner's Law. The damage is calculated as the ratio of predicted number of traffic repetitions to the allowable number of load repetitions (to some failure level) as shown in Equation (1).

$$D = \sum \frac{n_{i,j,k,l,m}}{N_{i,j,k,l,m}} \times 100 \tag{1}$$

Where:

- D = Cumulative damage;
- n = Number of load repetitions for condition indicated by subscript combination;
- N = Number of load repetitions to failure for condition indicated by subscript combination, see Equation (2);
- i = Month;
- j = Quintile;
- k = Axle type;
- l = Axle load; and
- m = Traffic path, assuming a normally distributed lateral wheel wander.

The number of load repetitions to failure is estimated using the classic empirical fatigue relationship given by Equation (2). The form of the model is a function of the tensile strain at the bottom of the asphalt pavement layer as well as the modulus of the asphalt layer. This model form is chosen because it directly links with the pavement response model,

$$N_f = Ck_1 \left(\frac{1}{\varepsilon_t}\right)^{k_2} \left(\frac{1}{E}\right)^{k_3} . \tag{2}$$

Where:

- N_f = Number of repetitions to fatigue cracking;
- ε_t = Tensile strain at the bottom of the asphalt concrete layer (from the pavement response model);
- E = Modulus of the asphalt concrete;
- k_1,k_2,k_3 = Calibrated coefficients (0.007566, 3.9492, and 1.281 respectively); and
- C = Equation (3) with V_a as the air void content and V_b as the asphalt content.

$$C = 10^{4.84\left(\frac{V_b}{V_a+V_b-0.69}\right)} \tag{3}$$

2.4.2.3 Rutting Prediction

To predict the cumulative rutting, the permanent deformation in each of the aforementioned sub-layers is first predicted using the model shown in Equation (4) for asphalt concrete and Equation (8) for aggregate base and subgrade. As seen in these equations, the vertical compressive strain from layered elastic analysis is used to link pavement response and pavement performance modeling for the case of rutting. The predicted permanent deformation is converted to rutting depth using the 1-D approximation shown in Equation (15), essentially taking the definition of strain to estimate that the change in geometry is equal to the product of permanent strain and sub-layer depth. Since the subgrade is treated as an infinitely deep layer this expression will not provide a reasonable answer and so an alternative form, shown in Equation (13) is used to estimate the subgrade rutting.

$$\varepsilon_p = \varepsilon_v \left[k_z 10^{K_1} T^{K_2} N^{K_3} \right] \tag{4}$$

$$k_z = \left(C_1 + C_2 z\right) 0.328196^z \tag{5}$$

$$C_1 = -0.1039 h_{ac}^2 + 2.4868 h_{ac} - 17.342 \tag{6}$$

$$C_2 = -0.0172 h_{ac}^2 - 1.7331 h_{ac} + 27.428 \tag{7}$$

$$\varepsilon_p = \varepsilon_v \left[\left(\frac{\varepsilon_0}{\varepsilon_r} \right) e^{\left(\frac{\rho}{N}\right)^\beta} \right] \beta_{mat} \tag{8}$$

$$\log \beta = -0.61119 - 0.017638 W_c \tag{9}$$

$$\log\left(\frac{\varepsilon_0}{\varepsilon_r} \right) = \frac{\left(0.15 e^{(\rho)^\beta}\right) + \left(20 e^{\left(\rho/10^9\right)^\beta}\right)}{2} \tag{10}$$

$$\rho = 10^9 \left[\frac{-4.89285}{1 - \left(10^9\right)^\beta} \right]^{\frac{1}{\beta}} \tag{11}$$

$$W_c = 51.712 \left[\left(\frac{M_r}{2555} \right)^{\frac{1}{0.64}} \right]^{-0.3586 \times GWT^{0.1192}} \tag{12}$$

Where:

ε_p = Permanent strain
ε_v = Vertical compressive strain at the mid-depth of the given sub-layer (from the pavement response model);
k_z = Equation (14);
T = Temperature at mid-depth of given sub-layer (°F);
N = Number of applied loading cycles;
z = Mid-depth at sub-layer of interest (inch);
h_{ac} = Overall asphalt pavement thickness (inch);
GWT = Depth to water table (feet);
B_{mat} = 1.673 for aggregate base and 1.35 for subgrade; and
M_r = Soil modulus (psi).

$$RD_{SG} = \int_0^{\infty} \varepsilon_p(z)\,dz = \frac{1}{k}\varepsilon_{p,z=0} \tag{13}$$

$$k = \frac{1}{6}\ln\left(\frac{\varepsilon_{p,z=0}}{\varepsilon_{p,z=6}}\right) \tag{14}$$

$$RD_{Total} = \sum_{i=1}^{N_{sublayers}} \varepsilon_p^i h^i + RD_{SG} \tag{15}$$

Where:
RD_{SG} = Subgrade rut depth (inch);
$\varepsilon_{p,z=0}$ = Permanent deformation at the top of the subgrade, from Equation (8);
$\varepsilon_{p,z=6}$ = Permanent deformation six inches below the top of the subgrade, from Equation (8);
RD_{Total} = Total pavement rut depth (inch);
$N_{sublayers}$ = Number of sub-layers;
ε_p^i = Total plastic strain in sub-layer i; and
h^i = Thickness of sub-layer i (inch).

The algorithm used to predict rutting over the pavement lifetime is based upon sequential damage accumulation scheme with the amount of accumulated permanent deformation from a given axle load being dependent upon the complete loading history prior to that axle. The process is briefly summarized in Figure 9.

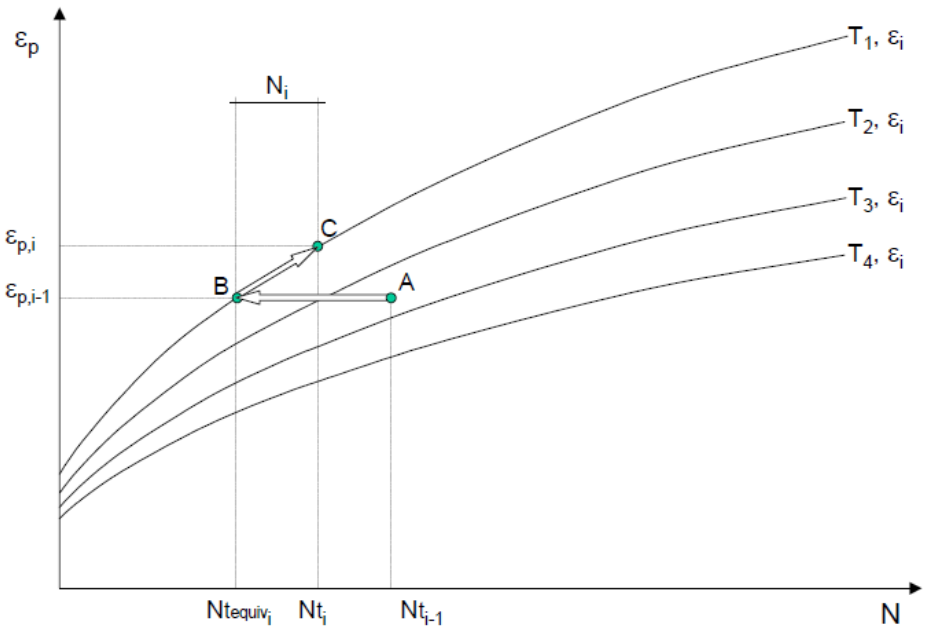

Figure 9: Permanent deformation accumulation.

For the purposes of this figure let $\varepsilon_{p,i-1}$ represent the permanent strain accumulated in one of the sub-layers at the end of sub-season *i*-1 (a sub-season here is a combination of month and quintile). Also, let the curve indicated as T_1 represent the value of the permanent deformation function from Equation (4) at the next sub-season, *i*. Point B is the link between the function that dictated the permanent strain accumulation in sub-season *i*-1 and the one that will control permanent strain accumulation in sub-season i. Points A and B are at an equivalent permanent strain level because the permanent strain between sub-seasons must be continuous. Finally point C represents the additional increment of permanent strain that would accumulate from the initial loading group in sub-season *i*. In reality the process is slightly more involved since both the temperature and the applied load level, indicated by the ε_v term in Equation (4), affect the permanent strain accumulation function. In this case careful attention must be given to the order of loading as well as the sub-season.

2.4.2.4 International Roughness Index

Ride quality is an important measure of functional performance. As shown in Figure 10, it is most often quantified by combining the measured longitudinal pavement profile with a mathematical model that simulates a single wheel on a vehicle, e.g., the International Roughness Index (IRI).

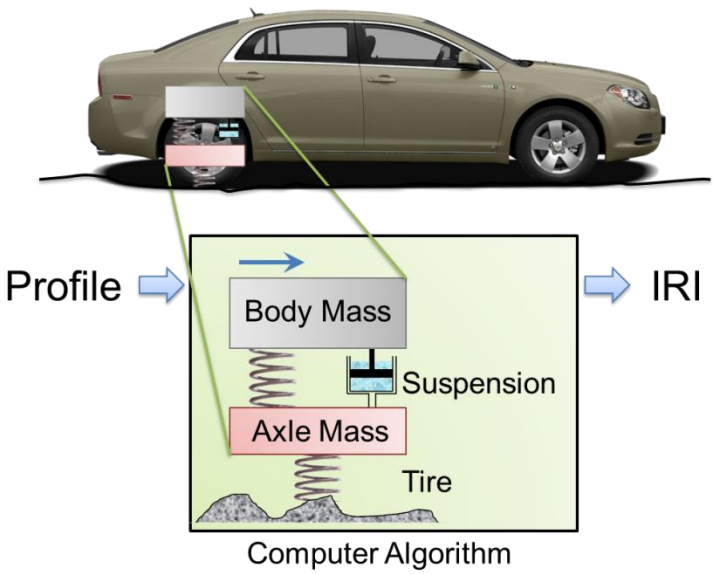

Figure 10: Schematic diagram of IRI parameter.

While the measurement of IRI is fairly straightforward, predicting how it evolves using mechanistic models is not so easy. In the mechanistic-empirical method used for this report, the IRI is estimated over the analysis period by using the distresses (cracking and rutting) predicted from other models. The mathematical model to accomplish this is shown in Equation (16).

$$IRI(t) = IRI_0 + \left(0.4FC + 40RD + 0.008TC + 0.015SF\right) \quad (16)$$

Where:

$IRI(t)$	=	Pavement smoothness at a specific time (inch per mile);
IRI_0	=	Initial smoothness immediately after construction (assumed = 63 in./mi);
FC	=	Total fatigue cracking (% of lane);
RD	=	Total pavement rutting (inch);
TC	=	Total transverse cracking (ft/mi); and
SF	=	Site factor, Equation (17).

$$SF = Age\left[0.02003\left(PI + 1\right) + 0.007947\left(Precip + 1\right)\right] + 0.000636\left(FI + 1\right) \quad (17)$$

Where;

Age	=	Pavement age (year);
PI	=	Plasticity index of the soil (%);
FI	=	Average annual freezing index, (°F days); and
$Precip$	=	Average annual precipitation, (in.).

2.4.2.5 Traffic

For the analysis in this report the initial year traffic volumes, in terms of Average Annual Daily Truck Traffic (AADTT) were obtained from the National Highway Planning Network (FHWA 2015) Traffic was considered using so-called Level 3 analysis, which means that the required input

(other than AADTT and traffic growth rates) were obtained from default values provided in the analysis software. These default values were established from a national level analysis of pavement loadings, and since this analysis was national in scope it was decided that such an approach would provide sufficient accuracy to meet the objectives of this study.

Figure 11 shows the map of current traffic in the form of AADTT values for various sections considered. Traffic input values form the basis of this analysis, as level of traffic carried by the section is the predominant factor in determining the various distresses caused and hence the performance of the structure. As expected, the traffic levels are particularly high along;

- Interstates 5, 10, and 15 around Los Angeles, California,
- Interstates 5 and 90 around Seattle, Washington,
- Interstates 35 and 10 around San Antonio, Texas,
- Interstate 10 through Dallas, Texas,
- Interstates 80 and 90 around Chicago, Illinois,
- Interstates 75 and 94 around Detroit, Michigan, and
- Interstate 95 around Miami, Florida and New York City, New York.

It can also be seen from the map that the traffic level is relatively less in the West-North central region and the northern part of the Mountains region.

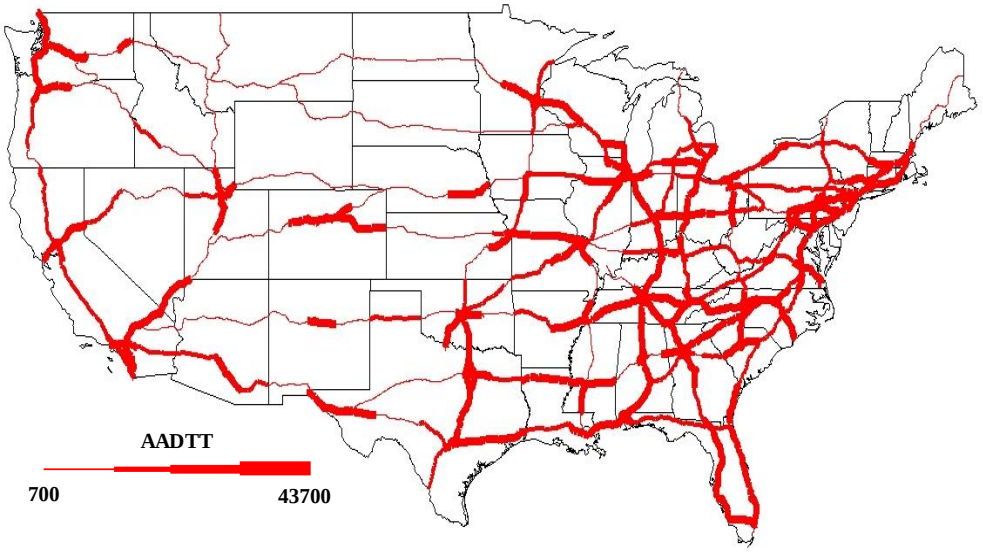

Figure 11: Interstates AADTT map.

Finally, each segment was analyzed with respect to the traffic growth values found from the website of each Department of Transportation. These rates are summarized for each analysis section in Appendix B, but in all cases were applied based on compound growth as shown in Equation (18).

$$AADTT_t = AADTT_{BY}\left(1+GR\right)^t \tag{18}$$

Where:

$AADTT_t$ = AADTT in t years from the base year;

$AADTT_{BY}$ = AADTT in the base year of analysis;
t = Time; and
GR = Growth rate as a percentage.

2.4.2.6 Materials

The key material properties used for pavement analysis are the moduli values of each paving layer. The moduli values relate stress and strain and are necessary to perform the layered elastic analysis, which as discussed below provides the response variables for performance predictions. In the case of the asphalt concrete the relevant modulus is the temperature and frequency dependent dynamic modulus. For the purposes of this analysis the dynamic modulus was estimated using the Witczak predictive model shown in Equation (19).

$$\log|E^*| = -1.249937 + 0.02923\rho_{200} - 0.001767(\rho_{200})^2 - 0.002841\rho_4 - 0.05809V_a - 0.082208\frac{V_{beff}}{V_{beff}+V_a} + \frac{3.871977 - 0.0021\rho_4 + 0.003958\rho_{3/8} - 0.000017(\rho_{3/8})^2 + 0.00547\rho_{3/4}}{1+e^{(-0.603313-0.313351\log f - 0.393532\log\eta)}} \quad (19)$$

Where:

ρ_{200} = Percentage of aggregate passing #200 sieve;
ρ_4 = Percentage of aggregate retained in #4 sieve;
$\rho_{3/8}$ = Percentage of aggregate retained in 3/8 - inch sieve;
$\rho_{3/4}$ = Percentage of aggregate retained in ¾ - inch sieve;
V_a = Percentage of air voids (by volume of mix);
V_{beff} = Percentage of effective asphalt content (by volume of mix);
f = Loading frequency (Hz); and
η = Binder viscosity at temperature of interest (10^6 P).

As shown in this equation the relevant material properties include gradation parameters, binder viscosity, and volumetric properties. The asphalt cement viscosity was estimated from the correlation between viscosity and specification grade of the asphalt binder. The required specification grade of the asphalt used in the pavement was obtained from either the state department of transportation or from the known climatic conditions at the site.

For unbound layers the elastic modulus at the optimum moisture content is first entered and then adjusted internally for the effects of moisture content changes over time. For sections with an aggregate base layer, the initial elastic modulus and Poisson's ratio were taken from the default model inputs for crushed stone as 30,000 psi and 0.35 respectively. In the case of the subgrade a two-step process was adopted. First, the extensive mapping effort completed under the NCHRP 9-23B project was used to determine the representative AASHTO classification for each analysis segment. The soils are denoted as A1, A2, A3, A4, A5, A6, or A7. These data which were earlier collected for the segmentation process was used here as the subgrade input for the MEPDG analysis. In the Level 3 analysis of MEPDG, the data required in the case of subgrade are the modulus, Poisson's ratio, and the coefficient of lateral pressure, k_o. The modulus values were taken to be the default MEPDG values for the corresponding AASHTO class of the soil (see Table 5),

the Poisson's ratio was taken as 0.35, and k_o was taken as 0.5. Other required material parameters included the thermal conductivity and heat capacity of the asphalt as well as the gradation, soil water characteristic curve parameters, and Atterberg limits of the unbound layers. The pre-programmed default values were used for all of these parameters.

Table 5: Soil Resilient Modulus Values Entered for Analysis.

Material Classification	M_r (psi)	Material Classification	M_r (psi)	Material Classification	M_r (psi)
A-1-a	29,500	A-2-6	20,500	A-5	15,500
A-1-b	26,500	A-2-7	16,500	A-6	14,500
A-2-4	21,500	A-3	24,500	A-7-5	13,000
A-2-5	21,000	A-4	16,500	A-7-6	11,500

2.4.2.7 Structure

The pavement structure is another major input factor. This input requires knowledge of the thickness and layer types used on each interstate. These details were obtained through direct communication and internet surveys of each of the applicable state departments of transportation. In some cases, structure details were unavailable and so they were assumed based on the structures from the adjacent and/or close by states. For example, the pavement structure details of the state of Virginia have been assumed from the structure details of North Carolina.

2.4.2.8 Climate

The local climate affects the material properties by dictating both the pavement temperature and the sub-surface moisture conditions. The relevant parameters include hourly temperature, daily precipitation, average amount of sunshine, wind speed, and latitude and longitude. As demonstrated schematically in Figure 12 each of these variables make contributions to heat and moisture flow in the pavement system. For example, the wind speed contributes to the convection process. As shown in Figure 13 the weather stations used to collect these data were distributed across the United States and provided pre-formatted files that contained a minimum of five years historical data. For each pavement section the weather stations closest to the project were selected. In the case of sections without a close weather station, the closest available stations were chosen, and the data interpolated to represent the climate along the entire section length. This approach was deemed acceptable based on the fact that climate was a determining factor in the segmentation process.

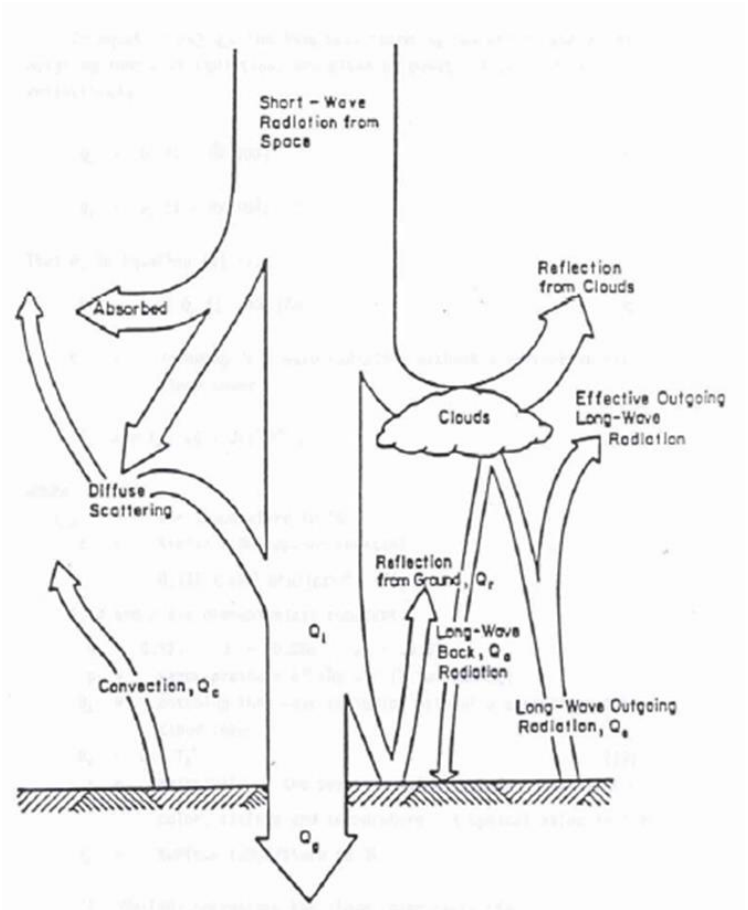

Figure 12: Relevant energy movements in process of heat transfer in pavement system (Lytton et al. 1990).

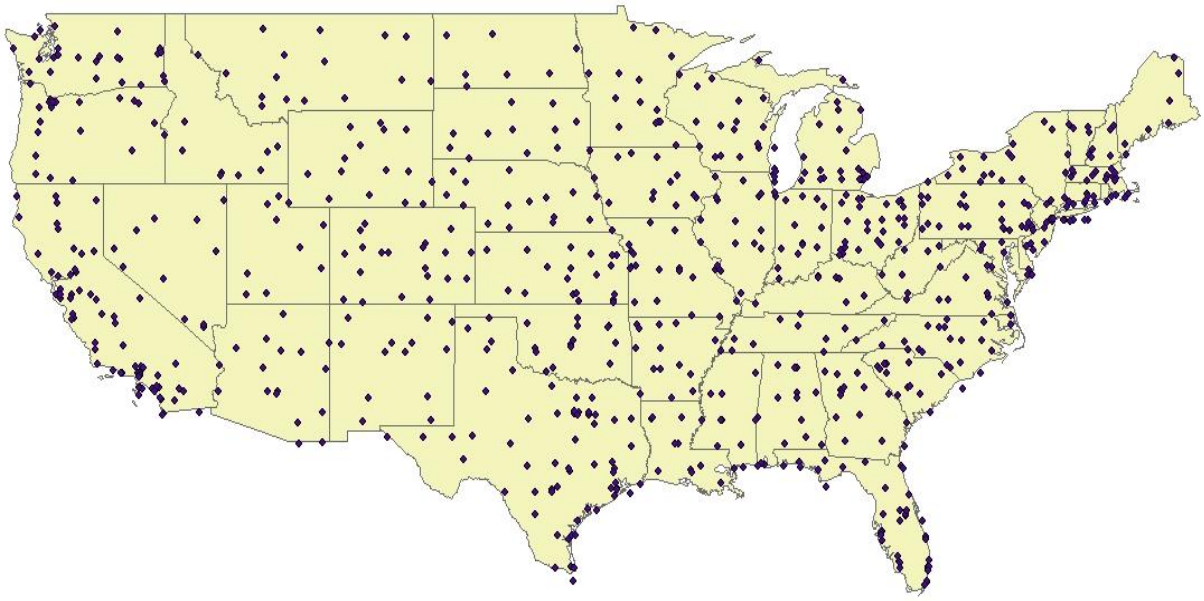

Figure 13: Weather stations across the US.

The future climate projections included daily maximum and minimum temperatures and monthly precipitation geospatially arranged in 12 km square blocks for the years 2006-2100. A MATLAB script was developed to automate the data extraction for only the years 2040-2060 and to perform geospatial interpolation for the block that was closest to the relevant weather station. Once the daily maximum and minimum temperature and monthly precipitation were extracted, the historical weather data was then obtained from the climate databases held in the AASHTOWare Pavement ME software. Since this analysis requires hourly temperature and precipitation data, and not just daily maximums and minimums or monthly averages, additional processing is needed.

The Modified Imposed Offset Morphing Method (M-IOMM) was adopted (Belcher et al. 2005, Sailor 2014) to create the future projected hourly data. The standard IOMM method shifts and stretches given hourly temperature data based on the predicted monthly mean temperature. In this study, since projected daily maximum and minimum temperature values are available the IOMM was modified. Historical data was first extracted and from this data the 20 years of daily temperature variation was obtained. To create the hourly climate data file for the future cases from this data the following procedure was used for each pavement section and for each of the 16 future cases in this study.

1. Daily minimum and maximum temperatures (T_{BMin} and T_{BMax}) were extracted from the historic climate database for each day of the 20 Year record.
2. Daily minimum and maximum temperatures (T_{FMin} and T_{FMax}) were extracted from the given projected climate data for each day of the 20 Year record (2040-2060).
3. The difference between the daily maximum and minimum temperatures for each day of the 20 years was calculated for both the historic climate data (T_{BMax}- T_{BMin}) and the predicted climate data (T_{FMax} - T_{FMin}).
4. Predicted hourly temperature (T_{iF}) was calculated using the hourly distribution of historic temperature (T_{iB}) and predicted maximum and minimum temperature, with Equation (20)

$$T_{iF} = \frac{(T_{FMax} - T_{FMin})}{(T_{BMax} - T_{BMin})} \times (T_{iB} - T_{BMin}) + T_{FMin} \quad (20)$$

For the cases where only temperature projections were considered the remaining climate input parameters (Wind Speed, Percent Sunshine, Precipitation and Relative Humidity) were taken from the historic climate files. For this analysis an average temperature history from an ensemble of 19 different climate models at Representative Concentration Pathway (RCP) 8.5 and RCP 4.5 were used for analysis. The current day temperature histories were used as the baseline. The period considered was mid-century, 2040-2060.

2.4.2.9 Output

The results from the mechanistic-empirical analysis are summarized in an output file that lists the average predicted distresses along with the reliability estimate of these distresses. An example output summary from the analysis of segment I94-MT-2 is shown in the table and figures below.

Table 6: Distress Output Summary.

Distress	Distress Predicted	Reliability Predicted
Terminal IRI (in/mi)	119.2	94.81
Alligator Cracking (%)	0.2	99.99
Permanent Deformation (in)	0.46	99.95

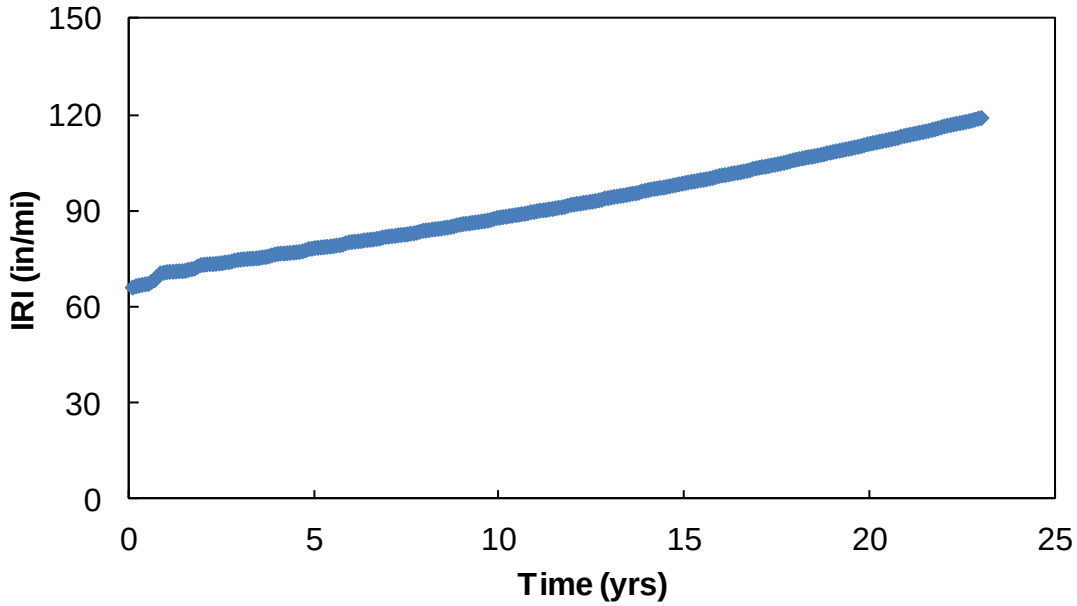

Figure 14: Example IRI results from MEPDG analysis.

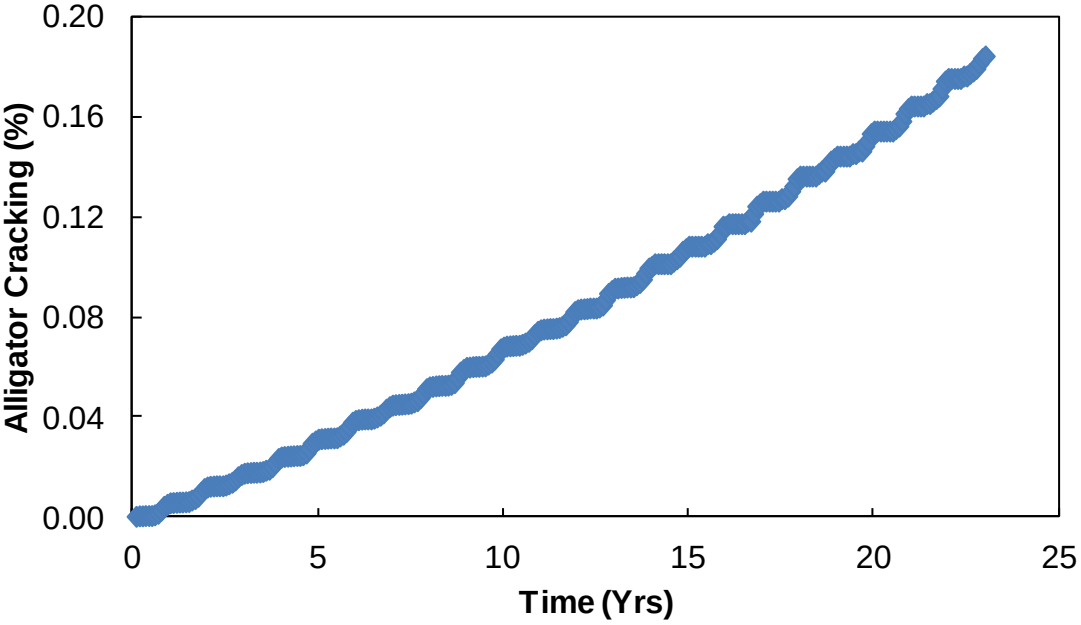

Figure 15: Example alligator cracking results from MEPDG analysis.

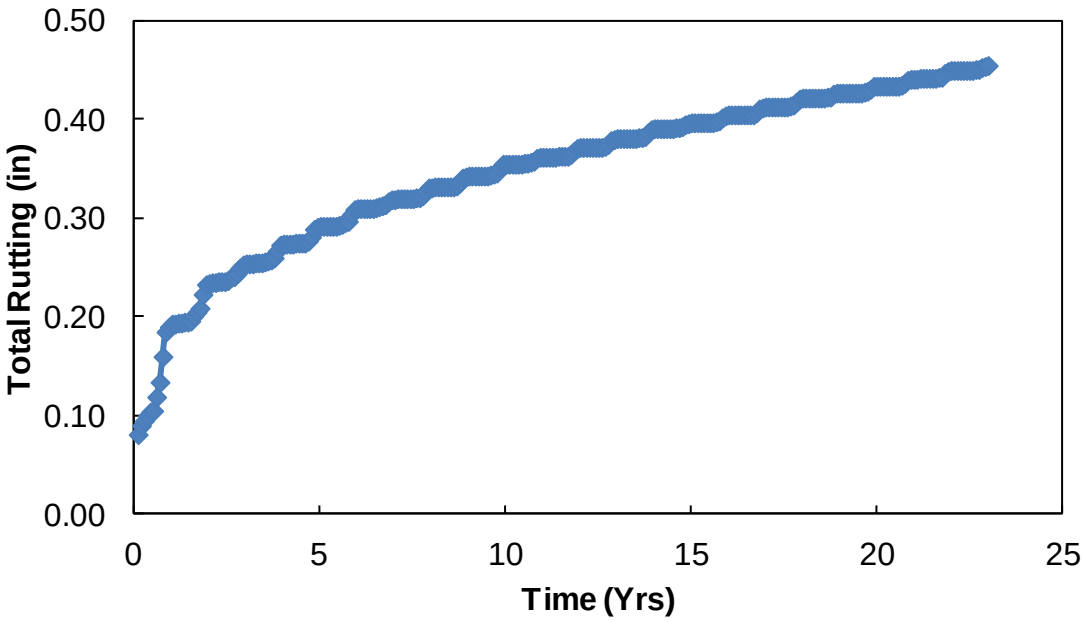

Figure 16: Example rutting results from MEPDG analysis.

2.5 RESULTS

The results from the Pavement Design ME analysis is shown in Figure 17 (fatigue cracking, Figure 18 (asphalt concrete only rutting), Figure 19 (total pavement rutting), and Figure 20 (IRI). The analysis shows that under the prescribed average model ensemble that the rutting distress is more vulnerable to changes compared to fatigue cracking. As expected this effect is greater under RCP 8.5 than it is under RCP 4.5. Although the number of sites available is limited, the effect in terms of percentage change is observed to be greater in in wet freeze and dry freeze locations (may not be absolute value but percentage change is much higher in these locations). With respect to fatigue cracking most of the freeway sections show an increase in fatigue cracking due to the projected temperature changes. Although not shown here, the percentage increase is observed to be greater in earlier years compared to end of the pavement life (20 years). So, while the ultimate amount of cracking at the end of the pavement life may not be as large as the rutting, the rate of accumulation is faster, possibly suggesting that early/more frequent maintenance activates may be triggered for the pavement sections. Interestingly, the fatigue cracking is also observed to be more in wet no freeze locations (VA, NC, TX, etc.) compared to other locations. Finally, the predicted change of IRI values is not as substantial as what occurs in the other distresses. The effect that is observed is greater in both dry and wet non-freeze regions compared to other regions.

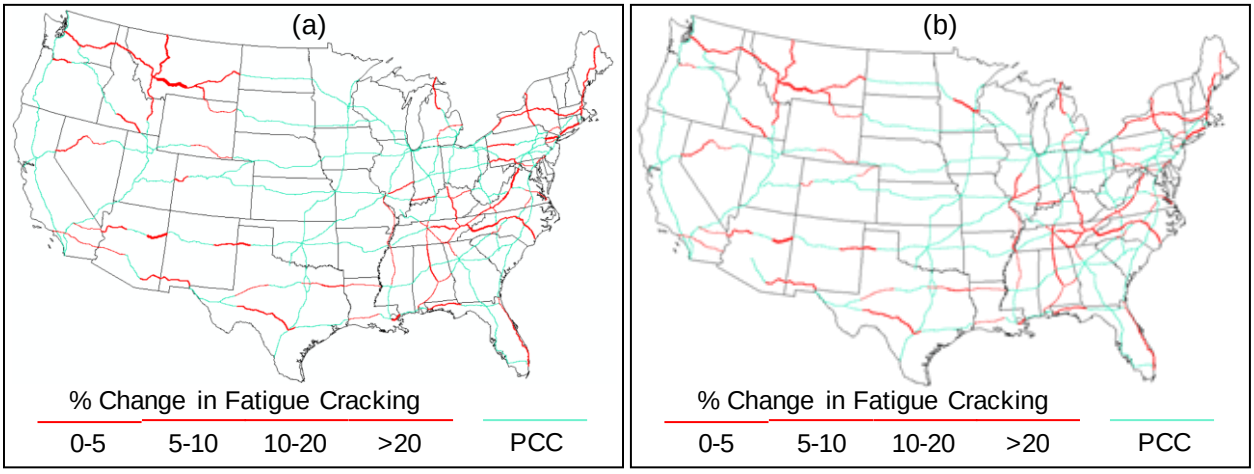

Figure 17: Impacts from projected temperature values on fatigue cracking for; (a) RCP 8.5 scenario and (b) RCP 4.5 scenario.

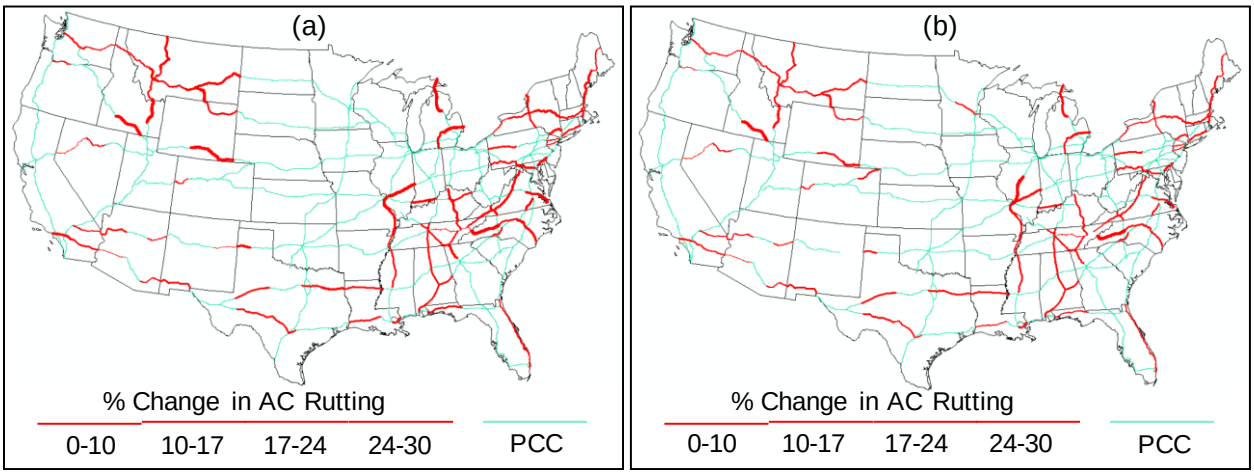

Figure 18: Impacts from projected temperature values on asphalt concrete rutting for; (a) RCP 8.5 scenario and (b) RCP 4.5 scenario.

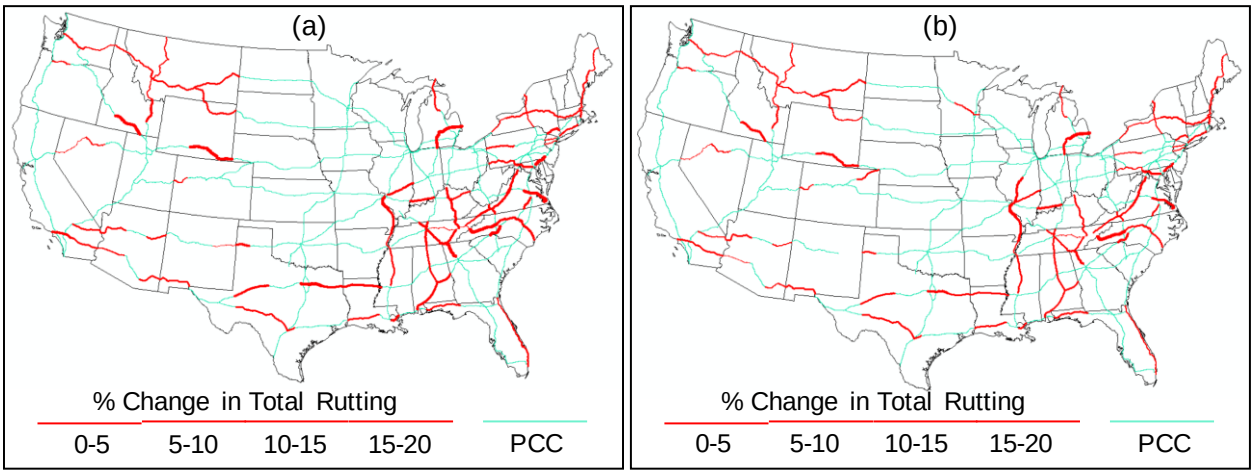

Figure 19: Impacts from projected temperature values on total pavement rutting for; (a) RCP 8.5 scenario and (b) RCP 4.5 scenario.

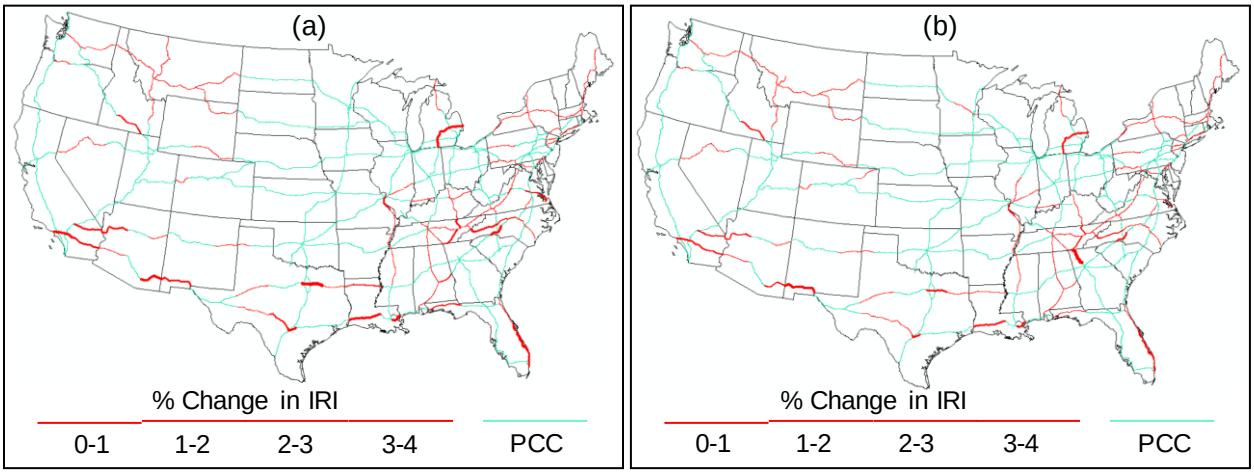

Figure 20: Impacts from projected temerature values on IRI for; (a) RCP 8.5 scenario and (b) RCP 4.5 scenario.

3.0 STUDY 2: EVALUATION OF CLIMATE FACTORS RELATED TO PAVEMENT PERFORMANCE

3.1 INTRODUCTION

The primary objective of study two is to predict the performance of freeway sections in different climate regions across the United States and for different climate models and in so doing address the gaps in the literature. Then, using these results in conjunction with performance predicted using historical climate data, quantify the impact of incorporating projected climate data.

3.2 METHODOLOGY

The overall approach followed in this study is shown in Figure 21. As seen in this figure the methodology involves conducting multiple pavement performance predictions using the, AASHTOWare Pavement ME software, to predict and compare the long-term behaviors of pavements under either historical or projected climate scenarios. Simulations using the historical database are referred to as the baseline cases, while those using the climate model data are referred to as the future cases. As detailed below, these future cases include representative concentration pathways (RCPs) 8.5 and 4.5 and multiple sections of real in-service pavements. In total sixteen different future climate cases are considered;

- Average of 19 models at RCP8.5 with temperature and with temperature + precipitation,
- Average of 19 models at RCP4.5 with temperature and with temperature + precipitation,
- MIROC-ESM at RCP8.5 and RCP4.5 with temperature and with temperature + precipitation,
- CCSM4 at RCP8.5 and RCP4.5 with temperature and with temperature + precipitation, and
- MRI-CGCM3 at RCP8.5 and RCP4.5 with temperature and with temperature + precipitation.

Performance projections for the baseline and each of the sixteen future cases were carried out using five different interstate locations; I-10 in Arizona (I10-AZ), I-90 in Montana (I90-MT), I-95 in Maine (I95-ME), I-64 in Virginia (I64-VA), and I-65 in Indiana (I65-IN). These locations have been chosen to represent different climate regions and because the respective states have calibrated the AASHTOWare Pavement ME models for their state/region. The analysis period in each simulation was 20 years in deference to standard practice.

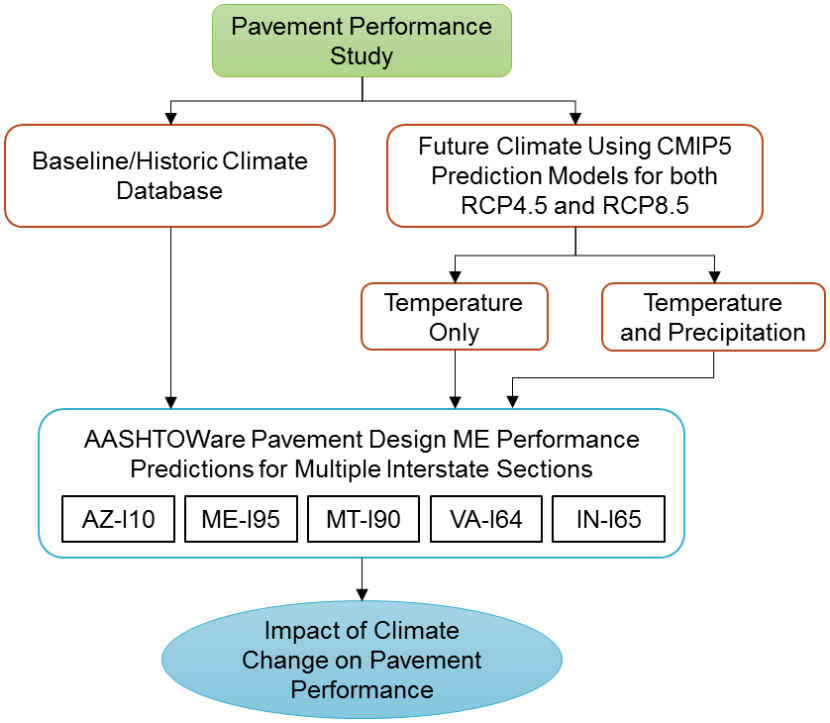

Figure 21: Framework for assessing the impact of climate change on the pavement performance.

The present (baseline) scenario was evaluated by using the climate files that exist within the Pavement ME software. Future scenarios are evaluated using the average of a multi-model ensemble of 19 different 12 km downscaled Global Climate Models (GCMs) as well as three of the individual models from this ensemble (Brekke et al. 2013). Table 7 shows 19 models used for ensemble climate projections in this study. The models chosen participated in the CMIP5 project and had both RCP8.5 and RCP4.5 downscaled data. During the Coupled Model Intercomparison Project Phase 5 (CMIP5), the IPCC established RCPs approach to consider future climate change in terms of policy decisions (IPCC 2007). The RCPs are four greenhouse gas concentration trajectories, but the two most often used are; 1) RCP8.5, which corresponds to a high greenhouse emissions pathway and is the upper limit of all RCPs (Riahi et al. 2011) and 2) RCP4.5, which is a scenario that assumes radiative forcing stabilizes by 2100 (Thomson et al. 2011). These two scenarios are chosen to encompass ranges of likely future scenarios where RCP8.5 assumes essentially no abatement of emissions and RCP 4.5 assumes intervention policies that result in greenhouse gas emissions reducing near mid-century. Many climate scientists agree that pathways below 4.5 are now unlikely (Knutti and Seldacek 2013, Schleussner et al. 2014, Makin et al. 2015) and so RCP4.5 serves as a lower bound estimate of climate change outcomes while RCP8.5 serves as an upper bound estimate.

Table 7: Climate Prediction Models Considered for Extracting Temperature and Precipitation Data from CMIP5 Database.

Modeling Center (or Group)	Institute ID	Model Name
Commonwealth Scientific and Industrial Research Organization (CSIRO) and Bureau of Meteorology (BOM), Australia	CSIRO-BOM	ACCESS1.0
Beijing Climate Center, China Meteorological Administration	BCC	BCC-CSM1.1
Canadian Centre for Climate Modeling and Analysis	CCCMA	CanESM2
National Center for Atmospheric Research	NCAR	CCSM4
Community Earth System Model Contributors	NSF-DOE-NCAR	CESM1(BGC)
Centre National de Recherches Météorologiques / Centre Européen de Recherche et Formation Avancée en Calcul Scientifique	CNRM-CERFACS	CNRM-CM5
Commonwealth Scientific and Industrial Research Organization in collaboration with Queensland Climate Change Centre of Excellence	CSIRO-QCCCE	CSIRO-Mk3.6.0
NOAA Geophysical Fluid Dynamics Laboratory	NOAA GFDL	GFDL-ESM2G GFDL-ESM2M
Institute for Numerical Mathematics	INM	INM-CM4
Institute Pierre-Simon Laplace	IPSL	IPSL-CM5A-LR IPSL-CM5A-MR
Japan Agency for Marine-Earth Science and Technology, Atmosphere and Ocean Research Institute, and National Institute for Environmental Studies	MIROC	MIROC-ESM MIROC-ESM-CHEM MIROC5
Max Planck Institute for Meteorology	MPI-M	MPI-ESM-LR MPI-ESM-MR
Meteorological Research Institute	MRI	MRI-CGCM3
Norwegian Climate Centre	NCC	NORESM1-ME

For each model, the daily maximum and minimum temperatures and average monthly precipitation data were extracted. Climate files for each model were downloaded from the Climate Analytics website. There, downscaling of temperatures were performed per the daily bias-correction and constructed (BCCA) analogs method (Brekke et al. 2013), while precipitation data was downscaled per the Bias-Correction Spatial Disaggregation (BCSD) method (Maurer et al. 2007). Although projections are available spanning the period from current day through 2100 only the period from 2040 through 2060 was considered in this study to evaluate the impact of climate change in future for a span of approximate pavement design life. This timeframe was chosen to estimate the mid-century impacts and encompass a period of time where impacts (if they existed) would be evident. Also, beyond mid-century, the uncertainty inherent in the GCMs becomes very large and therefore meaningful conclusions become more difficult to attain. The data itself was downloaded from the archives of the Climate Analytics Group (Brekke et al. 2013). The three models chosen for individual predictions were MIROC-ESM, CCSM4, MRI-CGCM3. These three models were chosen for specific reasons. The first was that they fell into different clusters of GCMs based on their simulation fields as defined by Knutti et al. (2013). The second was that after study of individual model predictions in several different geographical locations, these three models were found to approximate high-temperature, median-temperature, and low-temperature growth

scenarios. This finding generally agreed with those from others as well (Adaptwest 2016). It may be argued that these models do not accurately reflect North American conditions, since for example the MRI model originates in Japan. However, here the approach suggested by climatologists and articulated by Knutti et al. (2013) is adopted wherein each individual model is itself a representative sample of a future scenario given uncertainties and limitations in observations, imprecise or imperfect understanding of all individual and interactive physical mechanisms, and limited computational resources. As such the ensemble, itself (inclusive of all models), serves as the first order approximation of future uncertainty and any individual model that aligns at one end or the other of the ensemble can be extracted to bracket the outcomes.

3.3 PERFORMANCE PREDICTION PROCESS IN AASHTOWARE PAVEMENT ME SOFTWARE

In this study AASHTOWare Pavement ME software (described in Section 2.4.2) is the primary analysis tool to assess the impacts of climate on pavement performance. This study uses the AASHTOWare Pavement ME software due to its relatively widespread usage, its national scope at the development phase, and because calibration factors are available for many different-locations. The outputs of interest for flexible pavement analysis are the fatigue cracking and rutting, while transverse cracking and faulting are the primary distresses for rigid pavements. Traffic levels for these sections were estimated from National Highway Planning Network (NHPN) database (NHPN 2015).

Table 8: Pavement Design ME Input Parameters used for the Interstate Flexible Pavement Sections.

Input Type	Variable	AZ _I10	ME_I95	MT_I90	VA_I64	IN_I65
Traffic	AADTT[1]	7089	4860	2543	17750	11800
	Lanes	2	2	2	2	2
	Speed (mph)	75	75	65	70	70
Climate	Elevation (m)	455	15	1350	190	240
	Location	Phoenix, AZ	Portland, ME	Bozeman, MT	Charlottesville, VA	Indianapolis, IN
Layer 1- AC	Thickness (cm)	35.3	23.6	19.8	21.6	25.4
	Density (kg/m^3)	2370	2370	2370	2370	2370
	P_{be} (%)[2]	4.6	5	4.5	5.8	5
	Va (%)[3]	5.3	5	4.9	5.6	7
	Asphalt	AC 40	AC 20	PG70-28	AC 20	AC 20
Layer 2- Aggregate Base	Thickness (cm)	15.2	83.8	83.8	13	11.7
	Modulus (MPa)	210	210	210	210	210
Subgrade	Modulus (MPa)	115	115	80	80	90

[1]AADTT = Two way annual average daily truck traffic, [2]P_{be} = Effective asphalt cement content by mass, [3]V_a = Air void content

Soil data was obtained from the NCHRP 9-23b database (Witczak et al. 2006), and other relevant inputs were taken from state agencies. With respect to climate, the software uses hourly air temperature, wind speed, percent sunshine, precipitation, and relative humidity for analysis purposes. These data are stored in climate files that are read by the software at the time of analysis. These climate files generally contain five to ten years of climate data beginning around the mid

1990's. For analysis, the climate data is assumed to remain stationary throughout the entire design life and thus when analysis period exceed the extent of the climate record, the software simply reuses the same climate data repeatedly. Finally, it is noted that for the sites chosen, the performance models had been calibrated to the local/regional conditions. Studies have shown that there is a large difference in the damage prediction from between real pavements and predicted pavements when only the national calibration factors are used (Banerjee et al. 2009, Banerjee et al. 2010). The relevant details of these sections are shown in Table 8.

It should be mentioned here, that while the Pavement ME software explicitly considers the interactive factors that affect pavement performance, scientific proof that this method provides the most accurate estimation of pavement performance does not exist. In fact, there is a strong argument that can be for empirical models, like the ones used by Chinowsky and Arndt (2012) and Schweikert et al. (2014) that have been calibrated on large sets of data. Often the statistical rigor with which these methods assess performance exceeds that of mechanistic-empirical models (Banerjee et al. 2009, 2010). Thus, while it is the authors' opinion that the ME model provides a more accurate assessment of climatological changes on pavement since it explicitly separates material selection and climate (empirical models most often implicitly group material decisions and climate together), this belief is not rigorously confirmed.

3.4 PROCESSING CLIMATE PROJECTIONS

Climate data was processed in the same way as that described in Section 2.4.2.8 using the IOMM. For some cases in this study precipitation projections were also included into the climate file. To create hourly precipitation data, the IOMM approach was adopted by combining the hourly precipitation data from the historical record with the monthly average precipitation rate from the future cases. The following step-by-step procedure was adopted.

1. Cumulative monthly rainfall for the baseline case was extracted and used to calculate an average daily precipitation rate for the respective month.
2. Average daily precipitation of each month (R_{BMAvg}) was calculated from the historic climate data base.
3. Average daily precipitation of each month (R_{FMAvg}) was extracted from the given climate projection.
4. The hourly rainfall for future (R_{iF}) was calculated using the Equation (21).

$$R_{iF} = \left(\frac{(R_{FMAvg} - R_{BMAvg})}{R_{BMAvg}} \times R_{iB} \right) + R_{iB} \tag{21}$$

The hourly precipitation data calculated for future years from the above procedure was then input to the temperature modified climate database along with other climate input parameters (Wind Speed, Percent Sunshine, and Relative Humidity) to create a future case climate files. It should be noted that this analysis does not consider certain climate stressors that may affect pavement performance and these are acknowledged. For example, depth to water table changes due to sea level rise (Knott 2017), soil expansion/contraction due to both long-term and short-term water variations (Lytton 1994), and extremes in daily temperature variation are not explicitly considered within the analysis framework.

3.5 PAVEMENT PERFORMANCE STUDY ANALYSIS AND RESULTS

3.5.1 Impact on Flexible Pavements

Typical results from the AASHTOWare Pavement ME D simulation process are shown for the Arizona site and for the baseline and RCP8.5 future cases in Figure 22. The results are compiled for the three distresses of fatigue cracking, rutting in the asphalt concrete (AC) layer only, and total rutting for the entire pavement cross-section. From this figure, it is observed that irrespective of the predictive model, the distresses observed in the pavements are increasing when compared to the baseline. Although it is not shown here, similar observations are made from the other locations and for RCP4.5 cases as well.

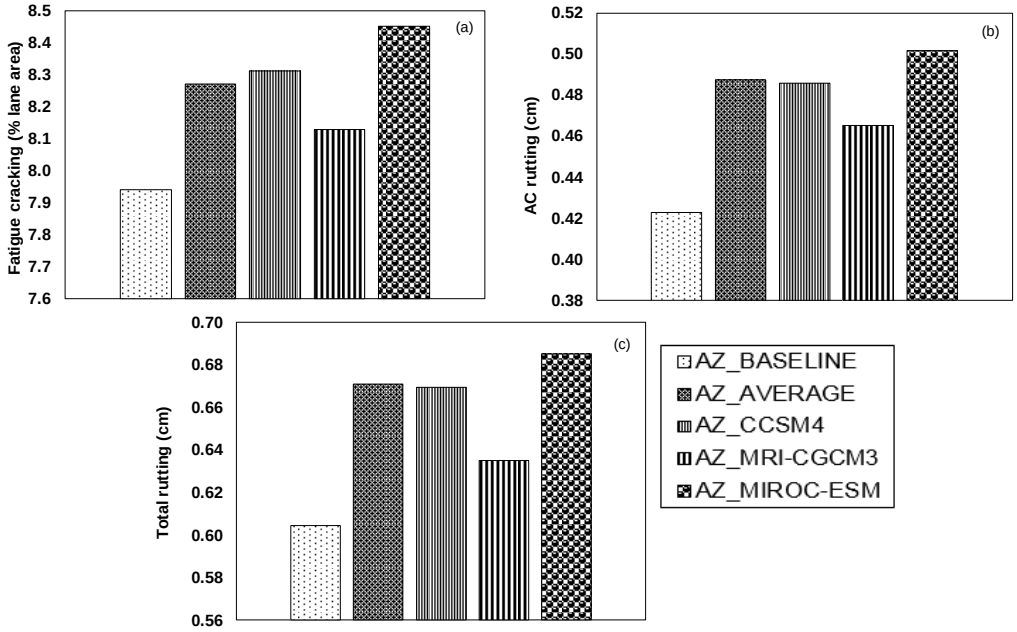

Figure 22: Pavement distress comparison across baseline and future climate prediction models for AZ section (a) Fatigue cracking, (b) AC layer rutting and (c) Total rutting.

To compare each case more effectively a percent difference increase function (*DI*), Equation (22) is defined.

$$DI = \frac{(Future\ scenario\ pavement\ Distress - Baseline\ scenario\ pavement\ distress)}{(Baseline\ scenario\ pavement\ distress)} \times 100 \qquad (22)$$

Using this definition for the data in Figure 22, the predicted impact of the climate projections is a 2-7% increase in the fatigue cracking, an 8-20% increase in the AC only rutting, and a 5-25% increase in total rutting at the end of the 20-year analysis period depending upon the model considered. The data in Figure 22 shows that there is considerable uncertainty in the range of predicted effects from temperature change. Thus, it is necessary to consider the impacts of climate change stochastically. Pavement performance results obtained after using different climate projections for both RCP4.5 and RCP8.5 are shown in the form of Box-and-Whisker plots. Climatologists are clear to not assign individual probabilities to the RCP scenarios and thereby consider them all as equally likely outcomes depending on technology as well as government and

individual choices. Thus, in this study the results obtained from both scenarios are grouped together in order to estimate the certainty or uncertainty in climate projection impacts. The Box-and-Whisker plots are used to demonstrate this uncertainty. The box is bounded by the first (25^{th} percentile of the results) and third (75^{th} percentile of the results) quartiles of the projections while the median is shown as a horizontal line in the interior of the box. The maximum and minimum values are shown as the error bars extending vertically from the box.

Figure 23 shows the variation of pavement performance in terms of percentage difference in fatigue cracking, AC rutting and total rutting across the five pavement sections considered in this study for the case where only temperature is adjusted. The first notable observation is that in the case of fatigue cracking, the Montana section (MT) shows very high difference relative to the other sections. However, after careful study it was observed that in the case of MT the fatigue cracking at the end of design life in the baseline scenario is very low (4.5%), which magnifies the true difference. In the most extreme model prediction this fatigue cracking increases to 7.3%, which is still considered a relatively small amount of fatigue cracking. To confirm this observation, the section was analyzed again by changing the pavement thickness so that at the end of the design life the pavement experienced more fatigue crackling in the baseline case. In this case, it is in fact found that the percentage increase in fatigue cracking from the climate models is in line with the rest of the sections. To be able clearly see the percentage increase in fatigue cracking, the rest of the four sections are plotted separately and shown in Figure 23 (c). In the case of AC rutting and Total rutting, the percentage increase in distress is more stable across all climate locations with fatigue cracking increase ranging from 2-11%, AC layer rutting from 9-45% and total rutting from 5-34% depending on the prediction model and climate location.

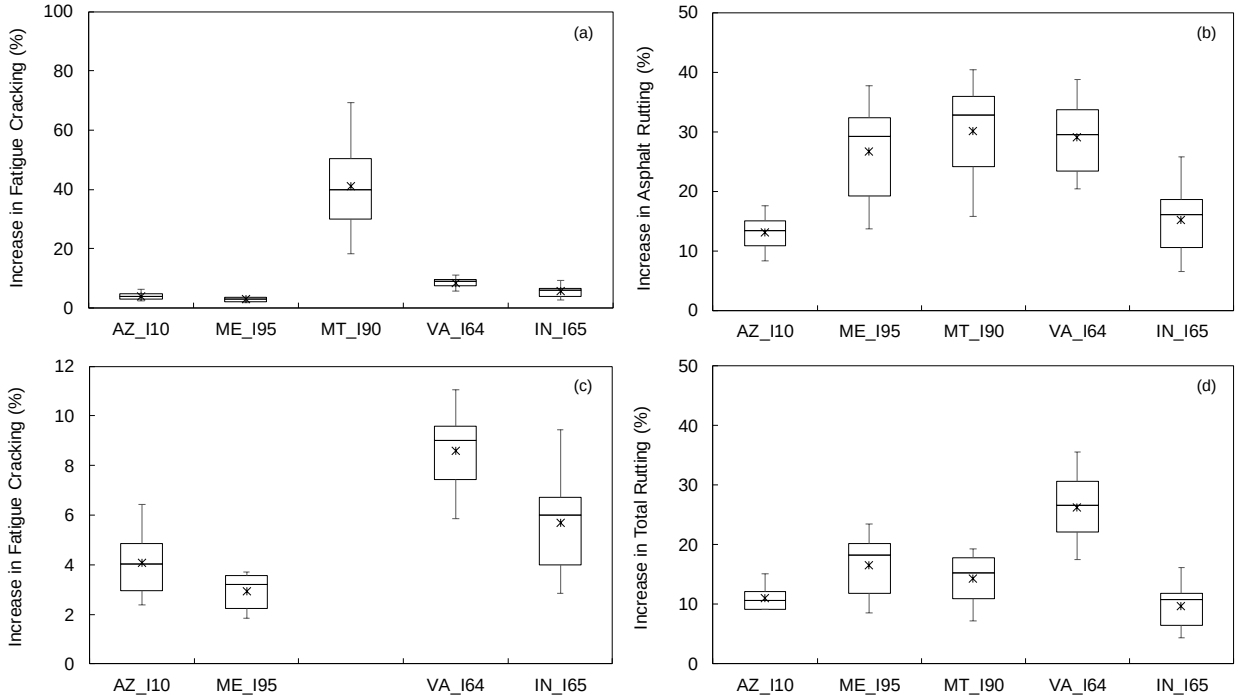

Figure 23: Variation of percentage difference across climate prediction models for study locations using only temperature data from predictions for; (a) fatigue cracking, (b) AC layer rutting, (c) fatigue cracking (for 4 locations), and (d) total rutting.

One important observation made from the results is that the percentage increase in rutting is more when compared to fatigue cracking, which is intuitive as rutting is largely a top of the pavement phenomenon where pavement temperatures due to climate change are expected to be the greatest. Conversely, fatigue cracking (as it is considered in the analysis model) is largely a bottom-up phenomenon where the thermal mass of the pavement structure provides some additional protection against future warming. In addition to percentage increase the figure also shows that the variation of percentage increase (difference between first and third quartiles) in both fatigue cracking and rutting varies across the different climate zones. All locations are showing substantial variation in the results however this variation is observed to be much more for Montana and Virginia as percentage increase in the distresses due to climate change is also high in these regions.

It is found that the impact of temperature changes can be approximated, at a first order level, by observing changes in the mean annual air temperature. For rutting the changes in performance showed greater correlation to the percentage change in mean annual air temperature (*N-MAAT*), Equation (23), than the direct change in temperature, Equation (24).

$$P-MAAT = \frac{\left(MAAT_{Future\ Scenario} - MAAT_{\text{Baseline } Scenario}\right)}{\left(MAAT_{\text{Baseline } Scenario}\right)} \times 100 \tag{23}$$

$$D-MAAT = \left(MAAT_{Future\ Scenario} - MAAT_{\text{Baseline } Scenario}\right) \tag{24}$$

where; *MAAT* = mean annual air temperature, *P-MAAT* = percentage change in *MAAT*, *D-MAAT* = change in *MAAT*, $MAAT_{Future\ Scenario}$ = the *MAAT* from a given climate model, $MAAT_{Baseline\ Scenario}$ = the *MAAT* for the baseline scenario. It is recognized that other climate factors may exist which provide similar or even better correlations. Mallick et al. (2017), for example, adopted the maximum air temperature and its rate of change over time. However, here, only these two climate factors are considered as discussed below.

Figure 24(a) shows how the predicted asphalt concrete layer rutting increases (as a percentage of the rutting predicted in the baseline scenarios) as a function of *N-MAAT*. The use of this climatic parameter suggests that with rutting it is the increase in temperature relative to the current temperature that will be most likely to cause detrimental performance. It is suspected that type of correlation exists because the materials are already engineered differently in locations with high-temperatures (e.g., the use of mixtures with larger stone and more stone-on-stone contact in Arizona). While material properties are an explicit input to the pavement analysis tool, not all factors are considered and local calibrations implicitly embed many of these differences into the prediction algorithm. Overall the correlation is high ($R^2 = 0.88$), but there is scatter, which can be attributed to differences in latitude (e.g., angle of incidence with short-wave radiation) and the fact that the correlation variable is a simple function of the annual air temperature change (recall this function is only expected to represent the first order approximation of performance correlation).

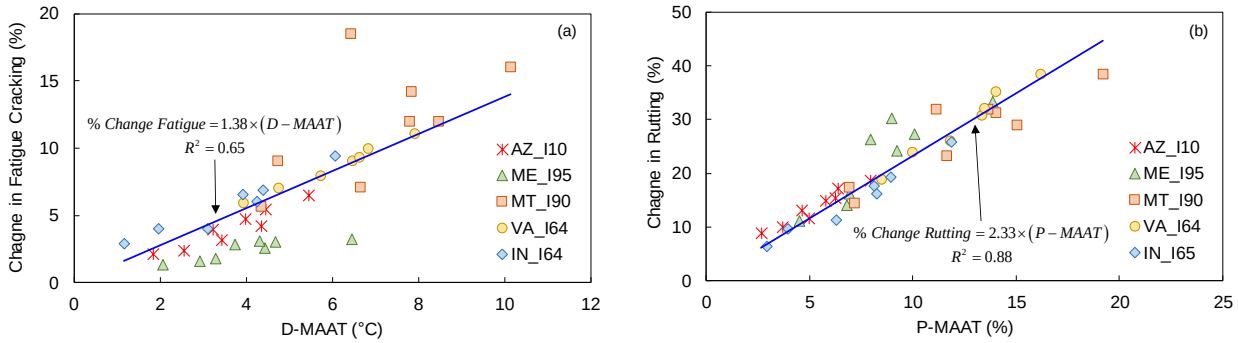

Figure 24: Correlation between change in pavement performance and climate indicators; (a) rutting and N-MAAT and (b) fatigue cracking and D-MAAT.

With fatigue, the greatest correlation was found between the change in predicted cracking and *D-MAAT*, Figure 24(b). This correlation may be a consequence of the fact that fatigue cracking correlations are more difficult to establish during local calibration and many agencies have relied on national calibration with or without some small adjustments. The lower correlation is also expected in the case of fatigue cracking because of the interactive relationship between cracking, structural configuration, and the level of anticipated pavement. Indeed, it is seen that the Maine simulations deviate from the correlation systematically and this may be attributed to the fact that the Maine pavement is very thick (total structural pavement thickness of 107.4 cm, but carries relatively little traffic. This discrepancy suggests that overdesign of a pavement structure under certain climatic conditions serves as one mitigating strategy against climate change influences on fatigue cracking, but less so with respect to asphalt concrete layer rutting. The Montana pavement, and the existence of the single point that is far above the correlation line (the CCSM4-RCP4.5 scenario) correlation also sheds light on another important aspect of pavement performance that the simple mean annual air temperature based correlations do not capture. As a rule, pavement performance does not degrade uniformly throughout the year. In fact, the performance algorithms embedded into the Pavement ME Design model suggest that pavement distresses grow faster during the warmer months than the cooler months, and that within these months it is the hottest part of the day that exhibits the greatest damage. Thus, predicted changes in not only the mean annual temperature, but also the timing of when projections will tend to be higher (e.g., greater or less warming in the summer versus the winter) will also affect performance.

To prove this effect, the first order approximation between change in fatigue cracking and *D-MAAT* is supplemented with a supposed second effect from the temperature differences between the square of the fifth quintile air temperature differences for July ($\Delta Q5$-*July*) from the baseline and future scenario cases is considered. Note, that the fifth quintile air temperature represents the temperature that is greater than 80% of all air temperatures within the month. When incorporating the change in temperature from the fifth quintile from the month July, the correlation for this model begins to look more consistent across the models, see Figure 25 which shows R^2 increases from 0.59 before including the fifth quintile temperature differences and 0.72 after its inclusion). Note that the x-axis is labeled as "Observed Change in Fatigue Cracking (%)", which are the changes in cracking based on the AASHTOWare predicted fatigue cracking. The y-axis is labeled as "Predicted Change in Fatigue Cracking (%)", which are the values predicted by either of the equations shown on the plot. Again, the relationship is not perfect, but it is not expected to be and the improvement in relationship is simply shows that identifying the impact from projected climate

changes must examine not only the mean annual air temperature increases, but also the changes that occur at different times of the year. What is most striking about these correlations are that they suggest that performance is not only positively correlated to the temperature change, but correlated such that differences in performance are magnified with respect to temperature changes (e.g., the slope of the relationships is greater than one).

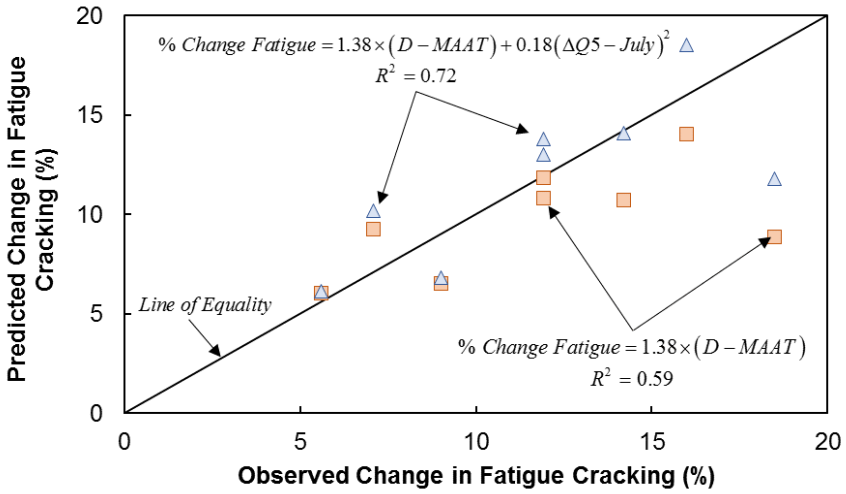

Figure 25: Comparison of performance correlation when including Q5 temperature changes.

These first order approximations have been applied to estimate the potential national impacts from future climate change. Baseline temperatures are extracted for each of the 808 weather stations available in the AASHTOWare Pavement ME Design software for the contiguous US. Climate projects are then extracted from the ensemble of 19 models for each of these locations and averaged. Here, only the average RCP 8.5 case is presented as it shows a slightly above median estimate of the impacts. Figure 26(a) presents the projected impacts with respect to fatigue cracking and Figure 26(b) presents those associated with rutting. In both, the values shown are the percentage increase in distress (fatigue cracking or rutting) that could occur if assumptions of climate stationarity continue. As expected the effects are more pronounced in rutting than in fatigue. The overall trend is similar with greater impacts to both fatigue and rutting expected in the northern latitudes (particularly the upper mid-west and northeast areas). Some small pockets of high impact are projected in the southern Nevada and Idaho-Montana/Idaho-Washington border areas, but this may be due to the presence of micro-climatic regions that are common in the western United States coupled to spatial sparse weather stations and imprecision in the downscaling algorithms, which may not reflect likely future events. In these cases, more careful study with better scaled and more regionally valid models may be needed to draw more accurate conclusions. With fatigue cracking a smaller overall impact is projected and some differences in relative scale are also observed.

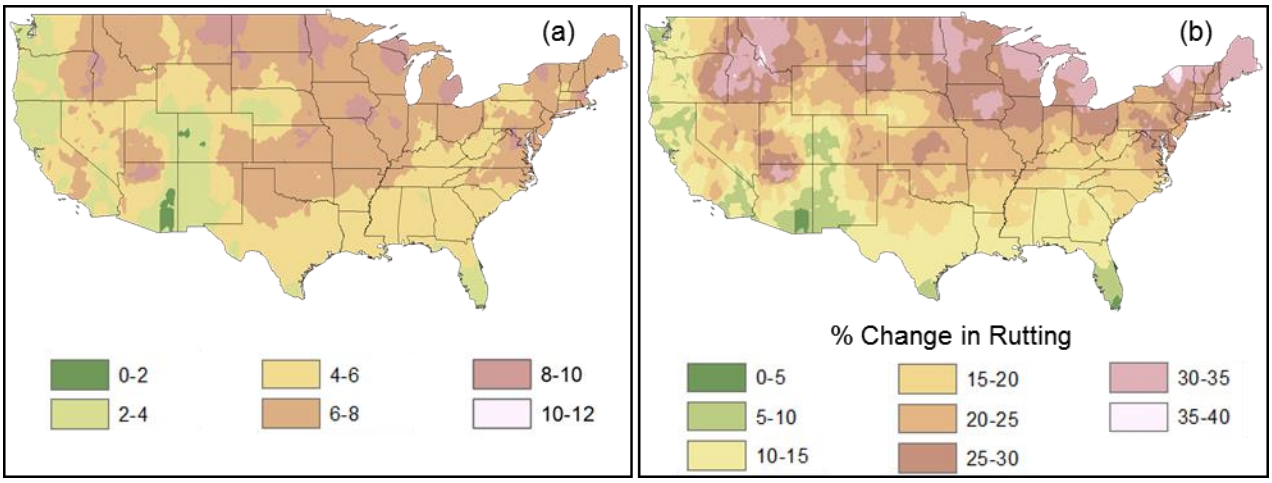

Figure 26: Projected national impacts from 2040-2060 climate change projects; (a) fatigue cracking and (b) rutting.

It should be kept in mind that the maps in Figure 26 represent only the potential for impacts as they do not consider the extent of the current transportation network, the types of roadways present, and the other second or third order effects that may be present. They also do not account for the real-world processes that go into engineering and maintaining pavements over time. Additional analysis similar to that presented elsewhere that incorporates the extent of the transportation infrastructure in place and/or the volume of traffic carried would be needed, but is beyond the scope of the current study (Espinet 2016; Mallick et al. 2016; Schweikert et al. 2014).

Similar comparisons were made from the results when both projected temperature and projected precipitation data were included, see Figure 27. The trends observed in this case are also in line with the temperature only case. Comparing Figure 25 and Figure 27 it is observed that the inclusion of the precipitation data does not substantially affect the pavement distresses for all the climate locations. The key exception to this case is the fatigue cracking in the MT location. While the average percentage change in the fatigue cracking and AC rutting with the incorporation of precipitation projections into the analysis was only about 1-2% for the other locations (and mainly in VA_I64 and ME_I95), the difference for the MT case is approximately 16-18%. The reason for such a striking difference largely lies in the small amount of cracking that was observed for the MT pavement (baseline cracking = 4.3%). Thus, while the percentage change is high, the actual differences between the cases is small. Among the remaining four pavement locations Maine is showing a higher difference in the increase of fatigue crackling when precipitation prediction data is also used from the prediction models. Even though it is not shown in the graphs similar observations are made with respect to AC rutting.

As with the temperature effects, these changes can be approximated at the first order by using simply the projected change in precipitation. In this case, the percentage change in mean annual precipitation (P-MAP), Equation (25), is used to track climatic changes.

$$P-MAP = \frac{\left(MAP_{Future\ Scenario} - MAP_{\text{Baseline } Scenario}\right)}{\left(MAP_{\text{Baseline } Scenario}\right)} \times 100 \tag{25}$$

where; *MAP* = mean annual precipitation, $MAP_{Future\ Scenario}$ = the *MAP* from a given climate model, $MAP_{Baseline\ Scenario}$ = the *MAP* for the baseline scenario.

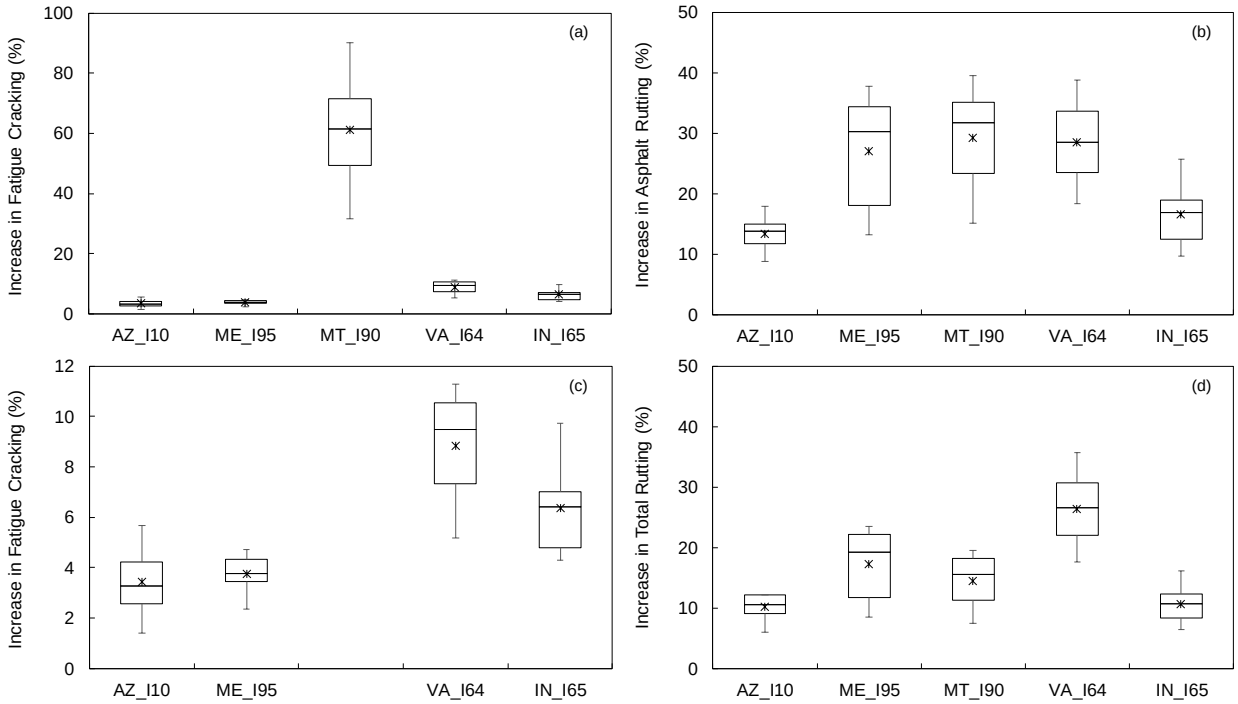

Figure 27: Variation of percentage difference across climate prediction models for study locations using both temperature and precipitation data from predictions for; (a) fatigue cracking, (b) AC layer rutting, (c) fatigue cracking (for 4 locations), and (d) total rutting.

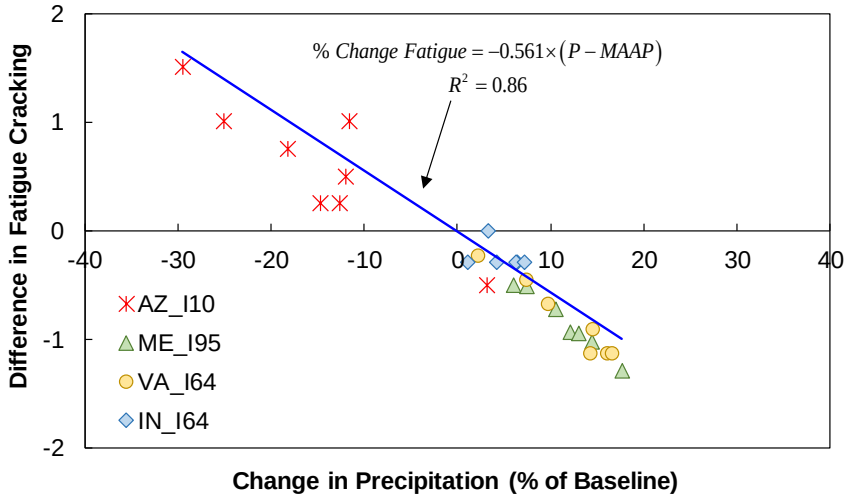

Figure 28: Correlation between change in fatigue cracking and P-MAP and fatigue cracking.

The change in fatigue cracking and asphalt concrete rutting with precipitation inputs are assessed by comparing the resultant distresses from predictions that include both temperature and precipitation changes with those from the same predictions using only temperature. Results of the

analysis are summarized for the fatigue cracking in Figure 28. As expected the effect of changing precipitation inputs is considerably smaller than changes in temperature. In general scenarios that predict less precipitation (e.g., P-MAP less than zero) results in less fatigue cracking. This result occurs because with less precipitation the base ad subgrade layers have a higher modulus and thus the pavement flexes less. Rutting of both the asphalt layer and total pavement show very little change (on the order of hundredths of a millimeter) and so no correlation is found. This finding is not entirely unexpected since surface infiltration is a very minor component in the overall moisture movement calculations embedded into the pavement analysis algorithms.

3.5.2 Impact on Rigid Pavements

Overall, the analysis of the flexible pavement section demonstrates that temperature projections may have a notable effect on pavement performance, but precipitation (at least in the context of monthly on-average increases) has a less important, but still quantifiable impact. It remains to be seen how these differences may manifest in rigid pavements where precipitation infiltration may be more substantial, but the strength of the paving material may conversely compensate for this infiltration. To study the impact of future precipitation data more clearly, the authors performed an analysis for one rigid section from the ME climate location. The reason for choosing ME in the rigid pavement analysis is due to the observed percentage increase in the fatigue cracking using precipitation data with the flexible pavement. The AASHTOWare Pavement ME analysis was again carried out for a rigid pavement section in ME for four different climate prediction models and the two different RCP scenarios. The distresses considered for the analysis purposes for rigid pavements are mean joint faulting and transverse cracking.

The simulation results for temperature only and temperature and precipitation are plotted together in Figure 29. From the figure, the first observation is that with increases in both temperature and precipitation, the mean joint faulting is expected to increase relative to the baseline scenario. This effect results because increases in temperature changes the expansion and contraction of the slabs thereby resulting in greater relative slab movement. The second observation is that in the case of transverse cracking, the rigid pavements appear to perform better under climate change scenarios. Rigid pavement cracking is a combined result of both load induced stresses and temperature induced curling of the slab. With the increase of temperature, the shrinkage phenomenon in the slabs might be decreasing and this resultant effect is showing as an improvement in the transverse cracking in rigid pavements. More likely the effect occurs because PCC pavements are inherently prone to negative built in temperature gradients and climate change induced temperature rise mitigates this effect. A negative built in temperature gradient refers to the fact that at construction, the pavement surface tends to be at its warmest possible state (pavements are generally constructed during the hottest parts of the year). Since pavements will set as a planar surface, the result is that for most of the pavement life, the surface is relatively cooler than its planar configuration and so there is a slight (imperceptible to the naked eye) curl to the slab. This curl generates stresses in the pavement slab that in conjunction with traffic loads lead to transverse cracking. The projected temperature increases would result in a greater proportion of the year having temperatures above the temperature at set and thereby reduce the overall impact of this built-in negative temperature gradient.

With respect to the effects of including precipitation projections, the data are not showing any difference in terms of pavement distresses for rigid pavements. In fact, the impact of future precipitation data is showing more in the case of flexible pavements compared to the rigid pavements. This observation is corroborating the study findings observed from the impact of Hurricane Katrina on the roadways (Gaspard et al. 2007).

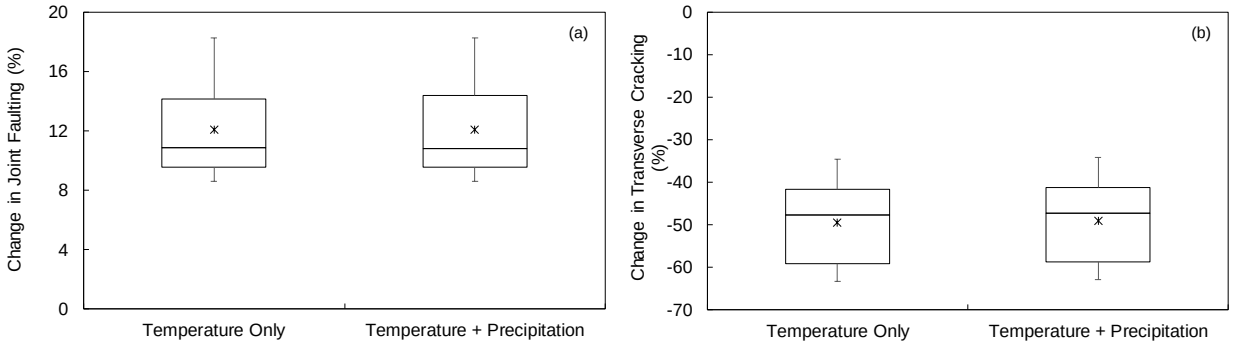

Figure 29: Variation of percentage difference across climate prediction models for rigid pavement section in Maine for temperature only, and for temperature and precipitation data from (a) mean joint faulting and (b) transverse cracking.

4.0 STUDY 3: EVALUATION OF MATERIAL SELECTION PROCESS ON PAVEMENT PERFORMANCE AND ECONOMIC COSTS*

4.1 INTRODUCTION

The current standard of roadway design guides engineers to use climate data from 1964-1995 to select materials. In this study, the economic effects of the continued use of this climate record by examining the impacts of non-stationarity on the asphalt grade in asphalt pavements, which constitute 90% of paved surfaces in U.S. and 99% worldwide (USDOT 2016), are quantified. This issue has been studied by others using techniques like the ones adopted here, but it is believed that these studies have one or more factors that limits the applicability of their findings. Some have focused heavily on climate projections but made correlations to infrastructure performance without supportive engineering analysis (Cambridge Syst. 2015), others have failed to recognize the totality of local factors (materials, construction practices, and climate) that occur when delivering infrastructure (Chinowsky and Arndt 2012, Chinowsky et al. 2013, Schweikert 2014), still others stopped short of linking potential engineering outputs to economic and social impacts (Viola and Celauro 2015, Fletcher et al. 2016), or have been too narrowly scoped to provide a complete geospatial and temporal perspective (Harvey et al. 2004, Meagher et al. 2012, Mills et al. 2009, Mndawe et al. 2013, Daniel et al. 2014). In short, many of the assessments conducted to date have focused on the correlation between climatological stressors and the presence of infrastructure, but without consideration for the engineering processes of the in-place infrastructure. By failing to consider these factors analyses systematically bias findings to locations where climate change is projected to have the greatest change in temperature and/or precipitation, but not necessarily where those changes will have the greatest impact on the pavement infrastructure.

Chinowsky and Arndt (2012) provided one of the first (and only) nationally scoped estimates of climate impacts on pavements. They developed an economic dynamic-stressor model based on empirical performance impacts from precipitation and temperature to examine the issue of climate change and roads. These models reflect, but do not necessarily predict the precise impact of climate change on materials since the empirical functions are calibrated with real-world data where material choices are correlated to climate. Follow-up studies then used this framework to investigate the economic cost of projected climate change on paved and unpaved roads across the United States (Chinowsky et al. 2013). Climate projections were made across a 2.5 by 2.5 grid of the United States under a scenario of business as usual growth (approximating the CMIP3 AIB scenario) and under a scenario of substantial reductions consistent with the Kyoto protocols. The authors concluded that by 2050 the annual adaptation cost would be US$785.0 million (in 2012 dollars) with the greatest impact in the Southeast and Midwest. A follow-up study applied to only the State of Colorado concluded that the benefits of adapting pavement strategies to climate change for that state could result in a US$22 million annual savings by 2050 (Schweikert 2014).

*Note: This study was conducted without financial support from the project, but under the same auspices and was unfunded.

While impressive in scope, the authors had to rely on generalizations of regional or international performance experiences to generate these estimates. Such estimates are questionable though given the highly local nature of materials, design, and construction practices. For example, in the case of heat impacts, costs were estimated based on the published costs of materials from the Colorado Department of Transportation. The authors did not consider that these costs would change as market conditions change (i.e., as local and regional temperatures change, the demand for certain grades would change and hence costs would adjust) and that the costs chosen assumed that low temperature grades would remain the same even. However, winter temperatures are also projected to increase and thus both high and low temperature grades will change jointly. When both grades change the complexity in producing the asphalt is reduced greatly and thus it is likely that costs would be substantially lower than what was estimated. This overestimation is quite important since the major contributor to costs in their analysis was the increased asphalt prices that climate change would bring.

The authors did attempt to address increased maintenance activities using these empirical models. However, to create a workable analysis, they had to assume a linear degradation of performance, which does not accurately reflect the behaviors of pavements, which degrade at an increasing rate (Huang 1993, Yoder and Witczak 1975). Mallick et al. (2016) addressed network performance in a more comprehensive way by first developing a Systems Dynamics model for individual pavement performance based on a set of simulations. They then applied this model under constrained economics and uncertainty to propose a framework to incorporate climate change projections (expressed as a mean and standard deviation) into decision making on pavement network management. While they did apply their model to several urban pavement systems they stopped short of making economic projections.

Viola and Celauro (2015) conducted an analysis for Italy. The authors analyzed historical and future climate projections in Italy and concluded that temperature rise occurring through 2033 would increase the required asphalt grade for 27% of the country by one standard increment. The future climate was projected based on linear extrapolation of the historical data trends. A similar study has also been conducted for urban areas in Canada using 10 models from the A2 scenario of the third phase of the Coupled Model Intercomparison Project (CMIP3) and found that 41% of the cities would likely require a higher asphalt grade by mid-century (Fletcher et al. 2016). Neither of these studies postulated on the nature of adaptation strategies or the cost impacts.

Researchers have also studied this issue at a finer, project level scale. Much of this work has focused on pavements in the New England region. In these cases, climate predictions were incorporated into the pavement design process and results were compared with design/analysis completed using the historical data. One study concluded that climate change predictions have a significant effect on pavement distresses specifically that the pavement life can decrease from 16 years to 4 years and maintenance cost may also increase by 100% (Daniel et al. 2014) while another found that changes in cracking for secondary roads and interstate pavements was negligible but for other roadways that the cracking increased by between 4% and 16% after 20 years (Meagher et al. 2012). The loss of performance and associated changes in construction and maintenance have been documented elsewhere too (Harvey et al. 2004, Meagher et al. 2012, Mills et al. 2009). Qiao et al. (2015) used a scenario in southern Virginia to estimate increases in total life cycle costs of 1-2% from climate change. The primary shortcoming in these project level assessments is a lack

of national or even regional scope, thus it is difficult to identify from these simulations the relative impact of climate change across the country.

While a body of work has developed that suggests future climate changes will have an impact on the costs of transportation infrastructure, the review above identifies some key limitations. Efforts using the most accurate and reliable performance predictions, are either limited in geospatial-temporal scope, do not consider the cost implications of those performance differences, or focus on developing a framework for project level assessment instead of conducting an economic assessment. On the other hand, research that has produced national impact assessment have had to rely on more questionable performance predictions and scenarios that may not be accurate reflections of practice. A hybrid of these two approaches using a limited set of accurate performance predictions in conjunction with a simpler performance metric is used here to balance accuracy with a workable analysis.

4.2 BASIS OF ECONOMIC ANALYSIS METHOD

National estimates of economic impact have all made assumptions that engineers would have information on climate change available and would make material selections to adequately compensate for heat rise. No estimates have been given that consider a scenario where engineers do not have perfect information and continue choosing strategies using a business as usual mindset. This aspect is quite important in estimating costs since it must be realized that the collection of institutions that design and construct the physical infrastructure of transportation networks are mature and have evolved gradually (Bergek et al. 2008, Carlsson and Jacobsson 1997, Kieft et al. 2016, Nego et al. 2012, Wieczorek and Hekkert 2012). This gradual evolution is driven largely by the fact that their actions rely on embodied information gained through learning by trial and error. This evolutionary process yields a direction bias with respect to actions and processes that has been well documented in the literature (Martin and Sunley 2006, and the sources therein). Standards, such as the ones that dictate the use of a 1966-1995 climate record for selecting the asphalt grade are an explicit expression of this bias.

Since the evolution of these standards occurs in the public domain, the drivers for change are often political, economic, social (as in public demand), and in some instances reactive to shock (as in when building requirements change after a high-profile collapse). Although the stressors that drive changes to these standards are largely social, their connection with the technical is apparent (Negro et al. 2012, Geels and Kemp 2007, Smith et al. 2005). It happens though that in mature institutions, generalizing technological know-how across the organization is typically slow and expensive because although data and experiences are shared (Casey et al. 2012, NCHRP 2016), adoption often requires repetition of experiences on systems that can take a decade or more to show their response. So, with respect to long-term heat rise from climate change, it is postulated that the issue of asphalt grade selection will go largely unnoticed by the public and will have relatively low priority politically. As such it is surmised that it is unlikely that the institutions would naturally embed climate projections into asphalt selection and make appropriate decisions based on these outcomes. Economic analysis is therefore conducted based on a scenario where institutions engaged in the engineering and delivery of transportation infrastructure would continue operating under a policy of material selection based on an outdated climate record and the implicit assumption of stationarity. Also, in an important advancement in the area of cost estimation for pavements, economic analysis is conducted for each individual model in both RCP 8.5 and RCP

4.5 scenarios of the analysis ensemble and results are presented in terms of the statistical range (interquartile and maximum/minimum) of expected costs. It is noted that others have also performed an economic analysis using different scenarios, but only used a single model with different forcings (Chinowsky et al. 2013).

Projecting climate change impacts on pavement infrastructure and its engineering is complicated because the system contains multiple feedback loops that affect decision making. Engineers also have numerous strategies to address performance challenges and it is recognized that they will likely respond to observed systematic decreases in performance, and can do so in many ways. For example, they could abandon the grading system entirely and make incremental empirical adjustments that that ultimately aligns with the new climatic reality. They could infer that errors exist in their engineering process and adjust their structural designs. They could also infer that changes to petroleum refining processes have negatively affected the asphalt cement and compensate by using asphalts modified with chemical or polymeric additives. While these changes will likely prevent the continuation of the status quo indefinitely, it is assumed for the purposes of estimating cost impacts, that it will take 30 years to recognize systematic reductions and incorporate broad changes into practice. This timeframe is assumed based on engineering practice that set pavement design life targets for initial construction and rehabilitation for pavements at the 15-20-year period, the total pavement life-cycle at 30-40 years, and the evolution of pavement design standards over the past 70 years (first established in the mid-1950s, and subsequent revision in the early-mid 1970s, early 1990s, and finally mid-2010s).

4.3 CLIMATE DATA

Two climate databases were used in this study; 1) the United States Historical Climatology Network (USHCN) and 2) a global climate model (GCM) ensemble of 19 climate models each under Representative Concentration Pathway (RCP) 8.5 and 4.5. In both cases the 1966-1995 climate record is used as the comparative reference because this is the current basis of binder selection in the United States. The objective in this analysis is to quantify the impacts from continuing to adhere to a static database, which means comparing future year effects to the current state of the practice and the condition that will exist if engineers continue to adhere to this practice.

4.3.1 USHCN Data Processing

The USHCN database was accessed through the U.S. Department of Energy portal and downloaded the daily maximum and minimum temperatures (http://cdiac.ornl.gov/ftp/ushcn_daily/). This database was chosen to determine the impact of present day temperatures on PG because although there are fewer weather stations in the database than others, they are quality controlled so that each station has minimal missing data and data records are available covering the period time of interest. Only those weather stations with complete daily temperature data from January 1, 1966 through December 31, 2014 are considered. In total, 799 weather stations met this criterion and their location are shown in Figure 1 of the manuscript. For each station, the data for the years 1966-1995 as well as the most recent 30-year period available (1985-2014) are extracted from the files using custom MATLAB scripts.

4.3.2 GCM Data Processing

GCM's were selected for the ensemble from those models that participated in the Coupled Model Intercomparison Project 5 (CMIP5), had daily maximum and minimum temperature data for RCP 8.5 and RCP 4.5 scenarios, and were available in 1/8° resolution (Maurer et al. 2007). The data were downloaded from the archives of the Climate Analytics Group (ftp://gdo-dcp.ucllnl.org/pub/dcp/archive/). For analysis, projections are grouped by 30-year periods. These periods begin in the first year of a decade (2010, 2040, and 2070) and are staged in 30-year increments. Results presented as "2010" are based on the temperature projections for the period from January 1, 2010 to December 31, 2039; data given as "2040" are based on data for 2040-2069, and so forth. For statistical analysis purposes, and to most easily compare current and future scenarios, the downscaled data is geospatially interpolated to the coordinates of the Superpave weather stations (Huber 1994). This extraction and interpolation is performed using custom MATLAB scripts.

4.3.3 Coordinating Roadways to Weather Stations

The roadways associated with each weather station are identified by using the built-in functionality of ArcMap (Version 10.3) to draw Thiessen polygons around the 5,417 weather stations in the database. These polygons define the nearest geospatial areas to each weather station. Roadway segments are then extracted from the National Highway Performance Network (NHPN) database, which contains details on all interstates, national routes, state routes, and paved local roads in the United States. Using Geographical Information Software, the total length of each type of roadway contained within each weather station polygon are then calculated.

4.4 SUPERPAVE METHOD OF ASPHALT CEMENT SPECIFICATION

In the U.S., asphalts are used per the Superpave Performance Grading (PG) system, which assigns a temperature-related grade based on the maximum and minimum temperatures between which that asphalt should exhibit adequate performance (AI 2003). A typical grade might be PG64-22, which means that the asphalt is Performance Graded for temperatures between 64°C and -22°C. Since the asphalt grade is based on pavement temperature and linked to pavement performance, it serves as a direct indication of how climate impacts pavement performance. Determining the required low and high temperatures for any location involves calculating the average and standard deviation of the minimum pavement temperature and the maximum seven consecutive day pavement temperature over a multi-decade period. In practice, the climate record used for this purpose is 1966-1995 and the averages are statistically adjusted to account for extremely cold or hot years and rounded to standard 6°C grade increments. In pavement engineering, other climate records may be used for structural design, but even in these cases the 1966-1995 climate record is the one used to select the materials for the design analysis. Thus, adherence to this record does have a substantial impact on the design and long-term behavior of pavements even though other records may be used for part of the design process.

To determine the asphalt grade, the standard performance grade (PG) method is followed. Equations (26) and (27) are then used to estimate the minimum pavement and seven consecutive day average maximum pavement temperatures, respectively (AI 2003). These temperatures are

used in the Superpave method because they relate to either thermal cracking (low temperature) or rutting (high temperature).

$$T_{pav,low} = 7.191 + 0.72\left(T_{air,low} - z \times \sigma_{air,low}\right) - 0.004Lat^2 - z\left(4.4 + 0.52\left(\sigma_{air,low}\right)^2\right)^{0.5} \quad (26)$$

$$T_{pav,high} = \left(\left(T_{air,high} + z \times \sigma_{air,high}\right) - 0.00618Lat^2 + 0.2289Lat + 42.2\right)\left(0.9545\right) - 17.78 \quad (27)$$

Where, $T_{air,low}$ = minimum average air temperature (° C), Lat = latitude (decimal degrees), z = standard normal deviate (50% reliability z = 0, 98% reliability z = 2.055), $\sigma_{air,low}$ = standard deviation of minimum air temperature (° C), $\sigma_{air,high}$ = standard deviation of 7 consecutive day hot temperature (° C), $T_{pav,low}$ = pavement hot temperature (° C), and $T_{air,high}$ = 7 consecutive day high temperature grade (° C). Latitude and longitude for GCM ensemble are the same as the Superpave weather stations and for the USHCN database they are extracted directly from the datafile. The daily maximum and minimum air temperatures at each location are extracted from the downloaded databases, arranged by year, and processed to determine the minimum air temperature and the highest seven consecutive day average maximum air temperature for each year in the record. Then, the average and standard deviation for these annual values are calculated.

The process accounts for exceptionally hot summers and cold winters by embedding statistical uncertainty into Equations (26) and (27). This is conventionally termed *reliability*, and is mathematically defined as the probability (expressed as a percentage) that the temperatures will not be exceeded in any given year. When the average of the annual air temperatures is used in these calculations, there is a 50% probability that a given year will exceed the average, and thus grades that are based on the averages are referred to as the asphalt grade at 50% reliability. Generally, engineers consider it to be too risky to use this grade and by convention choose a temperature that yields a 98% reliability.

The final step adjusts the calculated 50% or 98% reliability pavement temperatures to standard, six-degree temperature increments. For the high temperature grade, these are: 82, 76, 70, 64, 58, 52, and 46°C and for the low temperature they are -46, -40, -34, -28, -22, -16, and -10°C. This rounding process increases the true reliability of the given asphalt grade, but by convention it is still referred to as either the 50% or 98% reliability grade. Equations (26) and (27) can be rearranged to determine the true low temperature (R_{LT}) and high temperature (R_{HT}) reliability of a selected grade, Equations (28) and (29).

$$R_{LT} = 0.5\left[1 + erf\left(\frac{7.191 - LT - 0.004Lat^2 + 0.72T_{air,low}}{\left(0.72\sigma_{air} + \left(4.4 + 0.52\left(\sigma_{air}\right)^2\right)^{0.5}\right)\sqrt{2}}\right)\right] \times 100 \quad (28)$$

$$R_{HT} = 0.5\left[1 + erf\left(\frac{\frac{HT + 17.78}{0.9545} + 0.00618Lat^2 - 0.2289Lat - 42.2 - T_{air,high}}{\sigma_{air}\sqrt{2}}\right)\right] \times 100 \quad (29)$$

Where, LT and HT = low and high temperature grades against which the reliability is evaluated.

For the USHCN database Equations (26) and (27) are used to calculate the standard grade from both the 1966-1995 and 1985-2014 temperature record. Comparisons are made between these results to identify the stations where the two databases yield different grades. By using the stationary climate record, it is find that asphalt grades are already being improperly determined in many parts of the U.S. Figure 30 shows locations from the United States Historical Climate Network where the required asphalt grade based on temperature data from 1966-1995 differs from the one based on data from 1985-2014. In total, 35% of stations have a different high or low temperature grade (6% high temperature only, 26% low temperature only, and 3% both high and low temperature). High temperature grade changes are the primary performance concern since these sites will experience faster degradation, require greater maintenance, and possibly lead to earlier reconstruction. Underestimates of the low temperature value suggest that the location has additional protection against low temperature cracking, but implies that agencies are paying higher costs for materials that withstand lower temperatures than currently exist.

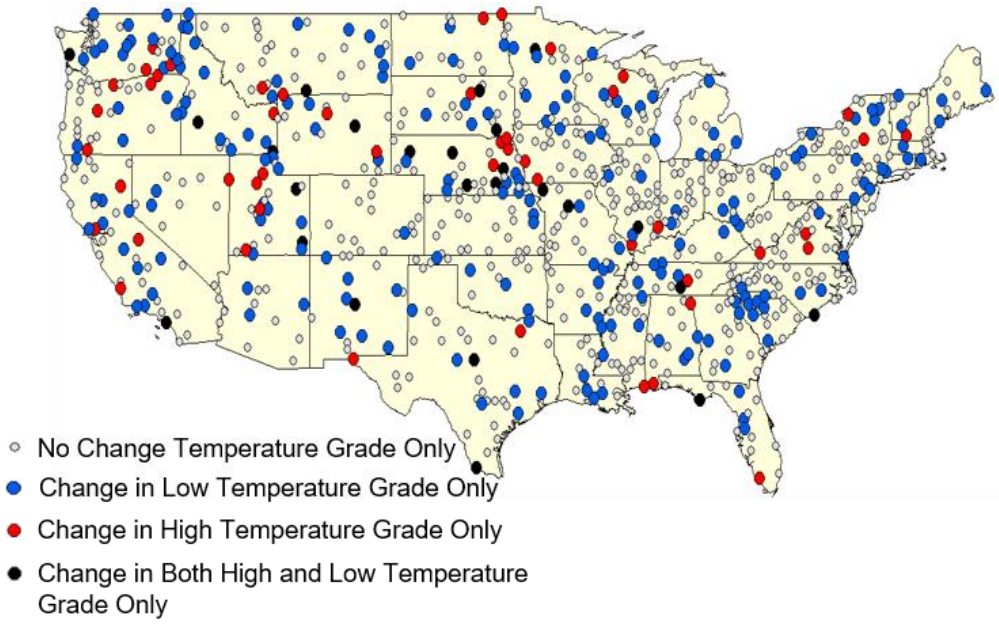

Figure 30: Weather stations evaluated to compare 1966-1995 climate database and 1985-2014 climate databases.

For each model in the GCM ensemble and for each time window in the study (2010, 2040, and 2070), the method above is applied to calculate the projected 98% pavement temperature for each time period and for each location. The difference between these temperatures when using the 1966-1995 climate record and from the median of the GCM ensemble are also calculated. The outcomes

from Equations (26) and (27) are also used to compute the standard grade (i.e., the grade in the standard temperature increments). These temperature differences are graphically depicted for the median RCP 8.5 scenario in Figure 31 and for the median RCP 4.5 scenario in Figure 32 . This grade is compared with the currently specified grade and the results are shown in Figure 33. Under future scenarios the Ohio Valley and Southeast regions of the country are expected to experience the greatest pavement temperature. The Southwest and Pacific coastal regions show relatively little change in the high temperature ensemble median. However, the low temperature median is projected to increase, particularly along the Rocky Mountains.

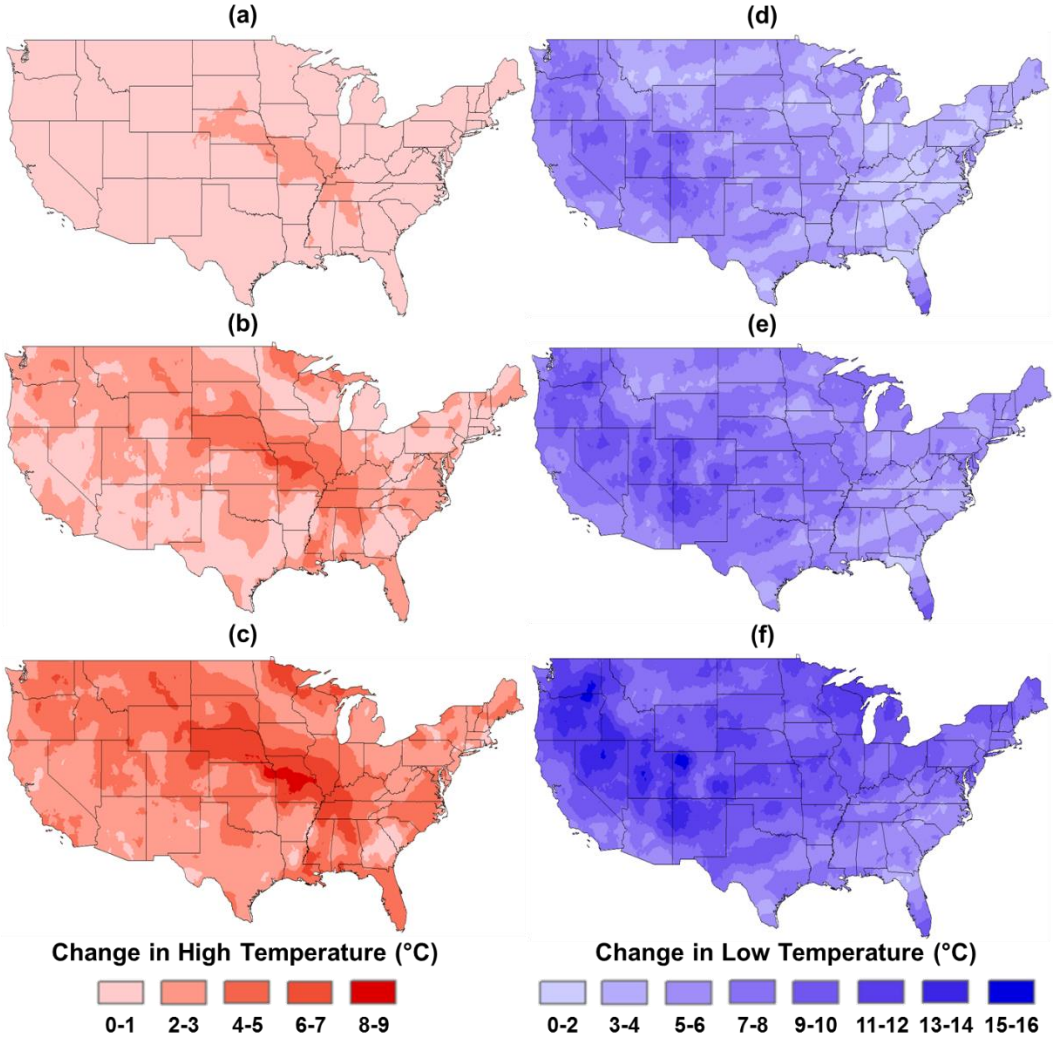

Figure 31: Expected median increases in pavement temperature based on the RCP 8.5 ensemble: (a-c) average 7-day maximum temperature and (d-f) average minimum temperature changes for 2010-39, 2040-69, and 2070-99 respectively relative to the 1966-1995 climatology.

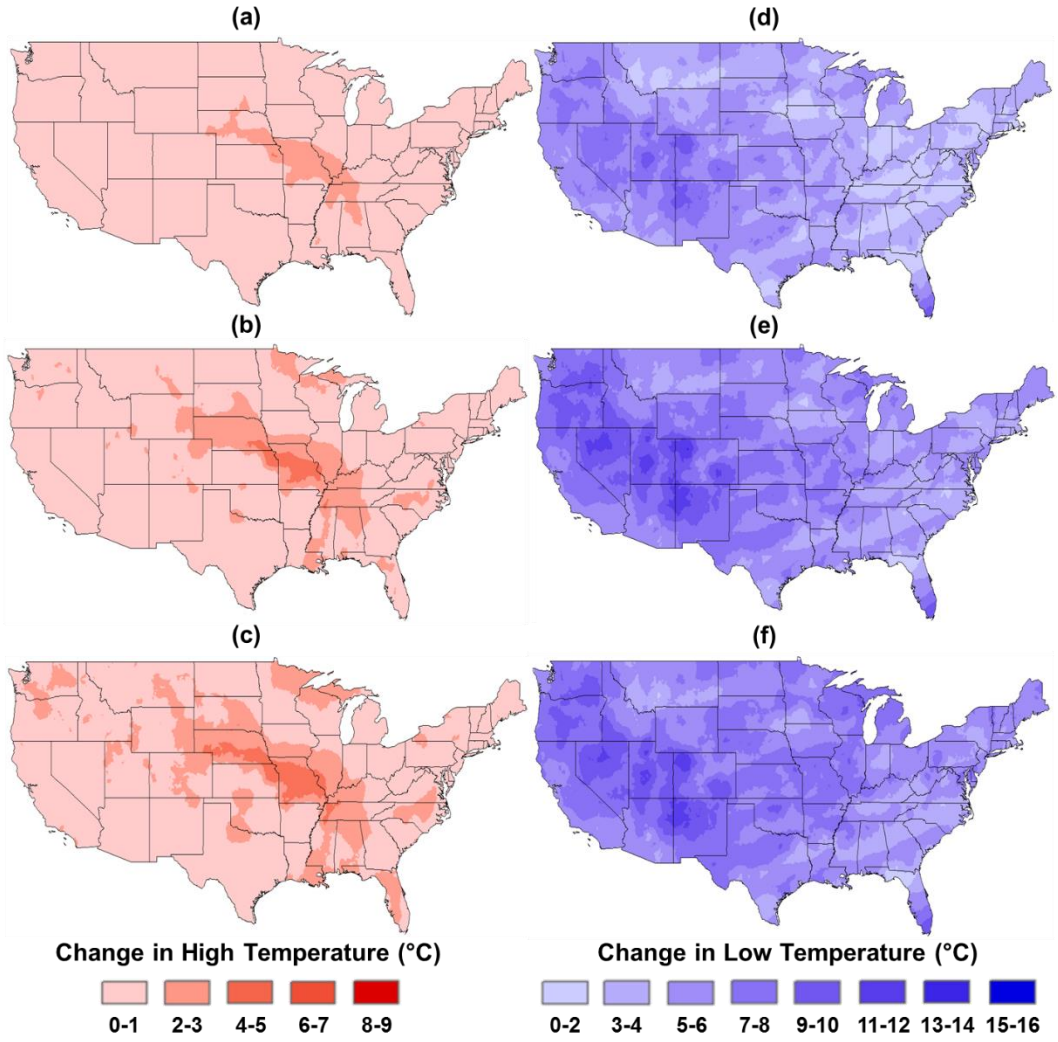

Figure 32: Expected median increases in pavement temperature based on the RCP 8.5 ensemble: (a-c) average 7-day maximum temperature and (d-f) average minimum temperature changes for 2010-39, 2040-69, and 2070-99 respectively relative to the 1966-1995 climatology.

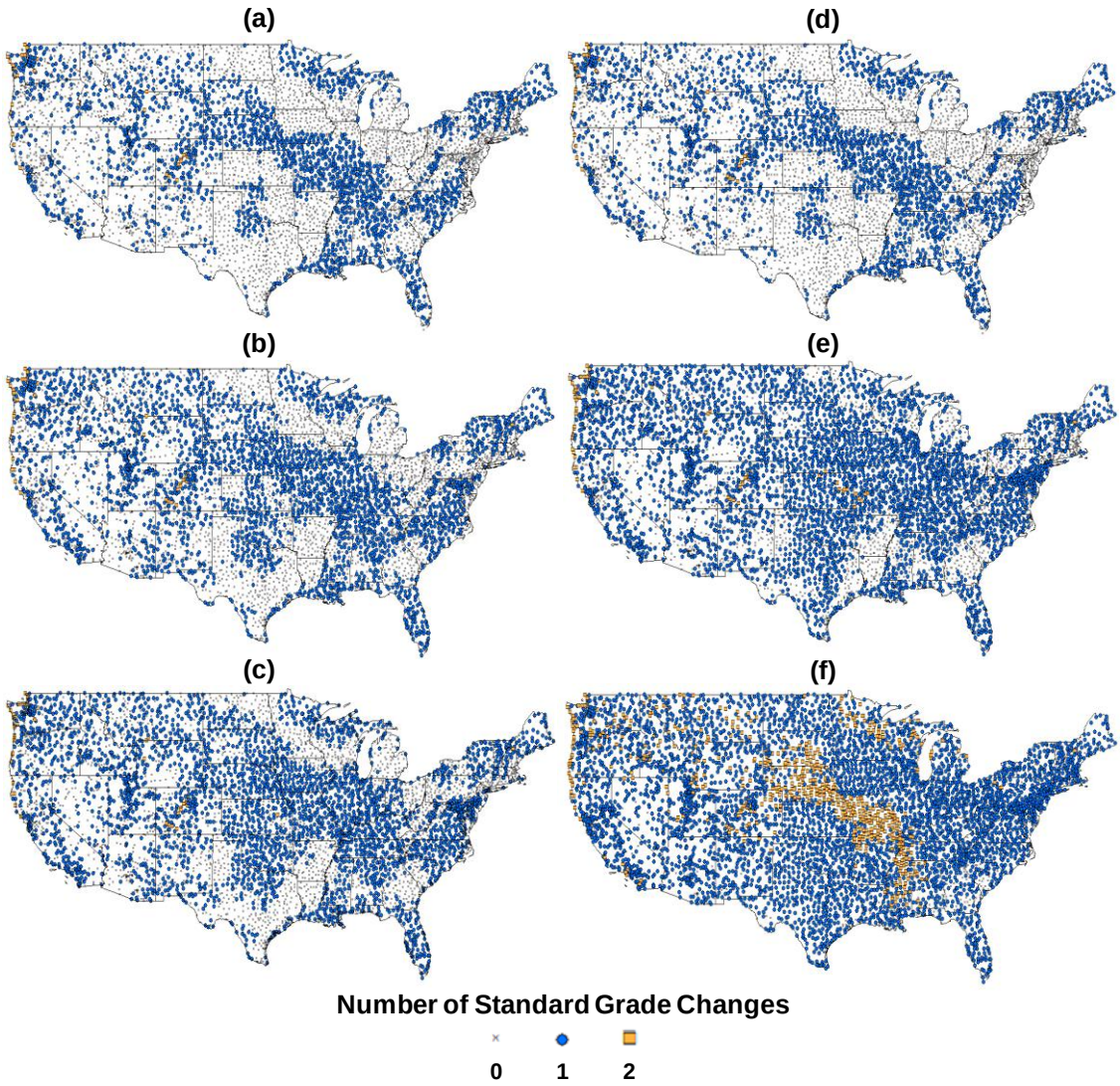

Figure 33: Expected number of increases in the standard high temperature grade increment for: (a-c) RCP 4.5 and for (a) 2010-2039, (b) 2040-2069, and (c) 2070-2099 and (d-f) RCP 8.5 and for (d) 2010-2039, (e) 2040-2069, and (f) 2070-2099.

4.5 UNCERTAINTY ANALYSIS OF PROJECTED IMPACTS

While the median projections show some trends, the model-to-model variation is high. To quantify this difference and the impact on interpreting the outcomes, the averages and standard deviations for the high and low temperatures are substituted into Equations (28) and (29) along with the current asphalt grade to estimate the future true reliability. The impacts are evaluated by state, region (defined using the National Climatic Data Center regions, Figure 34), and nation.

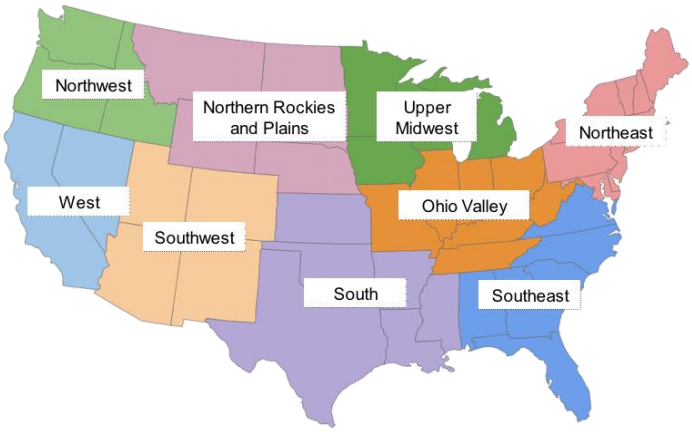

Figure 34: Regional boundaries used for this study.

The variability of the climate models is examined across regions by using the Beta Function, Equation (30). Characterization of this function reveals that the ensembles result in a skewed distribution of impacts, which is used to justify selecting the median as the central tendency measure of the ensemble. The median value is estimated by finding the parameters of the beta function (α, β, a, and c) using the Pearson method (Johnson and Kotz 1970) where their values are equated to functions of the mean, variance, skewness, and excess kurtosis.

$$P = \frac{\Gamma(\alpha+\beta)}{\Gamma(\alpha)\Gamma(\beta)}\left(\frac{x-a}{c-a}\right)^{\alpha-1}\left(1-\frac{x-a}{c-a}\right)^{\beta-1}\times 100 \tag{30}$$

Where, P = cumulative probability of given true reliability, x, α and β = beta distribution parameters, a and c = the maximum and minimum values of the distribution function, and $\Gamma()$ = gamma function.

The median estimates of true reliability for each region under RCP 4.5 and RCP 8.5 scenarios are shown in Figure 35 (a and b). It is found that the Southeast and Ohio Valley regions are projected to see the greatest impact while the Northeast and Northwest regions are the least impacted. However, as noted earlier, considerable variation exists and thus there is a certain probability associated with each of these median projections. The region-wise cumulative distribution of the reliability was computed using the beta function to better understand the likelihood of impacts. The results are shown for RCP 4.5 and RCP 8.5 for all regions and for the 2040 base year (e.g., considering years 2040-2070) in Figure 35 (c and d). The figure shows that in addition to having the greatest median impacts, the projections for the Ohio Valley and Southeast regions also have the greatest uncertainty. This uncertainty generally tracks with the median values as the Northern Rockies and Plains and Southwest regions follow the Ohio Valley and Southeast regions in both median and spread. From this figure, it can also be observed that the Northwest and Western regions have an almost bimodal distribution in the case of RCP 4.5 projections. One group of models suggest little to no impacts in reliability while a second group project higher impacts. In RCP 8.5 the models tend to project a more consistent albeit skewed distribution.

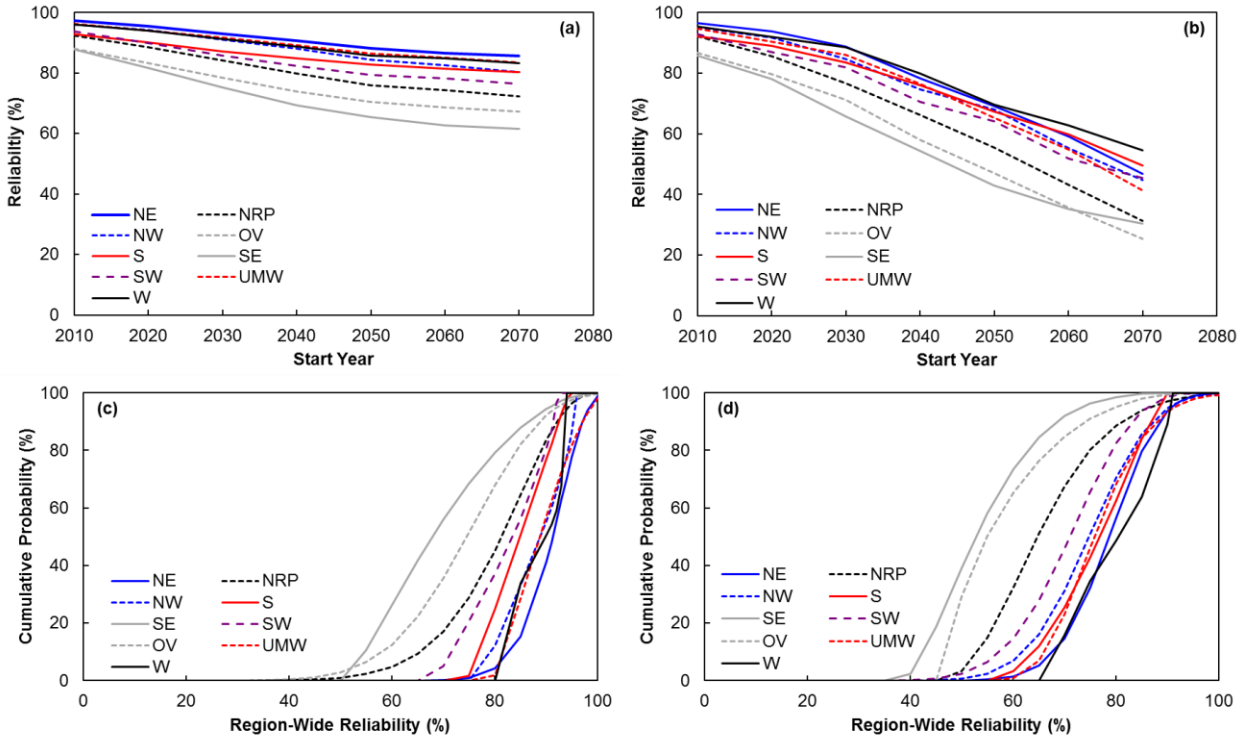

Figure 35: (a and b) Multimodal ensemble median predicted reliability by region for (a) RCP 4.5 and (b) RCP 8.5; (c and d) Cumulative probability distributions for regional reliability for (a) RCP 4.5 and (b) RCP 8.5 (Legend indicates region of interest, NE = Northeast, NRP = Northern Rockies and Plains, NW = Northwest, OV = Ohio Valley, S = South, SE = Southeast, SW = Southwest, UMW = Upper Midwest, and W = West).

4.6 IMPACT ASSESSMENT

To estimate the cost impacts, four steps are performed; 1) the nationally calibrated Pavement Design ME model is used to calculate performance reductions resulting from the temperature-induced shortfalls in grades, 2) changes to the construction, maintenance, and rehabilitation activities brought on by reduced performance and the life cycle costs of these scenarios are estimated, 3) roadway lengths are coordinated to the nearest corresponding weather station, and 4) the increased costs are calculated using life cycle cost analysis (LCCA).

4.6.1 Pavement ME Design Model

The Pavement Design ME simulation tool is used to estimate the performance impacts from using an incorrect asphalt grade. The decision was made to use Pavement Design ME because it is the only pavement analysis and design tool that has undergone extensive national calibration and one of the only that can directly consider asphalt grade in the performance prediction process. This tool explicitly considers the individual and interactive effects of local temperature, traffic, material (including the PG grade used), soil conditions, and the pavement structural configuration of the roadway types. To integrate these factors, Pavement Design ME uses a complex assemblage of models and routines that link the response of a pavement under trafficking to cracking, rutting, and ride quality changes over the lifetime of the pavement structure (approximately 20 years).

The performance of four roadway types (interstate, national route, state route, and local roads) in cold, moderate, and warm climate zones (Minneapolis, Minnesota; Raleigh, North Carolina; and Miami, Florida) are simulated. The pavements are simulated so that the correct asphalt has a service life of 18-22 years. The relevant inputs for each of the simulations are given in Table 9. For variables not explicitly given in this table (asphalt content, air void content, thermodynamic properties, etc.) the default parameters of the simulation tool are used. The climate records for each of these cities are available within the support files for the simulation tool and the soil properties are found using the soil survey tool available at (http://nchrp923b.lab.asu.edu/). For climate and roadway type, the simulations are first performed by inputting the correct asphalt grade for the current climate. Then subsequent simulations are carried out with a grade that is either one or two standard increments below the current grade. This approach was followed because of inconsistencies in using the GCM predicted climate input in the Pavement Design ME model. The pavement model uses hourly temperature values whereas the GCMs provide only daily maximum and minimum temperatures. Projecting the future hourly temperature variations and analyzing pavement performance under future climate grades would introduce additional uncertainty.

Table 9: Inputs used for AASHTO Pavement Design ME Simulations.

Climate	State Weather Station	Minnesota Minneapolis (94963)[1]	Florida Miami (12839)[1]	North Carolina Raleigh (13722)[1]
Asphalt Concrete Layer	Asphalts	PG 58-34, PG 52-34, PG 46-34	PG 70-10, PG 64-10, PG 58-10	PG 64-22, PG 58-22, PG 52-22
	Interstate Thickness (cm)	25.4	25.4	25.4
	National Route Thickness (cm)	15.2	15.2	15.2
	State Route Thickness (cm)	10.2	10.2	10.2
	Local Roads Thickness (cm)	7.6	7.6	7.6
Granular Base	Elastic Modulus (MPa)	207	207	207
	Interstate Thickness (cm)	38.1	38.1	38.1
	National Route Thickness (cm)	20.3	20.3	20.3
	State Route Thickness (cm)	15.2	15.2	15.2
	Local Roads Thickness (cm)	12.7	12.7	12.7
Subgrade	AASHTO Classification	A-2-4	A3	A-4
	Description	Silty Sand	Fine Sand	Silty Soil
	Elastic Modulus (MPa)	134	152	62
	Water Table (m)	15.2	3.4	16.8
Interstate Traffic	Truck Traffic Classification[2]	1	1	1
	Speed (km/h)	97	97	97
	Cumulative Truck Traffic	3,590,500	3,801,700	1,056,030
National Route Traffic	Truck Traffic Classification[2]	4	4	4
	Speed (km/h)	97	97	97
	Cumulative Truck Traffic	1,267,230	1,689,650	190,085
State Route Traffic	Truck Traffic Classification[2]	14	14	14
	Speed (km/h)	72	72	72
	Cumulative Truck Traffic	704,019	1,642,710	70,401
Local Road Traffic	Truck Traffic Classification[2]	17	17	17
	Speed (km/h)	48	48	48
	Cumulative Truck Traffic	352,010	938,693	32,854

[1] Weather station name and (number) from AASHTO Pavement Design ME software

[2] Truck Traffic Classification (TTC) are general distributions of trucks; 1 = Major single-trailer truck routes (Type I) I), 4 = Major single-trailer truck routes (Type III), 14 = Major light truck route (Type I), 17 = Heavy bus route

The basic prediction process followed in Pavement Design ME to predict fatigue cracking and rutting are given in Section 2.4.2. This analysis focused on the cracking and rutting distresses because the predicted values have greater certainty than others and because the focus here is on the structural performance of the pavements. Thermal cracking is also predicted from the Pavement Design ME model and is a distress that is directly related to climate. However, it is not considered in this analysis because as the data shown later demonstrates that future climate change results in a warming of the yearly cold temperature, which would result in less future thermal cracking. Other relevant performance measures do exist (raveling and pothole formation for example), and it is recognized that future climate changes will affect the mechanisms that cause these distresses. For example, higher temperatures will result in faster oxidation of the asphalt, which can embrittle the material and make it more likely to ravel. However, the science describing the mechanics of these distresses has not produced comprehensive mechanistically based models capable of reliably predicting the initiation and growth of these distresses. Empirical models do exist, but these may combine multiple confounding factors into single variables (for example a temperature variable in the empirical model may implicitly assume an asphalt type that is associated with that temperature), which makes it difficult to consider the effects of asphalt changes on the resulting performance.

For the structural inputs to the model it is recognized that pavement design methodologies can vary substantially between and within states. Even more, agencies do not always keep accurate records of the in-place designs or the standards that they follow. Although the specific designs for every roadway are difficult to identify, most pavement designs in the U.S. use a common paradigm: asphalt concrete is placed on a supporting layer of unbound and compacted granular base, which then rests on compacted native soil. The thickness of the pavement layers is a function of loading severity (both in terms of actual load levels and the number of repetitions). Loading severity strongly correlates with the roadway types: interstate (most severe loading), national route, state route, or local road (least severe loading). In this analysis, this effect is considered by creating four different representative pavement structures for the simulations. The thickness of these representative pavement types varies as shown in Table 9, with the thinner asphalt concrete pavements used for the roads with fewer trucks.

It is assumed that the pavements have reach structural failure when either the fatigue cracking reaches 20% of the total lane area (ARA 2004) or total pavement rutting is equal to 12.5 mm (FWA et al. 2011). The loss of performance from an incorrect asphalt by comparing the time to failure (to the half year) when the correct asphalt grade is used to the time to failure when an incorrect asphalt grade is used, Equation (31).

$$PL = \frac{t_{failure-baseline} - t_{failure-\Delta grade}}{t_{failure-baseline}} \times 100 \quad (31)$$

Where, PL = performance loss, $t_{failure\text{-}baseline}$ = years to failure when the correct asphalt grade is used, $t_{failure\text{-}\Delta grade}$ = years to failure when the asphalt grade used is wrong by either one or two increments.

After using these models, it is found that the predicted impact from choosing the incorrect asphalt grade varies more by roadway type than by climate region. In fact, the differences between climate regions Based on model predictions of the long-term pavement performance, an asphalt cement one standard grade below what is required leads to a 10% reduction in pavement life for interstates (coefficient of variation between predictions of 3.9%) and a 15% reduction for the other three roadways types (coefficient of variation of 5.6%). When using an asphalt cement that is two standard grades below the required level, the pavement life for interstates, national routes, and state and local routes decline by 20%, 25% and 30%, respectively (coefficients of variation of 5.8, 7.1, and 9.6 respectively).

It is interesting to observe that in terms of a reduction in pavement life, the impact from an incorrect asphalt grade is greater for the thinner roadways than the thicker ones. This effect is attributed to the way heat transfers in a pavement system. Pavements, as a rule are warmer than the surrounding air since in addition to experiencing conductive heating by the air, they also experience additional heating by absorbing the shortwave radiation emitted by the sun. There are additional mechanisms that also occur, for example surface convections and heat released and stored in the supporting soil, but the interaction between climate and roadway type can be understood by simply considering the conduction and radiation mechanisms. For the two main mechanisms, the heating occurs at the surface and diffuses downward through the pavement structure (note that the reverse effect occurs when the air temperature drops and the sun sets). Thus, surface temperatures are the ones affected most greatly by increases in air temperature. The diffusion that takes place is also important and is affected by the total thermal mass of the pavement layers, the conductivity, specific heat, etc. While it is the cumulative effect of temperature across all layers that dictates pavement performance, a careful examination of the governing PavementME equations reveals that the performance is weighted more heavily to loading that occurs at high-temperature (T is high, E is low, and ε is high). In roadways with a thicker asphalt concrete layer, the influence of surface temperature rise is mitigated first by having a larger thermal mass to reduce surface temperature rise the temperature, but also because the cumulative contribution of the surface damage to the total pavement damage decreases. By this same argument, when the wrong asphalt grade is used with thin pavements, the surface of the pavement is most greatly affected and the contribution of the damage that occurs at the surface is greater than it is in the case of the thick pavements. The net result of these phenomena is a greater loss in pavement life for lower class roadways relative to higher class roadways when temperature rise is not accounted for.

4.6.2 Maintenance and Rehabilitation Planning

To conduct the LCCA a 30-year life cycle plan is developed that supposes the timing of maintenance and rehabilitation activities. The schedule is first developed for the case where the correct asphalt is used (the reference schedule). The basis of this schedule is engineering experience, the guidelines for Indiana and New York (Lamptey et al. 2005, NYDOT 2002), and national guidance (Santero 2010, Walls and Smith 1998). Schedules are then developed for the case where the asphalt is wrong by one or two grades by modifying the timing of the individual activities in the reference schedule by the same amount as the performance loss. For example, it is estimated that the *PL* of an interstate pavement with an incorrect asphalt grade was 10%. In the reference schedule, a major rehabilitation will occur at year 16, but based on the 10% loss in performance this activity is now expected to occur in year 14.4 (16 x 0.9 = 14.4), which is rounded

in the final adjusted schedule so that it takes place in year 14. To establish the -1 and -2 grade schedule the timelines is adjusted proportionally to the loss in pavement life. This simple approach is used to estimate the life cycle schedule when the incorrect asphalt is chosen because it is assumed that agencies will continue operating as they do now, by relying on decision matrices based upon the time when certain thresholds of performance thresholds are met (rutting, cracking, raveling, potholes, etc.). It is recognized that this linear scaling is not a perfect representation of the pavement performance in individual years, but have adopted it for two specific reasons. First, most of the intermediate rehabilitations are related to pavement cracking phenomenon (crack sealing and patching), which do tend to grow linearly unless a pavement is poorly designed and experiences a near catastrophic failure. Within the analysis space adopted, it is assumed that engineers properly design and construct pavements and so these types of failures do not occur. The larger rehabilitations (overlays) occur within a few years of the pavement life predicted from the Pavement Design ME performance model so the extrapolation errors in the timing of these events is small. More sophisticated approaches would require establishing probability distributions for costs, timings, partial maintenance, and constrained economics of agencies. Such approaches can be characterized accurately for only specific project level conditions. Here, a large network analysis is conducted and it is believed that these approaches would introduce even greater uncertainty to the analysis.

Table 1: Construction, Maintenance, and Rehabilitation Schedule Considered for LCCA analysis.

Activity	**Year of Activity**					
	Correct Grade Schedule	*-1 Standard Grade Schedule*		*-2 Standard Grades Schedule*		
	All Roadway Types	Interstate	National, State, and Local Routes	Interstate	National Routes	State and Local Routes
Construction	0.0	0.0	0.0	0.0	0.0	0.0
Crack Sealing	4.0	3.5	3.5	3.0	3.0	3.0
Patching	8.0	7.0	6.5	6.0	6.0	5.5
Crack Sealing	10.0	9.0	8.5	8.0	7.5	7.0
Patching	13.0	11.5	11.0	10.0	9.5	9.0
Milling[1]	16.0	14.0	13.5	12.5	12.0	11.0
Overlay[1]	16.0	14.0	13.5	12.5	12.0	11.0
Crack Sealing	19.0	17.0	16.0	15.0	14.0	13.0
Patching	22.0	19.5	19.0	17.5	16.5	15.0
Crack Sealing	25.0	22.5	21.0	20.0	18.5	17.5
Patching	27.0	24.0	23.0	21.5	20.0	18.5
Milling[1]	--	27.0	25.5	24.0	22.5	21.0
Overlay[1]	--	27.0	25.5	24.0	22.5	21.0
Crack Sealing	--	--	28.0	26.5	24.5	23.0
Patching	--	--	--	28.5	27.0	25.0
Crack Sealing	--	--	--		29.0	27.0
Salvage Value	0.00	0.75	0.67	0.50	0.33	0.20

[1] For interstate pavements it is assumed that 5 cm are milled and 6.25 cm are overlaid for other classes it is assumed that 25 cm are milled and 37.5 mm are overlaid to account for traffic growth.

PL's change by roadway type and grade deficiency and so the timing varies accordingly. The performance losses are given above. Table 1 lists the activities for each of the scenarios sequentially where the numbers given in the table for each activity correspond to the year in which the activities occur. The Correct Grade Schedule is the expected strategy when the correct asphalt grade is used, whereas -1 and -2 Standard Grade Schedules are when the asphalt grades are wrong one and two grades, respectively.

4.6.3 Life Cycle Cost Analysis

LCCA analysis is conducted based on the maintenance and rehabilitation schedules in Supplementary Table 2. The unit of the analysis is a one-kilometer segment of the roadway type in question. The number of lanes assumed for each roadway type is based on national averages: interstate and national routes are four lanes wide, state routes are three lanes wide, and local routes have two lanes (USDOT 2016). Quantities of materials are estimated assuming that each lane is 3.7 m wide. The costs associated with each activity are based on values used by the North Carolina and Arizona Departments of Transportation. Both states have extensive transportation networks with multiple suppliers so they provide an overall representative indication of national costs. All costs are returned to the base year and summed according to Equation (32).

$$NPV = IC + \sum_{j=1}^{N} R_j \left[\frac{1}{(1+i')^{n_j}} \right] - Salvage \left[\frac{1}{(1+i')^{N}} \right] \tag{32}$$

Where, *NPV* = net present value, *IC* = initial cost, R_j = rehabilitation expenditure (single cost expenditure), *Salvage* = the salvage value at the end of the analysis period, i' = the discount rate, assumed 4% (Walls and Smith 1998), and n_j = year of expenditure. The salvage value is calculated by multiplying the construction cost by the proportion of remaining life.

The total *NPV* associated with each weather station is estimated by first determining which maintenance and rehabilitation schedule to follow. The number of lane kilometers for each type of roadway are multiplied by the *NPV* for the appropriate maintenance and rehabilitation schedule (see Table 10. So, for example a weather station with 10 kilometers of interstate would have a total estimated *NPV* of US$11,837,020 when the correct asphalt was used, while the same station would have a *NPV* of US$12,700,950 when the asphalt was wrong by one grade. The impact is quantified by the difference between the future scenario costs and the costs when all roadways have the correct asphalt grade. The results are then summed for all models and weather stations, and also disaggregate them by state and region. The regional and state costs are estimated based on a per lane kilometer cost by dividing the costs by the lane kilometers. For the ensemble of models, the median, maximum, minimum, and 75th ($NPV^{75th\ percentile}$) and 25th ($NPV^{25th\ percentile}$) percentiles are calculated. For analysis by state and region, outlying model predictions are identified using the interquartile range as shown in Equation (33) (NIST 2012).

$$Outlier = \begin{cases} NPV > NPV^{75th\ \textbf{percentile}} + 1.5\left(NPV^{75th\ \textbf{percentile}} - NPV^{25th\ \textbf{percentile}} \right) \\ OR \\ NPV < NPV^{25th\ \textbf{percentile}} - 1.5\left(NPV^{75th\ \textbf{percentile}} - NPV^{25th\ \textbf{percentile}} \right) \end{cases} \tag{33}$$

Table 10: Impacts by Pavement Type when using the Correct and Incorrect Asphalt Grade [Percent Difference from Using the Correct Asphalt grade shown in brackets].

Roadway Type	Correct Asphalt Grade	Asphalt Grade Incorrect by One Increment	Asphalt Grade Incorrect by Two Increments
		Net Present Cost (*US$/km*)	
Interstate	1,183,702	1,270,095 [6.80%]	1,312,235 [9.80%]
National Route	723,106	775,997 [6.80%]	807,514 [10.5%]
State Route	403,589	444,591 [9.20%]	472,737 [14.6%]
Local Road	231,742	257,804 [10.1%]	280,576 [17.4%]
		Net Present Cost (Not Including the Initial Construction Cost) (*US$/km*)	
Interstate	199,240	285,632 [43.4%]	327,773 [64.5%]
National Route	132,429	185,319 [39.9%]	216,837 [63.7%]
State Route	108,251	149,252 [37.9%]	177,398 [63.9%]
Local Road	84,072	110,135 [31.0%]	132,906 [58.1%]

When applied to the entire pavement network in the U.S. it is found that the implications of these costs are large. Projections are made for each of the models and from the median of the model ensemble for the sequential 30-year windows (2010, 2040, and 2070) in the dataset. The differences between these cases and the baseline scenario that assumes a stationarity climate represents the estimated impact from failing to adapt engineering practices to climate changes. The cost impacts are shown in Figure 36. The estimated costs across the U.S. based on RCP 4.5 are US$13.6 in 2010, US$19.0 in 2040, and US$21.8 billion in 2070. Cost estimates for the same periods based on RCP 8.5 are US$14.5, US$26.3, and US$35.8 billion, respectively. The variation in these costs are also large (as low as US$8.8 billion in 2010 to as high as US$45.5 billion in 2070) owing to the variability in model outcomes. To place the calculated impacts into perspective the cumulative baseline costs for the U.S. are approximately US$419 billion. Thus, the impacts from temperature increases add approximately 3-9% to the cost to build and maintain the infrastructure over each 30-year period.

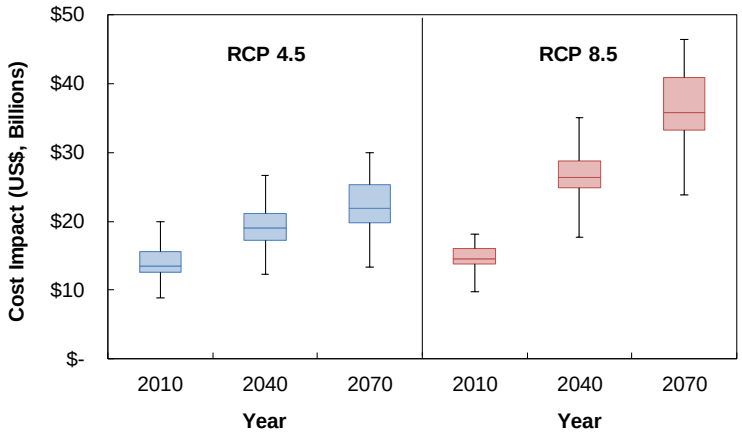

Figure 36: National cost impact from failing to adapt asphalt grade. Range of costs vary by year and RCP scenario considered. The projected costs are similar by RCP for the 2010-2040 period, but increases substantially by 2070-2100 period.

Since maintenance and rehabilitation is the responsibility of each individual state, the data is also cumulated by each state individually and by region. The results are shown in Figure 37. It is found that the total costs of failing to adapt to the projected changes disproportionately affect the Ohio Valley, South, and Southeast regions, which collectively account for approximately 54% of the total costs. Also based on total cost it is found that the four states most likely to experience elevated costs are Illinois, Texas, Florida, and California. Interestingly, the projected impacts in Texas substantially increase in RCP 8.5 scenario compared to the RCP 4.5 and scenario. These results are not entirely surprising as these states also have relatively large transportation networks. The costs are also examined on a per lane kilometer basis to account for differences in the state-level infrastructure network, Figure 38. This standardization produces similar results across states and regions but with some notable differences. The Ohio Valley and Southeast regions are expected to experience the greatest costs, especially under RCP 4.5. When comparing the RCP 4.5 and RCP 8.5 scenarios, it is also found that the Upper Midwest, Southern, Western, and Northeastern regions, along with the Ohio Valley and Southeast, are most sensitive to the RCP scenario. The results are most dramatic for the Upper Midwest, where the difference in cost by RCP varies by almost 90%. Other states that show high per kilometer cost differences between RCP scenarios are Ohio (75%), Delaware (75%), North Dakota (74%), New Jersey (72%), and Arkansas (68%). Conversely, Massachusetts, Maine, New Hampshire, Rhode Island, Vermont, Mississippi, and Alabama show small differences between the two scenarios.

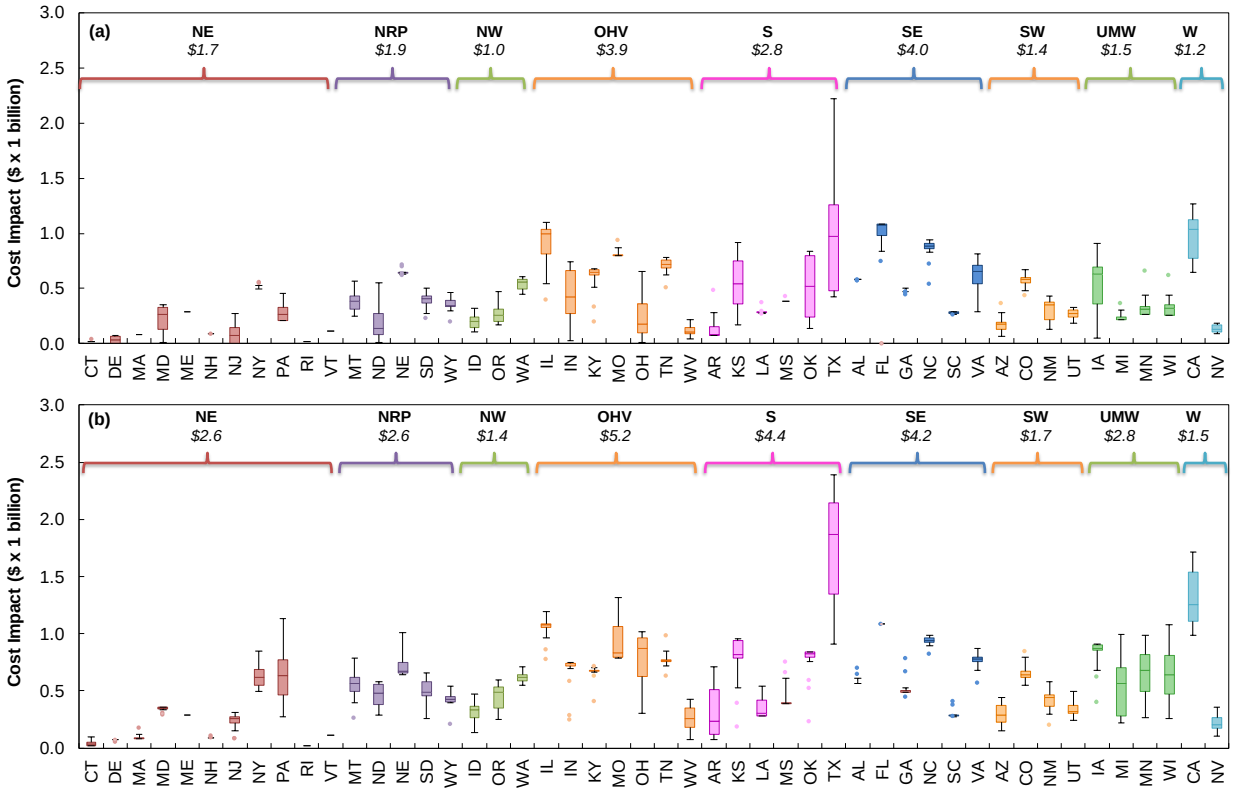

Figure 37: Projected median cost impact to pavement infrastructure on a total cost basis for 2040-2070 period from failing to successfully adapt asphalt cement grade; (a) RCP 4.5 and (b) RCP 8.5 (note costs are in US$ x 1 billion).

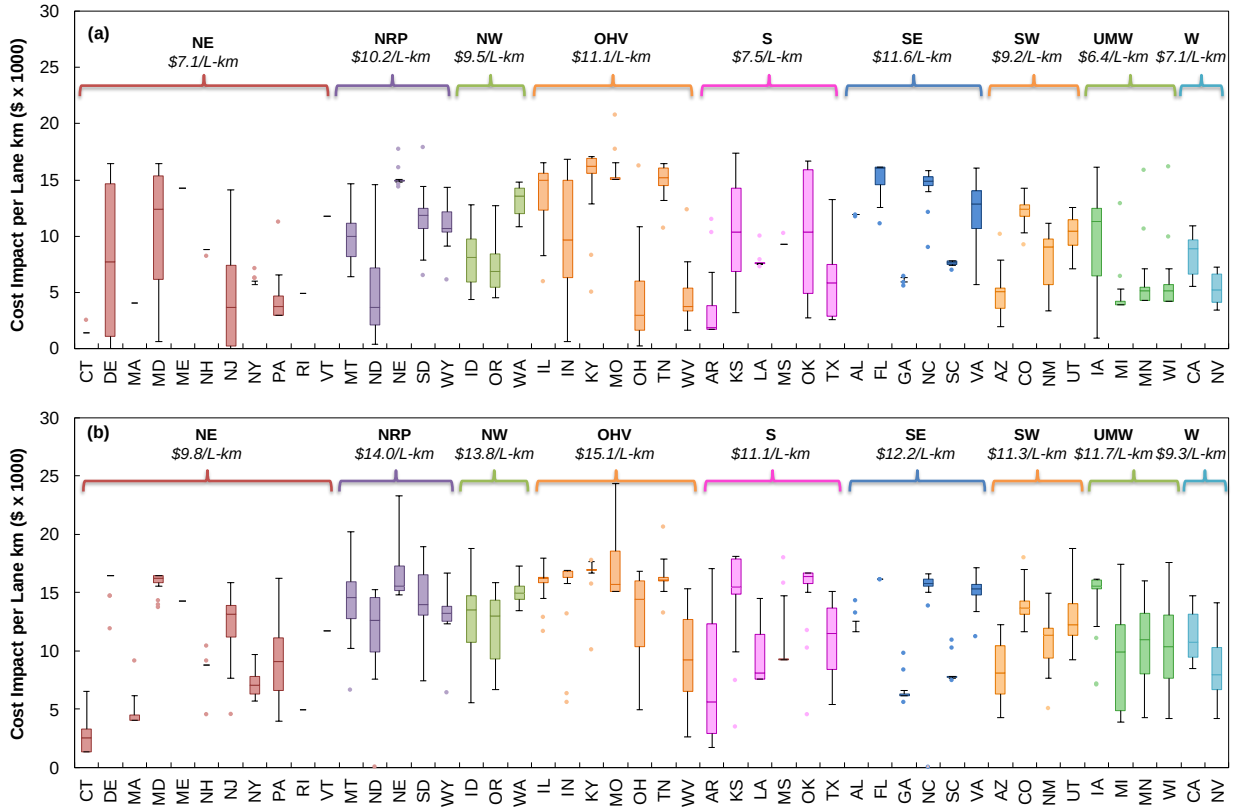

Figure 38: Projected median cost impact to pavement infrastructure on a per-lane kilometer basis for 2040-2070 period from failing to successfully adapt asphalt cement grade; (a) RCP 4.5 and (b) RCP 8.5 (note average costs are in US$ x 1000).

Finally, it is also seen that for a given scenario (RCP 4.5 or RCP 8.5) states have different levels of agreement between the models. In the most extreme case, Delaware under RCP 4.5, there is an estimated range of per lane kilometer costs between US$0 and US$16,500. Under RCP 8.5, the non-outlying predictions yield uniform agreement of US$16,500. This pattern of model convergence and then separation can be related to the discrete grade increments in the grading system. It is found that states along the east coast (Northeast, Ohio Valley, and Southeast) have a greater range in projected costs under RCP 4.5 than RCP 8.5, states in the South, Southwest, Northwest, West, and Northern Rockies and Plains have approximately equal range, while those in the Upper Midwest show a greater range under RCP 8.5.

The LCCA accounts for only a fraction of the total number of paved miles of the residential road network because details for these networks are not readily accessible in national data sources. However, the City of Phoenix, Arizona, is one network for which details are known. The city's network has more than 5,600 km of residential streets. By comparison the cumulative interstate, national route, and state route system in the entire state of Arizona is 9,900 km. These 9,900 km of roads are maintained and rehabilitated with an annual budget of approximately US$1.1 billion, whereas the City of Phoenix maintains its network on an annual budget of approximately US$57 million. Even when accounting for the greater number of lanes in the state system, the State has about 8.5 times more financing per lane km than Phoenix. At the same time, the projected impact from climate change in Phoenix is substantial. The median RCP 8.5 scenario suggests a total cost

impact for the period 2070-2100 of approximately US$0.15 billion in Phoenix alone. During this same period, the projected impact for the entire state of Arizona is US$0.53 billion.

Detailed information on the length of residential streets in Phoenix is available, but not on residential streets nationwide. To identify State's that may experience greater effects from the residential networks the relative proportion of local miles to other roadway types is used as a surrogate measure of the relative extent of the residential street network. Using this measure (see Figure 39) suggests that some states (California in particular) may be facing a substantially higher potential impact from what is estimated here.

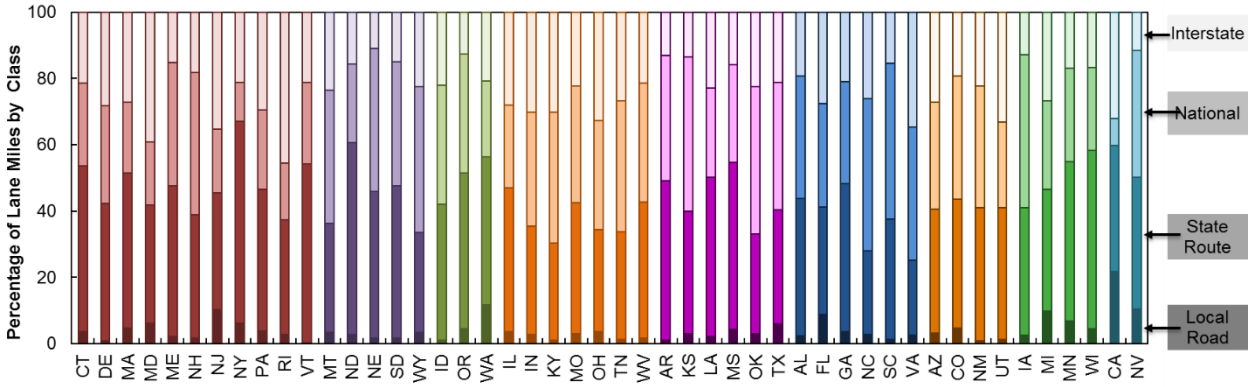

Figure 39: Percentage of roadways in analysis dataset by roadway type and by state.

4.7 COMPARISON WITH OTHER RESULTS

The economic assessment here is somewhat biased to underestimating the true cost of temperature related effects since costs due to construction delays from more frequent activities and increased vehicle operating costs because of degenerated pavement quality are not accounted for. These impacts carry a real economic burden, but estimates of their cost are difficult and/or vary geographically. Apart from the true capital infrastructure cost, these less apparent and more difficult to quantify factors are an important burden to government agencies and the public. In addition, the process of delivering and maintaining the pavement infrastructure carries an environmental burden. More frequent maintenance activities could thus result in environmental impacts. Although focus here is only on the economic impact, the exact environmental effects could be mitigated by selecting more environmentally friendly and sustainability minded strategies.

Only one other national estimate of cost similar in scope to what is done here has been identified in the literature. Chinowsky et al. estimated annualized costs of between US$0.75 and US$0.52 billion depending on the year of analysis (Chinowsky et al. 2013). These values are similar, but lower to the costs that are estimated here. There are other, more subtle differences though like the fact that the analysis here suggests that the costs will increase over time, while the others suggest a decreasing cost with time. As discussed in Supplementary Section 1, the method adopted by Chinowsky et al. (and the related papers by the same research group) estimate costs by assuming perfect adaptation into engineering practice, whereas the estimates here are based on the question of failing to adapt, which explains the differences in cost impacts over time. There are also differences in how material costs are estimated here and how the performance of pavements is

estimated. Nevertheless, these differing scenarios would seemingly represent the range of future possibilities and thus a comparative range of costs.

There have been a few localized studies of cost impacts that should be mentioned. Larsen et al. applied an adaptation approach (a precursor to the one used by Chinowsky et al.) and estimated the per km costs in Alaska for the period from 2006 to 2080 at between US$58,421 and US$42,545 (Larsen et al. 2008). Annualizing these costs (using the same discount rate that Larsen used) results in estimates of between US$1,762 and $1,283 per lane km. The estimates of annualized per km costs range from US$978 (Missouri under RCP 8.5) to US$79 (Connecticut under RCP 4.5). That Alaska might have a higher annualized impact is not surprising since evidence has suggested higher warming there than the rest of the contiguous U.S. (Chapin et al. 2014) However, this could also be related to the fact that performance losses were based on the authors' own judgements and not supported with any performance modeling. A more recent investigation of the same Alaskan network using the same model as in Chinowsky et al. (2013) results in number that are overall smaller than those estimated in the 2008 effort, but individual lane km costs are not reported (Melvin et al. 2016).

Mallick et al. estimated maintenance cost increases of more than 160% by 2100 for a relatively thin asphalt surfaced pavement (Mallick et al. 2014). This cost is greater than what is estimated here, but could be related to aggressive estimates of the impact of temperature on material properties, focus on a coastal roadway, and inclusion of soil saturation changes. Unfortunately, there are not enough details presented to postulate with greater certainty on other underlying causes. Qia et al. estimated a considerably smaller estimate of cost increase (1-2%) through 2050 (2015). There are a few relevant details that explain the difference between their estimate and the one developed in this paper. First, the authors considered only a single location and with a single GCM (high, medium, and low emission scenarios were considered though). Second, temperature was incorporated by linear scaling of all future climate according to the median annual predicted temperature rise. Pavement performance is more greatly affected by high temperatures and scaling by the annual air temperature increase does not consider future predictions of extreme hot (or cold) days. Finally, the estimate of 1-2% is based on a selection of optimal treatment options throughout the lifetime. In this case the estimate can be seen as another "best case scenario" assessment that taken in contrast to the estimates here (3-9% increases) provides an important perspective on the importance of quickly adapting to a non-stationary future.

5.0 CHALLENGES, CONCLUSIONS, AND FUTURE RESEARCH

In terms of both performance and cost, a failure to update engineering standards of practice and adapt to climate change may leave the pavement infrastructure in the U.S. at risk. Based on the analysis here, it is expected that the impacts will be greatest in geographically larger states, central and southeastern regions and local municipalities. The results of this analysis and comparisons between it and projections of mean air temperature rise across the US show that the impacts of climate change induced temperature rise cannot be uniquely related to the absolute value of air temperature or the change of this temperature in the future. The key contributors to this risk are: 1) the increase local in air temperature and year-to-year variation; 2) the geospatial location (notably the latitude), 3) the current engineering practices of the pavements inclusive of the current reliability of the asphalt grade; and 4) the density of the road network across roadway types. This study highlights that in given the temporal scale with which roadways are engineered to perform, in the future, it may be important that engineering practice incorporate up to date climate records and/or incorporate future climate projections to mitigate economic impact.

By examining the specific behaviors across interstate pavements, it is also learned that these effects will affect all regions of the US, but some areas may experience greater impacts for certain distresses (for example greater rutting impacts in wet freeze and dry freeze locations). Use of climate change projections shows substantial impact on the pavement distress irrespective of the climate location and prediction model data used. Though there is a variation in the magnitude of impact due to the climate projections all the projects models are indicting that pavements will experience higher distresses and early failure of the pavements. The percentage increase in fatigue cracking is observed to be less compared to the AC rutting, as temperature increase in the future will have more impact in terms of AC rutting. Overall impacts will vary depending on the analysis framework. Examining asphalt binder grade alone suggests that the Ohio Valley and Southeast may experience the greatest effects, while Pavement Design ME simulations suggest the upper Midwest and Northeast regions of the United States may experience greater effects. Incorporation of precipitation projection data along with temperature projections does not show any substantial difference in the pavement performance. Impact of climate change on rigid pavements sections considered in this study shows increase in joint faulting but decreases in transverse cracking.

In short, the study findings suggest, like others, that there may be a substantial impact on the pavement infrastructure due to the climate change. The uncertainty of these projections is large, but the message is consistent. And therefore, it may become increasingly important consider temperatures that deviate from historical norms when analyzing and designing pavements. Contextualizing the specific findings of this research into the broader literature suggests that continued reliance on a static climate record may result in more frequent maintenance and rehabilitation and ultimately greater costs from the transportation infrastructure.

6.0 REFERENCES

Adaptwest (2016). *Current and projected climate data for North America (CMIP5 scenarios)*, Online. <https://adaptwest.databasin.org/pages/adaptwest-climatena>. Accessed December 2016.

American Society of Civil Engineers (ASCE) (2013). *2013 Report Card for Americas Infrastructure*. Online. <http://www.infrastructurereportcard.org/>. Accessed January 2017.

Applied Research Associates (ARA) (2004). Guide for Mechanistic-Empirical Design of New and Rehabilitated Pavement Structures. Final Report. NCHRP 1-37A. National Cooperative Highway Research Program, National Research Council, Washington, DC.

Anderson, H., C. Beck, K. Gade, & S. Olmsted (2015). *Extreme Weather Vulnerability Assessment*. FHWA No. 0704-0188.FHWA, Arizona Department of Transportation, Phoenix, AZ.

Asphalt Institute (AI) (2003). *Superpave Performance Graded Asphalt Binder Specifications and Testing*, Superpave Series No. 1 (SP-1). Asphalt Institute, Lexington, KY.

Banerjee, A., J. Aguiar-Moya, & J.A. Prozzi (2009). *Calibration of Mechanistic-Empirical Pavement Design Guide Permanent Deformation Models: Texas Experience with Long-Term Pavement Performance*, Transportation Research Record: Journal of the Transportation Research Board, 2094, 12-20. doi: 10.3141/2094-02

Banerjee, A., J.A. Prozzi, & J.P. Aguiar-Moya (2010). *Calibrating the MEPDG Permanent Deformation Performance Model for Different Maintenance and Rehabilitation Strategies,* In Transportation Research Board 89th Annual Meeting, No. 10-2355.

Belcher, S.E., J.N. Hacker, & D.S. Powell (2005). *Constructing Design Weather Data for Future Climates*, Building Services Engineering Research and Technology, 26(1), 49-61. doi: 10.1191/0143624405bt112oa

Bergek, A., S. Jacobsson, B. Carlsson, S. Lindmark, & A. Rickne (2008). *Analyzing the Functional Dynamics of Technological Innovation Systems: A scheme of Analysis*, Research Policy, 37(3), 407-429. doi: 10.1016/j.respol.2007.12.003

Brekke, L., B.L. Thrasher, E.P. Maurer, and T. Pruitt (2013). *Downscaled CMIP3 and CMIP5 Climate and Hydrology Projections: Release of Downscaled CMIP5 Climate Projections, Comparison with Preceding Information, and Summary of User Needs*, US Army Corps of Engineers, US Geological Survey.

Cambridge Systematics, Inc. (2015). *Central Texas Extreme Weather and Climate Change Vulnerability Assessment of Regional Transportation Infrastructure*. FHWA No. 0704-0188. Capital Area Metropolitan Planning Organization, Austin TX.

Carlsson, B. & S Jacobsson (1997). *In Search of Useful Public Policies — Key Lessons and Issues for Policy Makers*. Chapter 10 in Technological Systems and Industrial Dynamics, Ed. B. Carlsson, Springer US.

Casey, D., P. Casey, & A.C. Lemer (2012). *Tracing Innovation's Spread: Impacts of the Domestic Scan Program*, *TR News*, 278, 3-8. Online < http://onlinepubs.trb.org/ onlinepubs/trnews/trnews278.pdf> Accessed August 2016.

Chapin, F.S., S.F. Trainor, P. Cochran, H. Huntington, C. Markon, M. McCammon, A.D. McGuire, & M. Serreze (2014). *Ch. 22: Alaska. Climate Change Impacts in the United States.*

The Third National Climate Assessment, J.M. Melillo, T.C. Richmond, & G.W. Yohe, Eds, U.S. Global Change Research Program, 514-536.

Chinowsky, P. & C. Arndt (2012). *Climate Change and Roads: A Dynamic Stressor-Response Model*. Review of the Development Economics, 16(3), pp. 448-462. doi: 10.1111/j.14679361.2012. 00673.x

Chinowsky, P.S., J.C. Price, & J.E. Neumann (2013). *Assessment of Climate Change Adaptation Costs for the US Road Network.* Global Environmental Change, 23(4), 764-773. doi: 10.1061/9780784413326.

Daniel, J.S, J.M. Jacobs, E. Douglas, R.B. Mallick, & K. Hayhoe (2014). *Impact of Climate Change on Pavement Performance: Preliminary Lessons Learned through the Infrastructure and Climate Network (ICNet),* In International Symposium of Climatic Effects on Pavement and Geotechnical Infrastructure 2013, Fairbanks AK. doi: 10.1061/9780784413326

Espinet, X., A. Schweikert, N. van den Heever, & P. Chinowsky (2016). *Planning Resilient Roads for the Future Environment and Climate Change: Quantifying the Vulnerability of the Primary Transport Infrastructure System in Mexico*, Transport Policy, 50, 78-86. doi: 10.1016/j.tranpol.2016.06.003

Federal Highway Administration (FHWA). (2013) *Freight facts and Figures 2013*, [Online] Available from: <http://ops.fhwa.dot.gov/Freight/freight_analysis/nat_freight_stats/docs/13facts figures/index.htm>. Accessed December 2014.

Fletcher, C.G., L. Matthews, J. Andrey, & A. Saunders (2016). *Projected Changes in Mid-Twenty-First-Century Extreme Maximum Pavement Temperature in Canada*. Journal of Applied Meteorology and Climatology, 55(4), 961-974. doi: 10.1175/JAMC-D-15-0232.1

Fwa, T.F., H.R. Pasindu, & G.P. Ong (2011). *Critical Rut Depth for Pavement Maintenance Based on Vehicle Skidding and Hydroplaning Consideration*, Journal of Transportation Engineering, 138(4), 423-429. doi: 10.1061/(ASCE)TE.1943-5436.0000336.

Gaspard, K., M. Martinez, Z. Zhang, & Z. Wu (2007). *Impact of Hurricane Katrina on Roadways in the New Orleans Area*, Technical Assistant Report No. 07-2TA, Louisiana Department of Transportation and Development.

Geels, F.W., & R. Kemp (2007). *Dynamics in Socio-Technical Systems: Typology of Change Processes and Contrasting Case Studies*, Technology in Society, 29(4), 441-455. doi: 10.1016/j.techsoc.2007.08.009

Harvey, M., P. Whetton, K.L. McInnes, B. Cechet, J.L. McGregor, K. Nguyen, N. Houghton, C. Lester, E. Styles, N. Michael, & T. Martin (2004). *Impact of Climate Change on Road Infrastructure*. Austroads Report No. AP-R243/04. Austroads and the Bureau of Transport and Regional Economics, Sydney.

Heitzman, M., D. Timm, E.S. Tackle, D. E. Herzmann, & D. D. Traux (2011). *Developing MEPDG Climate Data Input Files for Mississippi*. No. FHWA/MS-DOT-RD-11-232.FHWA, U. S. Department of Transportation.

Huber, G.A. (1994). *Weather Database for the Superpave Mix Design System*, SHRP-A-648A, Strategic Highway Research Program, Washington, DC.

Humphrey, N (2008). *Potential Impacts of Climate Change on US Transportation*, *TR news*, 256, 21-24.

Huang, Y.H. (1993). *Pavement Analysis and Design*. Prentice Hall, Upper Saddle River, NJ.

Intergovernmental Panel on Climate Change (IPCC) (2007). Working Group 3. *Climate Change 2007: Mitigation: Contribution of Working Group III to the Fourth Assessment Report of the Intergovernmental Panel on Climate Change: Summary for Policymakers and Technical*

Summary. Edited by Bert Metz, Ogunlade Davidson, Peter Bosch, Rutu Dave, and Leo Meyer. Cambridge University Press.

Johnson, N.L. & S. Kotz (1970). Continuous Univariate Distributions: Chapter 24 – Beta Distributions, Houghton Mifflin Company, Boston MA.

Kieft, A., R. Harmsen, & M.P. Hekkert (2016). *Interactions Between Systemic Problems in Innovation Systems: The case of Energy-Efficient Houses in the Netherlands*, Environmental Innovation and Societal Transitions, In Press. doi: 10.1016/j.eist.2016.10. 001

Koetse, M.J. & P. Rietveld (2009). *The Impact of Climate Change and Weather on Transport: An Overview of Empirical Findings*. Transportation Research Part D: Transport and Environment, 14(3), 205-221.doi: 10.1016/j.trd.2008.12.004

Knott, J. F., M. Elshaer, J.S. Daniel, J.M. Jacobs, & P. Kirshen (2017). *Assessing the Effects of Rising Groundwater from Sea Level Rise on the Service life of Pavements in Coastal Road Infrastructure*, Transportation Research Record: Journal of the Transportation Research Board, 2639, 1-10. doi: 10.3141/2639-01

Knutti R & J. Sedlacek (2013). *Robustness and Uncertainties in the New CMIP5 Climate Model Projections*. Nature Climate Change, 3, 369-373.

Knutti, R., D. Masson, D. & A. Gettelman (2013). *Climate Model Genealogy: Generation CMIP5 and How we got there*, Geophysical Research Letters, 40(6), 1194-1199. doi: 10.1002/grl.50256

Lamptey, G., M.Z. Ahmad, S. Labi, & C.S. Kumares (2005). *Life Cycle Cost Analysis for INDOT Pavement Design Procedures*, FHWA/IN/JTRP-2004/28. Indiana Department of Transportation, Indianapolis, IN.

Larsen, P.H., S. Goldsmith, O. Smith, M.L. Wilson, K. Strzepek, P. Chinowsky, & B. Saylor (2008). *Estimating Future Costs for Alaska Public Infrastructure at Risk from Climate Change*, Global Environmental Change, 18(3), 442-457. doi: 10.1016/j.gloenvcha.2008. 03.005.

Lytton, R.L. (1994). *Prediction of Movement in Expansive Clays*, In Vertical and Horizontal Deformations of Foundations and Embankments, ASCE Special Publication 40, Ed. A.T. Yeung and G.Y Felio, 1827-1845.

Makin, A., C.J. Klein, H.P. Possingham, H. Yamano, Y. Yara, T. Ariga, K. Matsuhasi, & M. Beger (2015). *The Effect of Applying Alternate IPCC Climate Scenarios to Marine Reserve Design for Range Changing Species*, Conservation Letters, 8(5), 20-328. doi: 10.1111/conl.12147

Mallick, R.B., J.M. Jacobs, B.J. Miller, J.S. Daniel, & P. Kirshen (2016). *Understanding the Impact of Climate Change on Pavements with CMIP5, System Dynamics and Simulation*, International Journal of Pavement Engineering. doi: 101080/10298436.2016.1199880

Mallick, R., M. Radzicki, J. Daniel, & J. Jacobs (2014). *Use of System Dynamics to Understand Long-Term Impact of Climate Change on Pavement Performance and Maintenance Most*, Transportation Research Record: Journal of the Transportation Research Board, 2455, 1-9. doi: 10.3141/2455-01

Martin, R., & P. Sunley (2006). *Path Dependence and Regional Economic Evolution*, Journal of Economic Geography, 6(4), 395-437. doi: 10.1093/jeg/lbl012

Maurer, E.P., L. Brekke, T. Pruitt, & P.B. Duffy (2007). *Fine-Resolution Climate Projections Enhance Regional Climate Change Impact Studies*, Eos Transactions, American Geophysical Union, 88(47), 504. doi: 10.1371/journal.pone.0071297

Meagher, W., J.S. Daniel, J. Jacobs, & E. Linder (2012). *Method for Evaluating Implications of Climate Change for Design and Performance of Flexible Pavements*. Transportation Research Record: Journal of the Transportation Board, 2305, 111-120. doi: 10.3141/2305-12

Mearns. L., R. Arritt, S. Biner, M.S. Bukovsky, S. McGinnis, S. Sain, D. Caya, J. Correia, D. Flory, W. Gutowski, E.S. Takle, R. Jones, R. Leung, W. Moufouma-Okia, L. McDaniel, A. M.B. Nunes, Y. Qian, J. Roads, L. Sload, & M. Snyder (2012). *The North American Regional Climate Change Assessment Program: Overview of Phase I Results*. Bulletin of American Meteorology Society, 93, 1337-1362. doi: 10.1175/BAMS-D-11-00223.1.

Melillo, J.M., R. Terese, & G.W. Yohe (Eds.) (2014). *Climate Change Impacts in the United States: The Third National Climate Assessment*. U.S. Global Change Research Program, 841 pp. doi:10.7930/J0Z31WJ2.

Melvin, A.M., P. Larsen, B. Boehlert, J.E. Neumann, P. Chinowsky, X. Espinet, J. Martinich, M.S. Baumann, L. Rennels, A. Bothner, D.J. Nicolsky, & S.S. Marchenko (2016). *Climate Change Damages to Alaska Public Infrastructure and the Economics of Proactive Adaptation*, Proceedings of the National Academy of Sciences, 114(2), 122-131. doi: 10.1073/pnas. 1611056113.

Meyer, M., M. Flood, J. Keller, J. Lennon, G. McVoy, C. Dorney, K. Leonard, R. Hyman, & J. Smith (2014). *Strategic Issues Facing Transportation, Volume 2: Climate Change, Extreme Weather Events, and the Highway System: Practioner's Guide and Research Report.* NCHRP Report 750, National Cooperative Highway Research Program, Washington, D.C.

Mills, B.N., S.L. Tighe, J. Andrey, J.T. Smith, & K. Huen (2009). *Climate Change Implications for Flexible Pavement Design and Performance in Southern Canada*, Journal of Transportation Engineering 135(10), 773-782. doi: 10.1061/(ASCE)0733-947X

Mndawe, M.B., J. Ndambuki, & W.K. Kupolati (2013). *Revision of the Macro Climatic Regions of Southern Africa*. OIDA International Journal of Sustainable Development, 6(1) 37-44.

Mndawe, M.B., J. M. Ndambuki, W.K. Kupolati, A.A. Badejo, & R. Dunbar (2015). *Assessment of the Effects of Climate Change on the Performance of Pavement Subgrade,* African Journal of Science, Technology, Innovation and Development, 7(2), 111-115. doi: 10.1080/20421338.2015.1023649

Moving Ahead for Progress in the 21st Century Act (MAP 21) (2012). Public Law 112-141, Title I Federal-Aid Highways, Subtitles A, B, D, and F.

National Cooperative Highway Research Program (2016). *US Domestic Scan Program*, National Cooperative Highway Research Program Project 20-68A(02). Online < http://apps.trb.org/cmsfeed/TRBNetProjectDisplay.asp?ProjectID=1570> Accessed August 2016.

National Highway Planning Network (NHPN) (2015). National Highway Planning Network - Tools - Processes - Planning Online <http://www.fhwa.dot.gov/planning/processes/tools/ nhpn/>. Accessed March 2015.

National Research Council Committee on Climate Change (NRC) (2008). *Potential Impacts of Climate Change on US Transportation*. National Research Council (US). Division on Earth, & Life Studies Transportation Research Board, Washington, D.C.

Negro, S.O., F. Alkemade, & M.P. Hekkert, (2012). *Why Does Renewable Energy Diffuse so Slowly? A Review of Innovation System Problems*, Renewable and Sustainable Energy Reviews, 16(6), 3836-3846. doi: 10.1016/j.rser.2012.03.043

New York Department of Transportation (NYDOT) (2002). *Comprehensive Pavement Design Manual: Chapter 5 Rehabilitation*. NYDOT Design Division and Technical Service Division. Albany, NY.

NIST/SEMATECH (2012). *e-Handbook of Statistical Methods*, National Institute of Standards and Technology. Online. <http://www.itl.nist.gov/div898/handbook/> Accessed June 2017.

Qiao, Y., A.R. Dawson, T. Parry, & G.W. Flintsch (2015). *Evaluating the Effects of Climate Cange on Road Maintenance Intervention Strategies and Life-Cycle Costs*. Transportation Research Part D: Transport and Environment, 41, 492-503. doi: 10.1080/10298436.2016. 1199880

Riahi, K., S. Rao, V. Krey, C. Cho, V. Chirkov, G. Fischer, G. Kindermann, N. Nakicenovic, & P. Rafa (2011). *RCP 8.5—A Scenario of Comparatively High Greenhouse Gas Emissions*, Climatic Change, 109(1-2), 33-57, doi: 10.1007/s10584-011-0149-y

Rosenzweig, C., W.D. Solecki, S.A. Hammer, & S. Mehrotra, (Eds.). (2011). *Climate Change and Cities: First Assessment Report of the Urban Climate Change Research Network*. Cambridge University Press. Cambridge, UK.

Sailor, D.J. (2014). *Risks of Summertime Extreme Thermal Conditions in Buildings as a Result of Climate Change and Exacerbation of Urban Heat Islands*, Building and Environment, 78, 81-88. doi: 10.1016/j.buildenv.2014.04.012

Santero, N. (2010). *Life Cycle Assessment of Pavements: A Critical Review of Existing Literature and Research*, Lawrence Berkeley National Laboratory, Online <https://www.osti.gov/scitech/servlets/purl/985846>. Accessed October 2016

Schleussner, C. F., Levermann, A., & Meinshausen, M. (2014). *Probabilistic Projections of the Atlantic Overturning*, Climatic Change, 127(3-4), 579-586. doi: 10.1007/s10584-014-1265-2

Schweikert, A., P. Chinowsky, S. Espinet, & M. Tarbert (2014). *Climate Change and Infrastructure Impacts: Comparing the Impact on Roads in Ten Countries through 2100*. Procedia Engineering, 78, 306-316. doi: 10.1016/j.proeng.2014.07.072

Smith, A., A. Stirling, & F. Berkhout (2005). *The Governance of Sustainable Socio-Technical Transitions*, Research Policy, 34(10), 1491-1510. doi: 10.1016/j.respol.2005. 07.005

Thomson, A.M., K.V. Calvin, S.J. Smith, G.P. Kyle, A.Volke, P. Patel, S. Delgado-Arias, B. Bond-Lamberty, M.A. Wise, L.E. Clarke, and J.A. Edmonds (2011). *RCP4.5: A Pathway for Stabilization of Radiative Forcing by 2100*, Climatic Change, 109(1-2), 77-94. doi: 10.1007/s10584-011-0151-4

United States Department of Transportation (USDOT) (2016). *National Transportation Statistics*. Bureau of Transportation Statistics, Washington, DC. Online < https://www.rita.dot.gov/bts/sites/rita.dot.gov.bts/files/publications/national_transportation_statistics/index.html >. Accessed March 2016.

United States Department of Transportation (USDOT) (2015a). *Transportation in the United States.* Bureau of Transportation Statistics Washington, DC.

United States Department of Transportation (USDOT) (2015b). *US. Beyond Traffic 2045: Trends and Choices*. US Department of Transportation, Washington, DC.

Viola, F. & C. Celauro (2015). *Effect of Climate Change on Asphalt Binder Selection for Road Construction in Italy*. Transportation Research Part D: Transport and Environment, 37, 40-47. doi: 10.1016/j.trd.2015.04.012

Walls, J. & M.R. Smith (1998). *Life Cycle Cost Analysis in Pavement Design - Interim Technical Bulletin*, FHWA-SA98-079, Federal Highway Administration, Washington, DC.

Wieczorek, A.J., & M.P. Hekkert (2012). *Systemic Instruments for Systemic Innovation Problems: A Framework for Policy Makers and Innovation Scholars*, Science and Public Policy, 39(1), 74-87. doi: 10.1093/scipol/scr008

Witczak, M.W., C.E. Zapata, & W.N. Houston (2006). *Models Incorporated into the Current Enhanced Integrated Climatic Model: NCHRP 9–23 Project Findings and Additional Changes after Version 0.7*. Final Report, Project NCHRP.

Woldemeskel, F.M., A. Sharma, B. Sivakumar, & R. Mehrotra (2016). *Quantification of Precipitation and Temperature Uncertainties Simulated by CMIP3 and CMIP5 Models*, Journal of Geophysical Research: Atmospheres, 121(1), 3-17. doi: 10.1002/2015JD023719

Wuebbles, D., G. Meehl, K. Hayhoe, T.R. Karl, K. Kunkel, B. Santer, M. Wehner, B. Colle, E.M. Fischer, R. Fu, A. Goodman, E. Janssen, V. Kharin, H. Lee, W. Li, L.N. Long, S.C. Olsen, Z. Pan, A. Seth, J. Sheffield, & L. Sun (2014). *CMIP5 Climate Model Analysis: Climate Extremes in the United States*, Bulletin of the American Meteorology Society, 95, 571-583, doi: 10.1175/BAMS-D-12-00172.1

Yoder, E.J., & M.W. Witczak (1975). *Principles of Pavement Design*. John Wiley & Sons, New York, NY.